ANSI/AIAA
S-131-2010

Standard

Astrodynamics – Propagation Specifications, Technical Definitions, and Recommended Practices

American National Standard

ANSI/AIAA
S-131-2010

American National Standard

Astrodynamics—Propagation Specifications, Technical Definitions, and Recommended Practices

Sponsored by

American Institute of Aeronautics and Astronautics

Approved 25 August 2010

American National Standards Institute

Abstract

This document provides the broad astrodynamics and space operations community with technical standards and lays out recommended approaches to ensure compatibility between organizations. Applicable existing standards and accepted documents are leveraged to make a complete—yet coherent—document. These standards are intended to be used as guidance and recommended practices for astrodynamics applications in Earth orbit where interoperability and consistency of results is a priority. For those users who are purely engaged in research activities, these standards can provide an accepted baseline for innovation.

American National Standard

Approval of an American National Standard requires verification by ANSI that the requirements for due process, consensus, and other criteria have been met by the standards developer.

Consensus is established when, in the judgment of the ANSI Board of Standards Review, substantial agreement has been reached by directly and materially affected interests. Substantial agreement means much more than a simple majority, but not necessarily unanimity. Consensus requires that all views and objections be considered, and that a concerted effort be made toward their resolution.

The use of American National Standards is completely voluntary; their existence does not in any respect preclude anyone, whether he has approved the standards or not, from manufacturing, marketing, purchasing, or using products, processes, or procedures not conforming to the standards.

The American National Standards Institute does not develop standards and will in no circumstances give an interpretation of any American National Standard. Moreover, no person shall have the right or authority to issue an interpretation of an American National Standard in the name of the American National Standards Institute. Requests for interpretations should be addressed to the secretariat or sponsor whose name appears on the title page of this standard.

CAUTION NOTICE: This American National Standard may be revised or withdrawn at any time. The procedures of the American National Standards Institute require that action be taken to affirm, revise, or withdraw this standard no later than five years from the date of approval. Purchasers of American National Standards may receive current information on all standards by calling or writing the American National Standards Institute.

Published by
American Institute of Aeronautics and Astronautics
1801 Alexander Bell Drive, Reston, VA 20191

Printed in the United States of America

Contents

Figures

Tables

Foreword

One of the most significant scientific and technological accomplishments since the beginning of the space era is the successful deployment of space systems and the necessarily ingenious application of astrodynamics to support these systems. Astrodynamics has been developed by extending the knowledge accumulated since the first recorded investigations into the motions of heavenly bodies.

The outgrowth of civilian and military rocket system developments has led to the establishment and implementation of numerous space systems, related physical models, and astrodynamics theories, algorithms, and procedures. With the proliferation of different and independent space systems and advancements in technology and astrodynamic sciences, the interfacing needed to ensure interoperability within space operations has become more complex.

The ASD/CoS charter is to *"Identify, establish, and publish astrodynamics standards, guides, and recommended practices to ensure the continued enhancement of aerospace-wide efficiency and productivity to meet the scientific, technological and operational demands."* To accomplish the chartered goals, the strategy is to:

— Research and establish the up-to-date status of the astrodynamics standards and practices currently available.

— Identify scientific, technological, and operational programs and system elements that have a need for astrodynamics standards and consensus practices.

— Perform in-depth analyses of the existing standards and practices and develop recommendations for possible adoption and/or modifications as AIAA standards or practices.

— Develop definition of standards and adopt formal guidelines and requirements of standardization.

— Recommend and propose the areas where new standards, guides, and recommended practices are required. Additionally, identify areas where standards are currently not appropriate.

— Identify, develop, and document candidate new astrodynamics standards, guides, and recommended practices for consideration.

— Perform independent verification and validation, including solicitation of in-depth reviews within industry, academia, and government laboratories for all proposed and documented standards, guides, and recommended practices.

— Submit proposed standards, guides, and recommended practices to the Standards Executive Council for approval and publication.

— Maintain all relevant technical materials and standards.

— Maintain technical coordination with scientific and astrodynamics communities nationally and internationally.

To help provide coherent direction for its activities in identifying and selecting topics, the committee approved a set of criteria. Fundamentally, the committee has taken the view that the objective of an astrodynamic standard is to provide guidance on practices that will ensure and enhance interoperability between organizations. Following are the criteria that have been useful in selecting topics that achieve this objective:

— Scope: Does the topic relate to processes associated with describing the motion of orbiting bodies? Although rather evident, the committee has occasionally found itself considering topics that really fall within the purview of a different area or responsibility.

— Utility: Is the topic of wide concern to the majority of the astrodynamics community, and does it deal with the process of information exchange among members of that community? If a topic is of only minor relevance to the community, developing standards may not be particularly useful. Thus, such standards should aim at facilitating the broadest information exchange across the community.

— Alternatives (Ambiguity): Does the topic involve alternative ways of performing a process or accomplishing an objective? In cases where multiple alternatives exist, we tried to give guidance on the variability of applications, indicating what the community consensus is. Where only one commonly accepted alternative existed, we determined if there was any potential confusion in its application.

— Practicality: Can agreement be achieved on standardization? Despite meeting all the above criteria, insufficient consensus may demand not treating the topic.

The ASD/CoS initial effort, *Recommended Practice, Astrodynamics—Part I,* was chaired by Dr. Joseph J. F. Liu. A *Part II* document was initiated by Dr. Hamilton Hagar, but was never officially finished in its original form. The current document supersedes the *Part I* and *Part II* and forms a unified document, including specific treatment of standards and recommended practices. The current version focuses on propagation for Earth orbiting satellites.

At the time of approval, the members of the AIAA Astrodynamics Committee on Standards were:

David A. Vallado, Chair	Center for Space Standards & Innovation
Rich Burns	NASA
David Finkleman	Center for Space Standards & Innovation
Michael Gabor	Northrop Grumman
Felix Hoots	The Aerospace Corporation
T.S. Kelso	Center for Space Standards & Innovation
Steve Nerem	University of Colorado
Daniel Oltrogge	1Earth Research, LLC
Glenn Peterson	The Aerospace Corporation
Paul Schumacher	U.S. Air Force Research Laboratory
John H. Seago	Analytical Graphics, Inc.
P. Kenneth Seidelmann	University of Virginia
Fred Slane	Space Infrastructure, Inc.
Jerome R. Vetter	Johns Hopkins University Applied Physics Laboratory

The above consensus body approved this document in August 2010.

The AIAA Standards Executive Council (Vice President, Wilson Felder, Chairman) accepted the document for publication in August 2010.

The AIAA Standards Procedures dictates that all approved Standards, Recommended Practices, and Guides are advisory only. Their use by anyone engaged in industry or trade is entirely voluntary. There is no agreement to adhere to any AIAA standards publication and no commitment to conform to or be guided by standards reports. In formulating, revising, and approving standards publications, the committees on standards will not consider patents that may apply to the subject matter. Prospective users

of the publications are responsible for protecting themselves against liability for infringement of patents or copyright or both.

Introduction

The American Institute of Aeronautics and Astronautics (AIAA) Astrodynamics Committee on Standards (ASD/CoS) has developed this open set of voluntary standards and recommended practices applying to propagation of orbits about the Earth. This document provides the broad astrodynamics and space operations community with technical standards and lays out recommended approaches to ensure compatibility between organizations. Applicable existing standards and accepted documents are leveraged to make a complete—yet coherent—document. These standards are intended to be used as guidance and recommended practices for astrodynamics applications in Earth orbit where interoperability and consistency of results is a priority. For those users who are purely engaged in research activities, these standards can provide an accepted baseline for innovation.

This document describes the technical specifications and requirements that comply with established and accepted guidelines, practices, and technical intent for propagation in Earth orbit. There are numerous examples of recommendations for implementation and approved variations. Accompanying resources will include algorithm and software code examples, as well as corresponding test cases, to establish confidence in the resulting products.

The remainder of this document is organized to provide a complete picture of the Earth orbit propagation application:

— Section 4 provides a glossary of terms used in the standards document.

— Section 5 lists the accepted and agreed upon units, constants, coordinates, and time systems, as well as consideration of conversions and precision.

— Section 6 describes the accepted force models used for Earth orbit propagation applications. These force models include gravity, atmospheric drag, third-body perturbations, solar radiation pressure, tides, and other perturbative forces.

— Section 7 describes application of analytical, numerical, and semianalytical approaches to orbit propagation.

— Section 8 summarizes the references used in the development of this set of standards and Annex A provides informative references.

1 Scope

This document provides the broad astrodynamics and space operations community with technical standards and lays out recommended approaches to ensure compatibility between organizations. Applicable existing standards and accepted documents are leveraged to make a complete—yet coherent—document. These standards are intended to be used as guidance and recommended practices for astrodynamics applications in Earth orbit where interoperability and consistency of results is a priority. For those users who are purely engaged in research activities, these standards can provide an accepted baseline for innovation.

2 Tailoring

When viewed from the perspective of a specific program or project context, the requirements defined in this standard may be tailored to match the actual requirements of the particular program or project. Tailoring of requirements shall be undertaken in consultation with the procuring authority where applicable.

For this document, there are no specific tailoring actions as the document contains recommended practices and approaches that are intended to cover specific implementations.

NOTE Tailoring is a process by which individual requirements or specifications, standards, and related documents are evaluated and made applicable to a specific program or project by selection, and in some exceptional cases, modification and addition of requirements in the standards.

3 Applicable Documents

The following documents contain provisions which, through reference in this text, constitute provisions of this standard. For dated references, subsequent amendments to, or revisions of, any of these publications do not apply. However, parties to agreements based on this standard are encouraged to investigate the possibility of applying the most recent editions of the normative documents indicated below. For undated references, the latest edition of the normative document referred to applies.

ISO 8601 (2004)	*Data elements and interchange formats — Information interchange — Representation of dates and times*
ITU-R 460 (2002)	Recommendation 460
Department of Defense	NIMA TR8350.2, World Geodetic System, 1984
AIAA G-003C-2010	Guide to Reference and Standard Atmosphere Models

4 Vocabulary

4.1 Acronyms and Abbreviated Terms

AAS	American Astronautical Society
AFGP4	Air Force General Perturbations Version 4
AFSPC	Air Force Space Command
AIAA	American Institute of Aeronautics and Astronautics
APL	Applied Physics Laboratory
AU	Astronomical Unit

BC	Ballistic Coefficient
BCRS	Barycentric Celestial Reference System
BIPM	Bureau International des Poids et Mesures (International Bureau of Weights and Measures)
CCD	Charge-Coupled Device
CEP	Celestial Ephemeris Pole
CIO	Celestial Intermediate Origin
CIP	Celestial Intermediate Pole
CIRA	COSPAR International Reference Atmosphere, (CIRA 90)
CIRS	Celestial Intermediate Reference System
CNES	Centre National d'Etudes Spatiale (National Center for Space Studies)
COSPAR	Committee On Space Research
CSR	Center for Space Research
CTIM	Coupled Thermosphere-Ionosphere Model
DCA	Dynamic Calibration of the Atmosphere
DE200	Development Ephemeris 200
DMA	Defense Mapping Agency
DSST	Draper Semianalytic Satellite Theory
DTM	Drag Temperature Model
ECMWF	European Centre for Medium-Range Weather Forecasts
EGM	Earth Gravitational Model
EOP	Earth Orientation Parameters
ET	Ephemeris Time
EUV	Extreme Ultraviolet
FK5	Fifth Fundamental Catalog
GAST	Greenwich Apparent Sidereal Time
GCRF	Geocentric Celestial Reference Frame
GEM	Goddard Earth Model
GEO	Geosynchronous Earth Orbit
GMST	Greenwich Mean Sidereal Time
GMT	Greenwich Mean Time
GOST	Russian atmospheric model

GPS	Global Positioning System
GRAM	NASA/MSFC Global Reference Atmospheric Model (GRAM 90)
GRIM	GRIM is a concatenation of the first two letters of GRGS (group de recherches de geodesie spatiale, Toulouse/France) and "I" and "M" from IAPG Munich (institute of astronomical and physical geodesy, technical university of Munich). Both institutes jointly prepared the first GRIM gravity models under the lead of George Balmino (GRGS) and Christoph Reigber (IAPG).
GSFC	Goddard Space Flight Center
HPOP	High-Performance Orbit Propagator
HWM	Horizontal Wind Model
IAG	International Association of Geodesy
IAU	International Astronomical Union
ICRF	International Celestial Reference Frame
ICRS	International Celestial Reference System
IEEE	Institute of Electrical & Electronic Engineers
IERS	International Earth Rotation and Reference System Service
ISO	International Standards Organization
ISS	International Space Station
ITRF	International Terrestrial Reference Frame
ITRS	International Terrestrial Reference System
ITU-R	International Telecommunication Union Radiocommunication Sector
IUGG	International Union of Geodesy and Geophysics
J70	Jacchia atmospheric models (J64, J70, J71, J77)
JD	Julian Date
JERS	Japanese Earth Resources Satellite
JGM	Joint Gravity Model
JPL	Jet Propulsion Laboratory
JR71	Jacchia-Roberts atmospheric model
LEO	Low Earth Orbit
LOD	Length of Day
MET	Marshall Engineering Thermosphere
MJD	Modified Julian Date
MOD	Mean of Date
MSFC	Marshall Space Flight Center

MSIS	Mass Spectrometer Incoherent Scatter, (MSIS 00)
NASA	National Aeronautics and Space Administration
NCAR	National Center for Atmospheric Research
NGA	National Geospatial Intelligence Agency
NIMA	National Imagery and Mapping Agency
NIST	National Institute of Standards and Technology
NMC	National Meteorological Center
NORAD	North American Aerospace Defense Command
NRL	Naval Research Laboratory
NSWC	Naval Surface Warfare Center
NTP	Network Time Protocol
OD	Orbit Determination
OSU	Ohio State University
PEF	Pseudo Earth Fixed
PPT3	Position, Partials, and Time Version 3
RMS	Root Mean Square
SALT	Semi-analytical Liu theory
SAO	Smithsonian Astrophysical Observatory
SI	Système International d'Unités (International System of Units)
SGP	Simplified General Perturbations
SGP4	Simplified General Perturbations Version 4
SLR	Satellite Laser Ranging
SRP	Solar Radiation Pressure
SSC	Space Surveillance Center
STK	Satellite Tool Kit
TAI	Temps Atomique International (International Atomic Time)
TCB	Temps-Coordonnée Barycentrique (Barycentric Coordinate Time)
TCG	Temps-Coordonnée Géocentrique (Geocentric Coordinate Time)
TDB	Temps Dynamique Barycentrique (Barycentric Dynamical Time)
TDT	Temps Dynamique Terrestre (Terrestrial Dynamical Time)
TEG	Texas Earth Gravity model
TEME	True Equator, Mean Equinox

TIGCM	Thermosphere Ionosphere General Circulation Model
TIO	Terrestrial Intermediate Origin
TIRS	Terrestrial Intermediate Reference System
TOD	True of Date
TT	Terrestrial Time
USNO	U.S. Naval Observatory
UCAC	USNO CCD Astrographic Catalog
USM	Universal Semianalytical Method
USSA 76	Standard Atmosphere, (USSA76)
UT	Universal Time
UT Austin	University of Texas
UT1	Universal Time One
UTC	Coordinated Universal Time
VLBI	Very Long Baseline Interferometry
WGS	World Geodetic System

4.2 Terms and Definitions

For the purposes of this document, the following terms and definitions apply.

Albedo
the reflecting power or the ratio of the light reflected to light received

Altitude (h)
height where the geoid is often used as a reference surface

Anomalies (E, M, ν)
the angles describing the position of a body in a reference frame as independent variables (see *eccentric, mean,* and *true anomalies*)

a_p
planetary amplitude of geomagnetic activity (every 3 hours)

NOTE The daily average of the a_p values is given the symbol A_p.

Apoapsis
the point of an elliptic orbit farthest from the focus occupied by the central body

Apogee
the point of a geocentric elliptic orbit that is at the greatest distance from the center of the Earth

Apsidal Line
the line connecting the periapsis with the apoapsis

Apsis
the point on a conic section where the length of the radial vector is maximum or minimum

Argument of Latitude (u)
the angle between the line of nodes and the radial vector of an orbiting particle, regarded as positive when measured from the ascending node to the radial vector in the direction of motion of the satellite; also, the sum of the argument of periapsis and the true anomaly

Argument of Periapsis (ω)
the angle between the line of nodes and the periapsidal line measured in the direction of motion

Ascending Node
the point in the equatorial plane, or in general, in the reference plane, where the body passes from south to north of the reference plane (see *right ascension of the ascending node*)

Astrodynamics
branch of space science and engineering dealing with the motion of artificial bodies in space (see also *celestial mechanics*)

Astronomical Unit *(AU)*
the semimajor axis of Earth's orbit; equal to the radius of a circular orbit in which a body of negligible mass, free of perturbations, revolves around the Sun in 2π/k days, where k is the Gaussian gravitational constant

Atomic Clock
an electronic resonating device used for time-keeping that derives its basic frequency standard from the electromagnetic radiation associated with the transition between a specific pair of atomic energy levels

Autumnal Equinox
the direction and date when the fictitious Sun crosses the equatorial plane from North to South in its apparent motion along the ecliptic

Auxiliary Circle
a circle circumscribing an elliptic orbit and having a radius equal to the semimajor axis of the orbit

Azimuth *(Az)*
the angle measured clockwise from North along the horizon of the celestial sphere to the great circle passing through the point of interest and the zenith

Ballistic Coefficient *(BC)*
a parameter used to model the satellite characteristics that influence the perturbative acceleration due to drag on a satellite,

NOTE 1 $\mathrm{BC} = C_D A / m$
where
- C_D is the drag coefficient,
- A is the effective frontal area, and
- m is the mass of the body.

NOTE 2 Recommended units are m2/kg.

Barycenter
the center of mass of a system of bodies

Barycentric Dynamical Time *(TDB)*
a time scale which has the same rate and epoch as Terrestrial Time and is used as the time argument of ephemerides

NOTE It is called T_{eph} in some cases.

Celestial Ephemeris Pole *(CEP)*
the reference pole for nutation and polar motion

Celestial Equator
the projection of the Earth's equator on the celestial sphere

Celestial Intermediate Pole *(CIP)*
the reference pole of the IAU 2000A precession-nutation model

NOTE The motions of the CIP are those of the Tisserand mean axis of the Earth with periods greater than two days.

Celestial Mechanics
branch of dynamical astronomy dealing with the motion and dynamics of natural bodies in space

Celestial Sphere
a hypothetical sphere of indefinitely large radius upon which celestial bodies are projected. It is centered on the origin (e.g., Earth's center or Sun's center) of the associated spherical coordinate system

Central Body
the primary body that is being orbited

Centrifugal Force
the apparent force in a rotating system, deflecting masses radially outward from the axis of rotation

NOTE It is equal and opposite to the centripetal force that acts to keep a particle stationary in the rotating frame.

Conic Section
the intersection of a cone and a plane

NOTE 1 The four intersections related to Keplerian (two-body) orbital motion are the circle, the ellipse, the hyperbola, and the parabola.

NOTE 2 Two degenerate types of theoretical interest are a line and a point.

Coordinated Universal Time *(UTC)*
the time available from broadcast time signals, and the basis of civil times in the world

NOTE It differs from International Atomic Time (TAI) by an integral number of seconds and is maintained within ±0.90 second of UT1 through the addition of leap seconds.

Coriolis Force
the apparent force attributed to a body in motion with respect to a rotating coordinate system

NOTE Coriolis force is experienced only by bodies with nonzero velocity in the rotating frame, unlike centrifugal force, which is independent of motion.

Covariance
a measurement of the tendency of two random variables to vary together

Cowell's Method
a process of special perturbations in which the total acceleration of an orbiting body is numerically integrated

Cross-section
the intersection of a three-dimensional object with a plane perpendicular to a particular reference direction

EXAMPLE The velocity direction.

Cross-track
see Sec. 5.5.8 for a discussion of satellite based coordinate systems

Date
day and time of day

Day (d)
an interval of time based on one rotation of the Earth

NOTE It is often subdivided into 86400 seconds, although the UTC day may be 86399, 86400, or 86401 SI seconds.

Declination (δ)
the angle between the celestial equator and a radius vector, regarded as positive when measured north from the celestial equator

Descending Node
the point in the equatorial plane, or in general, in the reference plane, where the body passes from north to south of the reference plane

Differential Correction
a process for correcting an initial estimate

NOTE It is used as an alternate name for orbit determination, estimation, least squares, and sequential batch operations.

Drag (D)
the retarding effect of the atmosphere on the motion of a body

Dynamical Astronomy
branch of astronomy dealing with the motion and dynamics of celestial bodies

NOTE It includes celestial mechanics, stellar dynamics, motion of binary stars, and positional astronomy.

Dynamical Time
the independent argument of dynamical theories and ephemerides (see *barycentric dynamical time* and *terrestrial time)*

Earth Rotation Angle
angle between the TIO and CIO measured along the intermediate equator of the Celestial Intermediate Pole

Eccentric Anomaly (E)
the angle at the center of an elliptic orbit, formed by the apsidal line and the radius vector drawn from the center to the point on the circumscribing auxiliary circle from which a perpendicular to the apsidal line will intersect the orbit and locate the body

Eccentricity (e)
term defining the specific shape of a conic section

NOTE 1 It is the ratio of the distance of a point on a conic section from the focus to the distance from the directrix.

NOTE 2 For ellipses — conic sections with an eccentricity of less than one—it is also the distance from the center of an ellipse to the focus divided by the length of the semimajor axis.

Eclipse
the obscuration of a celestial body caused by its passage through the shadow of another body

Ecliptic
the mean plane of Earth's orbit around the Sun

Elevation *(El)*
the angular distance of a point of interest above (+) or below (-) the horizon measured along the great circle passing through the point and the zenith

Ephemeris Time *(ET)*
the time scale used 1960-1984 as the independent variable in gravitational theories of the solar system later; subsequently replaced by dynamical time

Ephemeris
a table of locations (and rates) of natural or artificial bodies versus time

NOTE Its plural is "ephemerides", meaning multiple tables.

Epoch (t_0 or T_0)
a date that is usually prescribed as fixed and nonchanging, such as the date of the reference system to which celestial coordinates are referred, or a specific date to which an object's location has been referenced

Equator
the intersection of the surface of a body with the plane passing through the center of mass of the body, perpendicular to the axis of rotation

Equinox of Date
the instantaneous location of the equinox at a date, where the date may be changing according to a set of available observations or ephemeris

Equinox of Epoch
the instantaneous location of the equinox at an epoch that is usually prescribed as fixed or nonchanging

Extreme Ultraviolet Radiation *(EUV)*
high frequency ultraviolet radiation from the Sun that may have the most substantive influence on the density of the upper atmosphere of the Earth

Fictitious Mean Sun
an imaginary body having nearly uniform angular velocity in the plane of the Earth's equator; essentially the name of a mathematical formula that serves as the basis for mean solar time

Fiducial Direction
defining direction for a coordinate system

Flattening (f)
a measure of deviation of an ellipsoid from a spherical shape

NOTE 1 f = (a-b)/a

where

— a is the equatorial radius and

— b is the polar radius.

NOTE 2 Also known as oblateness, it is applied to a body generated by the rotation of an ellipse about its minor axis.

Fifth Fundamental Catalog *(FK5)*
a catalog of star positions prepared by the Astronomisches Rechen Institut in Germany and the basis for the IAU Reference System for J2000.0 from 1984-1998

Gaussian Gravitational Constant (k)
the gravitational constant expressed in terms of solar system units

NOTE It allows the motion of the planets to be accurately described without an exact knowledge of the scale of the solar system or the mass of the Sun and the planets.

General Perturbation Method *(GP)*
analytical or semianalytical solution of the differential equations describing a perturbed orbit

Geocenter ($\oplus$)
the center of mass of the Earth

Geocentric Coordinates
the latitude and longitude of a point on Earth measured as angles subtended at the center of Earth (see *latitude (geocentric)* and *longitude (geocentric))*

Geoid
an equipotential surface of the Earth that most closely approximates the mean sea level of the open ocean

Geosynchronous Satellite
a satellite whose orbital period is one sidereal day

Gravitational Constant (G)
the constant of proportionality in Newton's Universal law of gravitation

Gravitational Parameter ($\mu = GM$)
the product of the mass of central body and the universal gravitational constant

Gravitational Potential (U or V)
a function whose gradient yields the gravitational force

Great Circle
the path of intersection, circumscribing a spherical surface, when a plane intersects the sphere's center

Great Circle Path
a geodesic (shortest distance between two points) along a sphere

Greenwich Apparent Sidereal Time *(GAST)*
Greenwich mean sidereal time corrected for the shift in the position of the mean equinox due to nutation

Greenwich Mean Sidereal Time *(GMST)*
the hour angle of the Greenwich meridian relative to the mean equinox

Greenwich Meridian
the meridian from which terrestrial longitude is measured, passing through the Royal Observatory in Greenwich, England

Height *(h)*
the distance measured above a reference surface along a perpendicular to that surface

Heliocentric
sun-centered

Horizon
a plane normal to the zenith, passing through the observer or object of interest; also, the limb of a nearby celestial body

Hour Angle *(HA)*
angular distance on the celestial sphere measured westward along the celestial equator from the meridian to the hour circle that passes through a celestial object

Hour Circle
a great circle on the celestial sphere that passes through the celestial poles and is, therefore, perpendicular to the celestial equator

Inclination
the angle between the orbital angular momentum vector and the equator, or XY plane

Inertial Reference Frame
an unaccelerated and nonrotating reference frame in which Newton's Laws are valid

NOTE The inertial qualifier is sometimes used with other quantities to indicate unaccelerated and nonrotating behavior, such as the inertial ecliptic.

International Celestial Reference Frame *(ICRF)*
a quasi-inertial reference frame defined based on the radio positions of 212 extragalactic sources distributed over the entire sky

NOTE The resulting International Celestial Reference Frame has been adopted by the International Astronomical Union as the fundamental celestial reference frame, replacing the FK5 optical frame as of 1998 January 1.

International Celestial Reference System *(ICRS)*
the set of prescriptions and conventions together with the modeling required to define at any time a triad of axes

NOTE 1 The System is realized by VLBI estimates of equatorial coordinates of a set of extragalactic compact radio sources, the International Celestial Reference Frame (ICRF).

NOTE 2 The ICRS can be related to the International Terrestrial Reference System (ITRS) by use of precession-nutation theory and corrected by Earth-orientation parameters.

International Terrestrial Reference Frame *(ITRF)*
the International Terrestrial Reference Frame is a set of points having three-dimensional Cartesian coordinates which realize an ideal reference system, the International Terrestrial Reference System (ITRS), as defined by the IUGG resolution No. 2 adopted in Vienna, 1991

International Terrestrial Reference System *(ITRS)*
a set of prescriptions and conventions, together with the modeling, required to define origin, scale, orientation and time evolution of a Conventional Terrestrial Reference System (CTRS)

NOTE The ITRS is an ideal reference system, as defined by the IUGG resolution No. 2 adopted in Vienna, 1991. The system is realised by the International Terrestrial Reference Frame (ITRF) based upon estimated coordinates and velocities of a set of stations observed by VLBI, LLR, GPS, SLR, and DORIS.

International Atomic Time *(TAI)*
the time scale of the Bureau International des Poids et Mesures of atomic time standards

NOTE The unit is the SI second.

In-track
see Section 5.5.8 for a discussion of satellite based coordinate systems

Invariable Plane
the plane containing the center of mass of the solar system and perpendicular to the angular momentum vector of the solar system

NOTE Sometimes known as the Laplacian plane.

J2000.0
standard epoch of the FK5 coordinate system (12^h TDB 2000 January 1)

NOTE JD = 2451545.0

Julian Date *(JD)*
the date measured as an interval since Greenwich noon, 1 January 4713 BC

K_p
planetary index of geomagnetic data

Laplacian Plane
for a system of satellites, the fixed plane relative to which the vector sum of the disturbing forces has no orthogonal component (see also *Invariable Plane*)

Latitude
the angular distance north (positive) or south (negative) of the primary great circle or plane, as on the Earth or the celestial sphere

Astronomical: the angle measured from the equatorial plane to the direction of gravity (plumb line) (ϕ_{as})

Celestial: the angle on the celestial sphere measured from the ecliptic plane to the radius vector from the observer to the point of interest (ϕ_{ecl})

Geocentric: the angle measured from the equatorial plane to a line to Earth's center of mass (ϕ_{gc})

Geodetic: the angle measured from the equatorial plane to the local normal to the reference spheroid (ϕ_{gd})

Leap Seconds
the one-second interval added or subtracted from the end of the UTC month to maintain UTC to within ±0.90 seconds of UT1

Line of Nodes ($\overline{n}$)
the line connecting the ascending and descending nodes

Local Horizon
apparent horizon tangent to the position vector at a particular location

NOTE This can also be applied to satellite positions.

Longitude
the angular distance along the primary great circle measured eastward from the reference meridian, as on Earth or the celestial sphere

Astronomical: the angle measured from the plane of the Greenwich meridian to the plane perpendicular to the equatorial plane that contains the direction of gravity (plumb line) (Λ)

Celestial: the angle on the celestial sphere measured eastward along the ecliptic from the dynamical equinox to the great circle passing through the point of interest and the ecliptic poles (λ)

Terrestrial: the angle measured from the plane of the Greenwich meridian to the plane through the polar axis and the radius vector from Earth's center of mass (λ_E)

Longitude of the Ascending Node
the angle measured eastward along the Earth's equator from the Greenwich meridian to the position of the ascending node with respect to the equator

Longitude of Perigee (ϖ)
the sum of the angles of the longitude of the ascending node and the argument of perigee

NOTE The general terminology is longitude of periapsis and the angle may be the addition of angles in separate planes if the orbit is inclined.

Low-Earth Orbit *(LEO)*
orbit below the near-Earth radiation belt (altitude approximately 3000 km)

NOTE 3000 km is an arbitrary point of differentiation.

Mean Anomaly *(M)*
the product of the mean motion and the interval of time since periapsis passage

NOTE An angular measure with a period equal to the period of the orbit.

Mean Elements
elements of an adopted reference orbit that approximates the actual perturbed orbit

Mean Equator and Equinox
the celestial reference system determined by ignoring small short-period variations in the motion of the celestial equator

NOTE 1 Mean Equator of date is defined as a specific instance of the secular precession of the Earth's rotational axis about the North ecliptic pole.

NOTE 2 Mean equinox of date is the intersection of the mean ecliptic and mean equatorial planes.

Mean Motion *(n)*
the value of a constant angular velocity required for a body to complete one revolution within one orbit period

Mean Sea Level
average level of the oceans determined through worldwide tide gauges and satellite observations

Meridian
the great circle between the North and South poles (terrestrial and celestial) which passes through the point directly above the observer

Modified Julian Date *(MJD)*
the Julian date minus 2400000.5

Nadir
the point on the celestial sphere diametrically opposed to the zenith

Newton's Universal Law of Gravitation
the gravitational force between bodies is proportional to the product of their masses and inversely proportional to the square of the distance between them

Node
either of the points at which the orbit intersects the reference plane

Nutation
the short-period oscillation of the pole of a gravitationally perturbed rotating body

NOTE 1 The oscillation occurs perpendicular to a central axis.

NOTE 2 For Earth rotation, it consists of the two components, nutation in celestial longitude ($\Delta\psi$) and nutation in obliquity ($\Delta\varepsilon$).

Oblateness
see *flattening*

Obliquity (ε)
the angle between the mean equatorial and orbital planes

Orbit
the trajectory of a body subject to the gravitational force of a neighboring body or bodies

Orbit Determination
process of finding the orbit of a satellite by processing measurements of the object

Orbital Elements
a selected set of six variables describing the orbit

NOTE The classical orbital elements are:

- a (semimajor axis),
- e (eccentricity),
- i (inclination),
- Ω (right ascension of the ascending node),
- ω (argument of periapsis), and
- M_0 (mean anomaly at epoch).

Penumbra
the near or partial shadow cast by an eclipsing body (see also *umbra*)

Periapsis
the point of an orbit closest to the focus occupied by the attracting body

Perigee
the point of a geocentric orbit closest to the center of Earth

Period *(P,T)*
the interval of time required to complete one revolution in an orbit or one cycle of a periodic phenomenon, such as a cycle of phases

Periodic Motion
a motion which repeats itself in equal intervals of time

Periodic Variations
variations due to perturbations which can be expressed as periodic functions

Phase Space
a mathematical space with one point for every possible state of the system, having as many dimensions as there are degrees of freedom in the system

Polar Motion
the irregularly varying motion of Earth's pole of rotation with respect to Earth's crust

Precession
the uniformly progressing motion of the mean pole of rotation with respect to the celestial sphere

Propagator
a computational process predicting the state of a dynamical system at a time of interest based on a set of initial conditions

Proper Motion
the projection on the celestial sphere of the motion of a star relative to the solar system

Radial
see Section 5.5.8 for a discussion of satellite based coordinate systems

Radiation Pressure (p_{SR})
the pressure acting on a surface exposed to incident electromagnetic radiation caused by the momentum transferred to the surface by the absorption and/or reflection of the radiation

Random Errors
those errors that can be described only statistically; errors arising from events whose causes or specific times of occurrences cannot be explicitly predicted

Reference Orbit
an orbit that is used as a baseline for comparison

Reflectivity
measure of the amount of radiation that is not absorbed by an object

Revolution
one complete orbit around the central body

Right Ascension (α)
the angle between the vernal equinox and the projection of the radius vector on the equatorial plane, regarded as positive when measured eastward from the vernal equinox

Second
International System of Units (SI): the duration of 9192631770 oscillations of the radiation corresponding to the transition between two hyperfine levels of the ground state of the cesium-133 atom

Sectoral Harmonic Coefficients (J_{mm}, C_{mm}, S_{mm})
coefficients of the terms in the Legendre series expansion of the gravitational potential that depend only on the longitude

NOTE The degree equals the order.

Secular
constant change over time

Selenocentric
referred to the center of mass of the moon

Semianalytical Techniques
propagation techniques that combine analytical and numerical methods

Semimajor Axis (a)
the distance from the center of an ellipse or hyperbola to an apsis

Sidereal Time
a measure of time defined by Earth's diurnal rotation with respect to the vernal equinox

Solar Flux
solar radiation emanating from the Sun and influencing satellite in the drag regime

Solar Radiation Pressure
force exerted on a satellite from the particles originating from the Sun

Special Perturbation Method *(SP)*
numerical integration of the differential equations describing perturbed motion

Spherical Harmonics
mathematical representation of a complex surface or shape

NOTE 1 The Earth's gravity field is modeled through this technique. These are the coefficients in the associated Legendre series expansion of the gravitational potential (J_{nm}, C_{nm}, S_{nm}).

NOTE 2 See also *zonal, sectoral,* and *tesseral harmonic coefficients.*

Spheroid
an oblate ellipsoid which closely approximates the mean sea level figure of Earth or the geoid.

NOTE A "spheroid" is an ellipsoid in which two of the three axes are equal; an "oblate spheroid" has the rotation of an ellipse about the minor axis; and, a "prolate spheroid" is the rotation of an ellipse about the major axis.

Standard Atmosphere
a static model of atmospheric density, pressure and temperature as a function of altitude that is accepted as a standard and used as a model to portray average values for these quantities

Standard Epoch
a date that specifies the reference system to which celestial coordinates are referred

State Vector
any set of parameters (e.g., position and velocity) which uniquely define an orbit at a selected epoch

Stationkeeping
the procedure necessary to maintain position (that is, either vehicle attitude or vehicle spatial position) after the space vehicle has been established on orbit

Stellar Dynamics
branch of astronomy dealing with the motion and dynamics of stars and stellar systems

Sun-synchronous Orbit
an orbit that precesses about the central body at the same mean angular rate as the central body orbits the Sun

Tangential
See Section 5.5.8 for a discussion of satellite based coordinate systems

Terrestrial Time *(TT)*
the independent argument for apparent geocentric ephemerides

NOTE 1 The unit is 86,400 SI seconds at mean sea level and TT = TAI + 32.184 s.

NOTE 2 Previously known as *terrestrial dynamic time*.

Terrestrial Longitude (λ_E)

the angle between the Greenwich meridian and the meridian of a geographic location, measured eastward along Earth's equator

Tesseral Harmonic Coefficients (J_{nm}, C_{nm}, S_{nm})

coefficients of the terms in the Legendre series expansion of the gravitational potential which depend on the latitude and longitude

NOTE Degree and order are not equal, and order is greater than zero.

Topocentric

referenced to a point on the surface of Earth

Tracking

the process of a sensor following a satellite while collecting observations of the satellite's relative position and velocity

Trajectory

the path describing the motion of an object as a function of time

Transverse

See Section 5.5.8 for a discussion of satellite based coordinate systems

Tropical Year

the period of time for the Sun to advance 360 degrees in longitude

True Anomaly (ν)

the angle at the focus (nearest the periapsis) measured from the apsidal line directed toward the periapsis to the radius vector of the orbiting body in the direction of motion

True Equator and Equinox

the celestial coordinate system determined by the instantaneous positions of the celestial equator and ecliptic

NOTE The Equator is often given an "of date" qualifier to specify the exact orientation.

True Equator and Mean Equinox

coordinate system formed by the projection of the mean equinox of date onto the true equator of date

NOTE This system is used exclusively with the SGP4 analytical propagation technique.

Two-body Motion

General: the dynamics of two gravitationally interacting point masses

NOTE Two-body dynamics refers to the situation where an orbit is propagated considering only the two bodies of interest, the satellite and the central body. Two-body orbit is used when referring to the orbit generated using only two-body dynamics. The two-body problem or model refers to the situation where only two bodies are present in the solution of propagating a satellite orbit.

Restricted: the modification of the general problem to the case when the mass of one of the bodies is much smaller than the other so that it does not influence the motion of the larger body

Umbra

the darkest part of the shadow cast by an eclipsing body in which all light from the source has been obscured

Universal Time *(UT)*
a measure of Earth-rotation angle, whose rate is based on the mean diurnal motion of the Sun, and is the basis of civil timekeeping

NOTE Coordinated Universal Time (UTC) is a particular form of Universal Time based on the SI second (see *Coordinated Universal Time (UTC)* Section 5).

Universal Time One *(UT1)*
a time scale based on rotational angle of the Earth's determined from astronomical observations

Variation of Parameters
perturbation technique in which the constants of the two-body orbit or of the analytical solution of an approximation to an actual problem are allowed to vary

Vernal Equinox
the direction where and the date when the Sun crosses the equatorial plane from South to North in its apparent motion along the ecliptic (its apparent longitude is zero); the ascending node of the ecliptic on the uniformly moving mean equatorial plane

Vertical
Astronomical: line parallel to the direction of gravity at the observation point (i.e., line normal to the geoid)

Geodetic: line normal to the surface of the reference spheroid and passing through the observation point

Year
time to complete one revolution of the Earth around the Sun

Anomalistic: the mean interval between successive passages of the Earth through perihelion

Tropical: the period of one complete revolution of the mean longitude of the sun with respect to the dynamical equinox

Zenith Distance
angle measured along the great circle on the celestial sphere from the zenith to the celestial object

Zenith (z)
for any given point, the intersection on the celestial sphere of the local vertical direction, which points opposite to the gravitational force at that point

Zonal Harmonic Coefficients (J_n)
The terms in the associated Legendre series expansion of the gravitational potential which depend only on the latitude

NOTE The order equals zero.

5 Units, Precision, Time, Constants, and Coordinates

The field of astrodynamics has a rich legacy of astronautical and astronomical terminology and practices. To produce effectively precise results, numerous definitions and specifications are required to operate within a framework of self-consistent coordinate and time systems. This section introduces some of these concepts, provides references that define some standard approaches, and recommends practices that aid in the sharing of data between organizations performing analyses.

5.1 Units

Standard units simplify the meaningful exchange of numeric data. The need is illustrated by numerous units historically used for the exchange of the orbital element semimajor axis: for example, kilometers, meters, statute miles, nautical miles, feet, Earth radii, or astronomical units. Another example, consistent

with ancient astronomical practice, is that angular measurements may be expressed in degrees of arc, arc minutes, arc seconds, and fractions thereof, whereas computing machinery will usually require angles expressed in radians.

Units of length, such as the SI meter, are defined in terms of the speed of light c and time interval Δt, that is, distance $d \equiv c\Delta t$. As the quantity Gm/c^2 has units of length, and assuming the values for c and the gravitational constant G remain the same in every frame of reference, the adopted masses of gravitating bodies (m) must also be compatible with the adopted units of time and length within the context of relativity.

5.1.1 Presentation of Units

Use of the International System of Units (SI) is recommended. Units should be described within the data itself, or via supplementary documentation, using conventional names or abbreviations, as recommended by National Institute of Standards (NIST). A few common exceptions exist, such as the use of angular degrees instead of radians, or "sec" instead of "s" as an alternate abbreviation for "seconds." The retention of full precision (significant digits) is necessary when converting or rescaling units.

Canonical units are units normalized by specific parameters and constants. Canonical units are especially useful in celestial mechanics for academic developments and manual calculations, because many parameters of the equation normalize to unity to provide for simplified mathematical derivations and faster numerical evaluation. Excepting situations where they may be mandated by a specialized theory, the routine use of canonical units is no longer recommended in high-accuracy systems. The reason is that the absolute scaling of canonical units changes as system parameters or constants incrementally improve with time, resulting in unnecessary operational complications and incompatibilities later. Also, because some mathematical terms almost always appear in tandem, it is often unclear in software what specific variables may have been normalized, e.g., Gm versus m. Keeping track of proper units and discovering programming errors can be more difficult, because many canonical variables are unitless or lack named units.

5.1.2 Recommended Practice

1) Use SI units exclusively, or use units that are approved for use with SI, such as angular degrees. Canonical units cannot be generally recommended.

2) In all cases of numerical presentation, scale units and frames of reference should be clearly identified.

5.2 Precision, Accuracy, and Uncertainty

The concepts of accuracy and precision are easily confused. Accuracy describes how close an experimental outcome is to the true value, whereas precision describes mutual agreement amongst a population of experimental outcomes. High precision tends to infer a lack of random errors, and is related to the repeatability or reproducibility of a result, regardless of where truth is, while high accuracy implies a lack of systematic errors or bias relative to truth. As a result, precision can refer to the exactness of presentation, i.e., the number of significant digits to be retained from a result. Accuracy is more closely related to the error uncertainty of a single experimental outcome. Deviation is the difference of an actual outcome from an expected or desired outcome. Error is deviation from the truth outcome.

Often, astrodynamic systems are assessed by their ability to reproduce an expected result given specific inputs, such as a series of test cases advocated in this standard. *These types of tests tend to gauge precision rather than accuracy*. Claims of accuracy usually require some detached representation of truth, and, generally, describe a single outcome rather than a population. For example, as it pertains to measurement of atomic time and time interval, "precise time and time keeping" is the terminology most often encountered and accepted because atomic time is maintained according to the *relative* agreement of many atomic resonators with respect to each other, rather than an independent time scale of greater

uniformity. Likewise, precision orbit determination refers to the use of the most highly detailed orbital models that reduce random errors; however, the quantity and quality of contributing observations actually determine the accuracy of the individual outcomes.

Testing administrators and software developers should remain aware of what constitutes a significant loss of precision in their own computing environments, due to the limitations of finite-word arithmetic in their computing machinery. The loss of numerical significance in initial conditions or nodes of interpolation can adversely affect resultant propagated values, so it is good operating practice to avoid approximations and numerical round-off. Exact constants (e.g., an adopted value of GM) should remain exact, and derived constants (e.g., the value of π) should be maintained to full computing precision, to preserve computing precision and maintain reproducibility.

5.2.1 Expression of Uncertainty

Expression of uncertainty should generally conform to the guidelines by Taylor and Kuyatt (1994). The most common expression of single-value uncertainty is the square root of the variance (σ^2), which is called the standard deviation, σ. It is not the only measure of distributional spread, but it is most convenient as a standard because (a) the variances of estimated parameters may be conveniently obtained from their theoretical relationship with respect to the variances of the observations (or, observation deviations), and (b) its sample estimator is simple and not specific to any particular distributional shape, providing that the sample is not too small. Likewise, if more than one parameter is estimated and the theoretical parameter deviations are (linearly) related, then the parameter covariance provides a measure of that relation as well.

The textbook estimator for sample variance, s^2, is a standard scale measure for a (complete and uncensored) population of deviations e, usually calculated as the sum of the square of the deviations

$$\mathrm{Var}[e] = \sigma^2 = \int_{-\infty}^{\infty} (e - \mu_e)^2 \, f(e)\, de \approx \frac{1}{n-1} \sum_{i=1}^{n} (e_i - \hat{e})^2 \tag{1}$$

Where μ_e is the true population mean, and $\hat{e}$ is the sample mean. s^2 is sensitive to changes in the extremities of a sample, and for this reason, extreme or outlying deviations are often rejected prior to use. This practice may be questionable but nonetheless necessary to achieve estimator robustness.

Unfortunately, uncertainty estimates tend to be slightly optimistic (biased too small) when outliers have been removed using a probabilistic criterion such as *Wright's Rejection Procedure* (i.e., reject all e_i beyond $\hat{e} \pm 3\sigma$). Where data seem suspect, it is recommended that technical expertise instead be used to identify and eliminate all deviations representing physically impossible conditions. If suspect (highly improbable, yet not impossible) deviations remain, it often suffices to replace the offending deviation(s) with the largest sample deviation that is not seriously suspect, a technique known as *Winsorization*. Of course, the subjective criteria that define "highly improbable" or "not seriously suspect" are part of the (co)variance estimator, so the adopted criteria should be presented with the resultant (co)variance estimates whenever outlying observations have been identified and accommodated.

An important question to understand is whether the sample variance of an estimated parameter is a measure of parameter precision, or parameter accuracy. When a nearly optimal estimator is used, the result is usually considered to be the "best" estimate of truth available given the sample data, so the parameter variance is considered an expression of accuracy. However, this interpretation is only justified if knowledge about the distribution of errors in the underlying mathematical model(s), and the observational data, are completely expressed. In practice, observation errors may be correlated in ways that are unknown or not easily modeled, and that lack of knowledge may further result in biased (co)variance estimates. Small sample sizes also increase (co)variance uncertainty. Unless there is compelling (preferably independent) methods of verification, it is often reasonable to question the validity

of parameter (co)variances as estimates of parameter accuracy, and consider them measures of precision.

5.2.2 Recommended Practice

1) Preserve numerical precision in each arithmetic operation, understanding the fundamental limitations of computing machinery.

2) Avoid approximations for computational convenience if possible.

3) When presenting results, distinguish whether uncertainty measures are describing accuracy (probability of bias of an individual outcome relative to truth) or precision (random fluctuation of the ensemble or population).

4) Use conventional measures of uncertainty.

5) Declare the criteria used to define outliers, and report which method(s) (rejection, Winsorization) were used to accommodate them.

6) Verify accuracy estimates wherever possible.

5.3 Time Systems

The standard unit of time interval most useful for scientific, practical, and legal purposes is the System International (SI) second, defined as 9192631770 periods of the radiation emitted from cesium 133 at 0 K. The SI definition of time interval is proper under general relativity. Proper time is simply the time kept by a clock fixed with the observer, along whatever trajectory and gravity field the observer is located. This is in contrast to coordinate time, which is one of the four independent variables used to characterize a locally inertial reference frame in general relativity (i.e., its value assigns chronological order to sequentially occurring events within the coordinate frame). In general, coordinate time will not be kept by any physically real clock; rather, it is the independent argument of the equations of motion of bodies in its frame.

When referencing observations to a time scale that is not coordinate time, renormalization of the time interval could carry over into units of length and gravitational mass. Partly for these reasons, there are a number of relativistic time scales with associated lengths and masses; and it becomes necessary to address the differences between them when seeking high precision.

International Atomic Time (TAI) is a physical time scale, is affected by the Earth's gravitational and rotational potential (the geoid), and can be deduced from a weighted average of various international frequency standards. Relative weighting is based on the historical stability of the individual standards. TAI is maintained by the Bureau International des Poids et Mesures (BIPM) and is a reference basis of other time scales. Global Positioning System (GPS) Time is the reference time scale of the GPS navigation system; ideally, it is steered to lag TAI by nineteen (19) seconds (GPS Time = TAI – 19 s).

Universal Time (UT1) is the angular measure of Earth rotation inferred from observations of extra-galactic radio sources. The Earth-rotation angle provides a sequentially increasing continuum that is everlasting and widely apparent, and serves as the astronomical basis of civil time of day. Earth rotation is only regular to about one part in ten-million per day. Being an observed quantity, it is measured and predicted by the International Earth Rotation and Reference System Service (IERS) and distributed as a differential quantity relative to atomic UTC, ($\Delta UT1 = UT1 - UTC$). Specifically, Universal Time indicates how the Earth's terrestrial reference frame is oriented relative to the celestial reference frame used by satellites.

Coordinated Universal Time (UTC) is a civil broadcast standard governed by ITU-R Recommendation 460, providing both astronomical time of day and atomic-time interval. UTC is atomic time kept within ± 0.9 s of UT1 by the introduction of so-called leap seconds, and for this reason, is a legally recognized proxy for mean solar time in most countries. UTC is always offset from TAI by an integer number of

seconds, and is thus a carrier of precision frequency and time interval for broadcast standards based on the SI second. Although atomic UTC is completely sequential and coherent (continuous) within the prescriptions of the UTC standard, the length of UTC day is non-uniform, owing to the possible addition or subtraction of an intercalary leap second at the end of the UTC month, usually June or December. DUT1 is a prediction of the difference between UT1 and UTC in tenths of a second and is available in advance.

Terrestrial Time (TT) is a theoretically ideal time at the Earth. A practical realization is TT = TAI + 32.184 s. $\Delta T = TT - UT1$ is the difference between this ideal time scale and the actual rotation of the Earth. TT was formerly known as Terrestrial Dynamical Time (TDT), a successor of pre-relativistic Ephemeris Time (ET).

Geocentric Coordinate Time (TCG) is a coordinate time for the geocenter. Its rate equals that of a theoretical clock co-moving with the center of the Earth, yet unaffected by Earth-moon gravity or rotation. It is related to TT by (using the Julian Date JD)

$$TCG = TT + L_G \times (JD - 2443144.5) \times 86400 \text{ s} \tag{2}$$

where $L_G \equiv 6.969290134 \times 10^{-10}$, a scale constant accounting for the Earth's gravitational and rotational potential affecting the rate of clocks. IAU Resolution B1.9 (2000) recommends L_G as a defining constant based on the best estimate at the time of adoption, so the relationship between TCG and TT does not change should there be future improvement in knowledge of the Earth's gravitational potential.

Barycentric Coordinate Time (TCB) is the coordinate time for the barycenter of the solar system. It differs from TCG by both secular and periodic terms. The complicated relationships between TT, TCG, and TCB are based on relativistic Lorentz transformations, although, an approximation of $(TCB - TCG)$ can be expressed as

$$(TCB - TCG) = \frac{L_C \times (TT - TT_0) + P(TT) - P(TT_0)}{(1 - L_B)} + \frac{\mathbf{v}_e \cdot (\mathbf{x} - \mathbf{x}_e)}{c^2} \tag{3}$$

Here, TT_0 corresponds to JD 2443144.5 (1977 January 1, 0 h) TAI, and the values of L_C and L_B are standard constants. Periodic terms, denoted by P(TT), have a maximum amplitude of around 1.6 ms and can be evaluated by the "FB" analytical model (Fairhead and Bretagnon, 1990). Alternatively, a numerical time ephemeris may provide $P(TT) - P(TT_0)$, such as TE405, which provides values with an accuracy of 0.1 ns from 1600 to 2200. Irwin (2003) has shown that TE405 and the 2001 version of the FB model differ by less than 15 ns over the years 1600 to 2200 and by only a few ns over several decades around the present time.[11] The HF2002 series has been fit to TE405 over the years 1600–2200 to provide $\{L_C \times (TT - TT_0) + P(TT) - P(TT_0)\}$ as a function of TT (Harada and Fukushima, 2003). This fit differs from TE405 by less than 3 ns over the years 1600–2200 with a residual RMS of 0.5 ns.[1] In theory, units of length and mass do not change between the TCB and TCG coordinate origins.

Barycentric Dynamical Time (TDB) was originally intended to serve as an independent argument of barycentric ephemerides and equations of motion and was defined by an IAU 1976 resolution to differ from TT only by periodic terms (Muller and Jappel, 1977). Later, it became clear that this condition cannot be rigorously satisfied. The IAU 2006 resolutions clarified TDB to be linearly related to TCB

$$TDB = TCB - L_B \times (JD_{TCB} - T_0) \times 86400 + TDB_0 \tag{4}$$

where $T_0 = 2443144.5003725$, $L_B = 1.550519768 \times 10^{-8}$, and $TDB_0 = 6.55 \times 10^{-5}$ s are defining constants. Operationally, each ephemeris realization defines its own version of TDB; the linear drift between TDB

[1] In the computation of (TCB – TCG), TT is used as a time argument, while the actual argument of the different realizations is T_{eph}. The resulting error in (TCB – TCG) is, at most, roughly 20 ps.

and TCB is usually chosen so that the rate of TDB matches TT as closely as possible for the time span covered by the particular ephemeris. The above equation is expected to represent the ephemeris particular expression very closely. TDB is sometimes designated as Barycentric Ephemeris Time (T_{eph}) when used as the time scale of the JPL Development Ephemerides (Standish, 1998). When TDB is used, the units of length and mass may differ slightly from the geocentric and barycentric reference systems, and the astronomical unit may need to be rescaled, depending upon the frame of reference and the accuracy required. TT is a commonly accepted proxy for T_{eph}, the barycentric coordinate-time scale of the JPL planetary ephemerides.

For more detailed discussion on the history and development of timing systems, see Seidelmann (ed., 1992) and Vallado (2007, Chapter 3). (See Seidelmann & Seago, 2005, for specific references.)

5.3.1 UTC Leap Seconds

A leap second is an intercalary, one-second adjustment that keeps atomic broadcast standards for time of day, UTC, within 0.9s of the rotation of the Earth time, UT1. A positive leap second begins at T23:59:60 and ends at T00:00:00 of the first UTC day of the next month.

A UTC clock is a specialized timepiece that must be able to distinguish between specific UTC days, some of which are one second longer (or shorter) than other UTC days. Most timekeepers manufactured today are arguably generic UT clocks that cannot correctly display the 60^{th} (leap) second; to compensate for a leap second, the indicated time before and during a leap second may incorrectly result in two consecutive seconds with the ambiguous labels. Such coercion often results in a mischaracterization of the UTC standard as lacking sequence or coherence (i.e., is discontinuous).

Another mischaracterization is that leap seconds can only be positive. Systems should also be operationally robust to the possibility of a negative leap second. A negative leap second is realized by omitting the last second of the UTC day. The possibility of a negative leap second precludes the use of simple yes/no logic flags indicating the presence of a leap second. To accommodate negative leap seconds, format fields in data tables or ephemerides could include space for a possible minus sign, for example. Negative leap seconds have not taken place to date and are unlikely with the current trend in the rate of rotation of the Earth.

Still another mischaracterization is that leap seconds must occur at the end of June or December only, which may be partly due to the historic wording of IERS Bulletin C leap-second announcements. Operationally, a leap second may be added to the end of any Gregorian calendar month given eight weeks notice. It is recommended that systems be able to accommodate a leap second at the end of an arbitrary UTC day. Based on the current standard of UTC, it is recommended that consumers routinely check the status of leap-second forecasts monthly.

To accurately determine atomic-time intervals using UTC, it is good practice to maintain UTC day and time of UTC day as separate and distinct quantities in software. Multivalue time tags, partly in units of day and partly in units of seconds of day, generally suffice. Canonical time units and decimal-valued representations of epoch do not promote proper conversions between UTC and TAI.

Network time protocols (NTP) and internal computer clocks have not tended to follow the above recommendation, but have historically attempted to store and manipulate system-clock dates as a single decimal or whole integer value, such as $T - T_{1970\text{-}01\text{-}01}$ in units of seconds under POSIX-standard for Unix[2]. This form of time keeping is internally consistent with UT clocks, but not UTC. Users maintaining UTC on a computer operating system should be aware of the likely limitations in operating-system clocks. For example, NTP servers may not provide the correct time step within one-second of leap-second insertion. Differential POSIX-standard time, stored as a signed 32-bit integer, will overflow in 2038. Proposals to extend functionality for real-time applications exist outside the current POSIX standards.

[2] ISO/IEC 9945-1:2003 Information Technology-Portable Operating System Interface (POSIX)-Part 1: System Application: Program Interface (API) [C Language]. Also, IEEE Standard 1003.1:2001.

When dealing with satellite ephemerides tabulated on UTC intervals of, Δt s, there is a possibility of an interval having $(\Delta t + 1)$ s containing a leap second. It is recommended that interpolation software accommodate these as unevenly-spaced nodes. If the opportunity is available, users should introduce UT1, UTC, and TAI as separate concepts in software.

5.3.2 Presentation of Time

The use of UTC is generally recommended for data exchange regarding events on or near the Earth. It is recommended that UTC time tags conform to Standard ISO 8601 (2004), which provides multiple conventions for the display of UTC time and time interval, including leap seconds. GMT is a synonym for UT, but its use is considered obsolete and is not recommended for precision applications. Greenwich Mean Time (GMT) is used for local civil time in the UK, and may be used in that context to imply UTC, or colloquially, British Summer Time (UTC plus one hour).

TT is recommended in situations where the lack of uniformity in UTC may be intolerable (such as very long-term predictive satellite ephemerides), unless an ephemeris-specific timescale is otherwise required. The use of GPS system time is not encouraged unless directly related to that navigation system or its spacecraft. (The label GPS time is generally ambiguous, for in some applications it implies UTC derived from a GPS receiver.) In all cases, the time scale in use should be clearly identified.

Users of precision time should reference the latest ITU-R Recommendation 460 that defines the UTC broadcast standard. This recommendation may be available from the ITU-R free of charge.[3] There are many descriptions of UTC in textbooks and on the Internet beyond this defining ITU-R Recommendation, but they are often incomplete, obsolete, or misleading.

5.3.3 Earth Orientation Parameter Data

Earth Orientation Parameter (EOP) data defines the specific orientation of the Earth as derived from multiple sources (IERS, NGA, and USNO, for instance). It consists of the difference of UT1 and UTC (ΔUT1), polar motion coordinates (x_p, y_p), and the excess length of day (LOD). It's needed for precise coordinate system operations and is available from a variety of sources. Some operational software use National Geospatial Intelligence Agency (NGA) polynomial coefficients to compute EOP parameters, instead of interpolating tabulated EOP estimates. This is acceptable for many applications; however, significant errors may result in ΔUT1 if the coefficients are much older than one week. Consider Figure 1 that uses about a year of predictions compared to the measured data to show sample performance of the indices over a 100-day span.

[3] http://www.itu.int/publications/bookshop/how-to-buy.html#free.

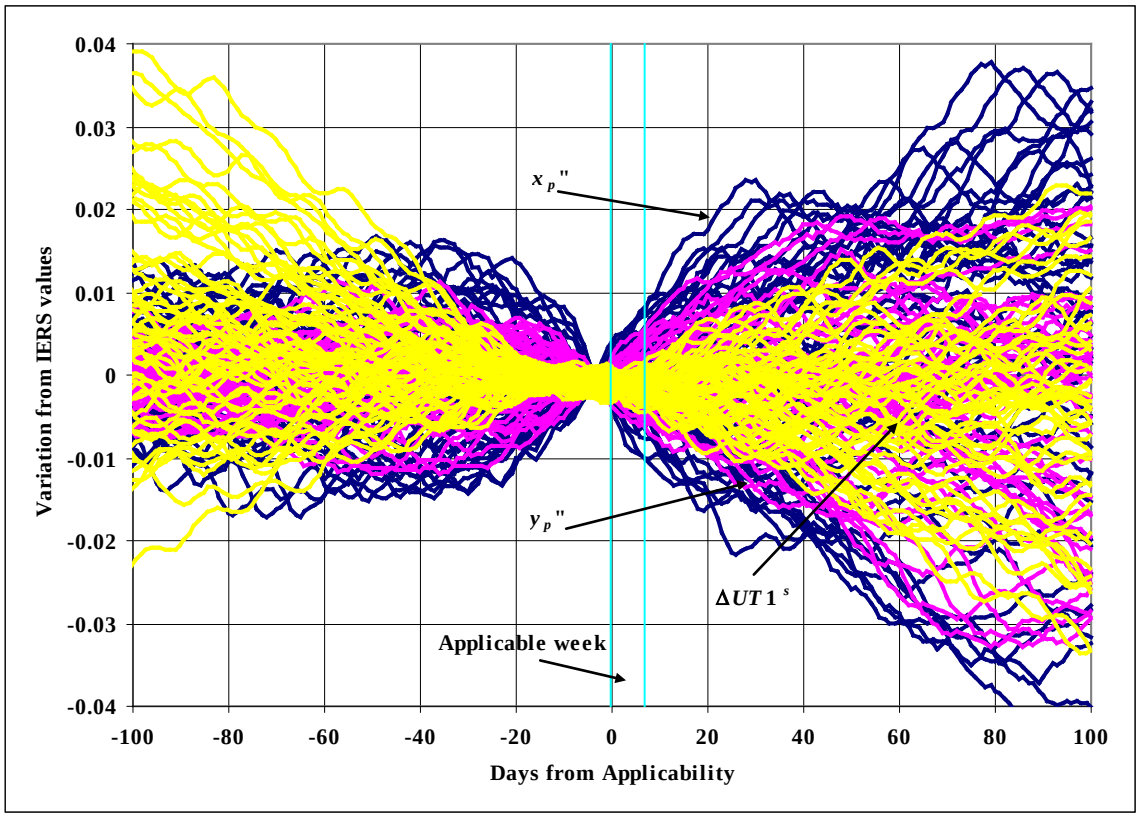

NOTE Numerous weekly coefficients were used to calculate values that were then compared to actual measurements over 200 days from the effective date of the coefficients. The vertical axis contains mixed units per the labels. Notice that the week before the week of applicability shows the best match—a consequence of least squares processing.

Figure 1 — Long-term EOP coefficient performance

5.3.4 Data Sources

The sources of data for EOP and solar weather are somewhat standard. However, there may be small differences between sources of EOP data (IERS, NGA, and USNO, for instance), but the impact on overall results is usually small (a few meters or so). Vallado and Kelso (2005) analyzed the data sources and recommend several sites to assemble a single file for operational use. The combined files may be found at http://celestrak.com/SpaceData/.

5.3.5 Recommended Practice

1) The IERS EOP data is recommended for all applications. A combined set of past, present, and future IERS and USNO data is available at http://celestrak.com/SpaceData/.

2) Specify which timescale is used for a particular operation or dataset using precise nomenclature (TT, TAI, UTC, etc.), avoiding the use of GMT.

3) Use time labels appropriate for the operation. Use of MJD is recommended for sequential labeling where date change is defined at midnight.

4) UTC time tags should conform to ISO 8601.

5) Use TT where the lack of uniformity in UTC may be intolerable. Use GPS time when dealing with elements of that system.

5.4 Constants

At the end of the 19th century, when astronomical data were manually reduced, there was significant emphasis on consistent systems of so-called fundamental constants. The last official list of constants—the 1976 IAU System of Astronomical Constants—is now mostly obsolete. Today, there are best estimates from the IAU, IERS, IAG, and various originating authors. No single list of constants can be recommended above all others. Thus, precision-data providers must cite the constants and reference frames used. The JPL Ephemerides of the solar system already include such listings. The *Astronomical Almanac,* and other national almanacs, similarly include lists of constants and their sources that are the basis for the information in those publications.

Mathematically speaking, the motion of a satellite represents a solution to a set of initial-value, second-order, ordinary differential equations of motion. The solution can be expressed either as a set of initial conditions with the corresponding system of equations, or as a tabular ephemeris representing the evolution of the solution over time. The solution is highly dependent on the fidelity of the theoretical equations themselves, as well as the accuracy of the observations from which the solution was inferred. Generally, these values will differ across operational environments due to the level of complexity of the system of equations, or differences in the adopted constants and frames of reference, even when identical observations are being used. Since a solution is optimal only for the specific theory and its associated constants, the initial values of one set of equations should not duplicate the results of a different theory or set of equations unless the model differences are accounted for. Likewise, systems of constants cannot be easily interchanged or modified without potentially degrading the accuracy of the overall system and its solutions.

There are three primary distinctions for physical constants: fundamental defining parameters, the associated gravitational model, and the astronomical constants. Gravitational models use many of these physical parameters as part of the model and are discussed in Section 6.2.

5.4.1 Fundamental Defining Parameters

Recommended values of the fundamental physical constants are found in the *Department of Defense, World Geodetic System, 1984, NIMA TR8350.2, Jan 2000*. The value of GM must be consistent with the application and the gravity field being used. In the EGM-96 model, 3.986004415×10^5 km^3/s^2 is compatible with applications operating in the Terrestrial Time (TT) scale. The value of 3.986004418×10^5 km^3/s^2 is compatible with geocentric applications operating in the Geocentric Coordinate Time (TGC) scale.

5.4.2 Astronomical Parameters

The International Astronomical Union (IAU), IERS, and IAG are sources of best estimates for constants for astronomical and geodetic applications. The recommended values of astronomical constants are taken from the annual publication, *The Astronomical Almanac*. A complete list of constants would be difficult to assemble as there are numerous sources, and different applications will require various parameters. Some values are subject to change as better measurements are taken. See http://www.usno.navy.mil.

5.4.3 Recommended Practice

1) Specify which constants were used for a particular operation.

2) Use exact conversions whenever possible, avoiding derived conversions.

3) Adopt those constants consistent with the original physical and gravitational models in use. Do not mix or substitute constants between models.

4) Use constants that are consistent with the required accuracy for the given problem.

5) Avoid embedding model-specific constants, or constants derived from such in computer software, which become obscure over time.

5.5 Coordinate Systems

The application of astrodynamical principles requires both *celestial* (where the equations of spacecraft motion are simply expressed) and *terrestrial* (where gravity is modeled and spacecraft observations tend to be taken) reference systems. Differential equations of satellite motion are valid relative to the celestial system and its corresponding barycentric or geocentric reference frame. The terrestrial system defines a rotating, Earth-based reference frame where satellite observations may originate. For near-Earth orbit determination and other astrodynamical applications, it is convenient to adopt the geocentric celestial reference systems conventionally defined by astronomers. However, the improved accuracy of astronomical theory and observations is now requiring a more relativistically consistent approach to the conventional transformation methods.

The conventional reference systems in common use, and the relationships between them, are approved and maintained by various international organizations, such as the International Astronomical Union (IAU), and the International Union of Geodesy and Geophysics (IUGG) with its associations. A variety of resolutions and theories exist to accomplish these transformations. Figure 2 illustrates the relevant timeline. A brief description of these resolutions and theories follows in the subsequent sections.

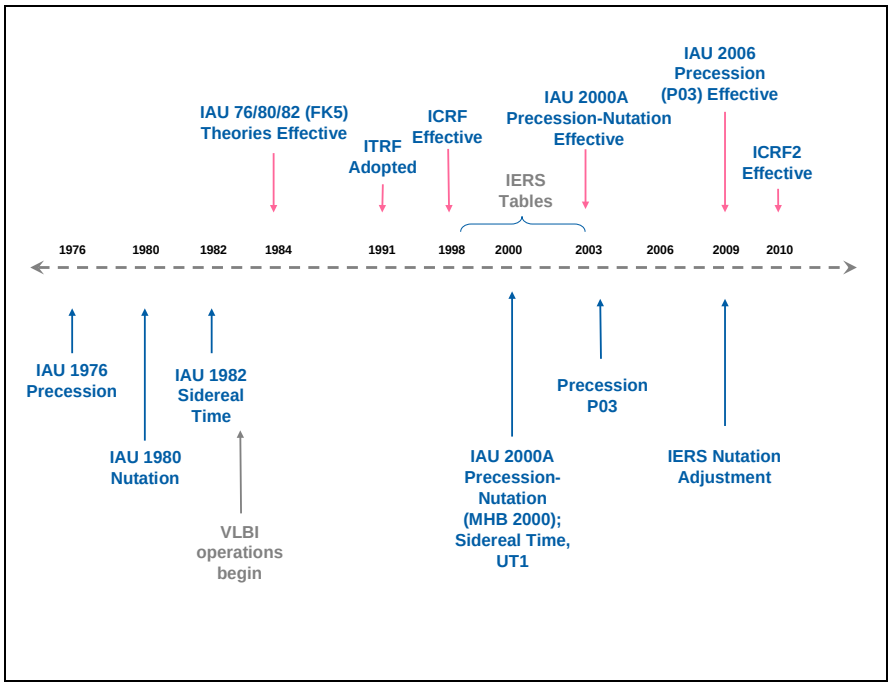

NOTE Theoretical development and adoption precede operational implementation. The effective dates indicate operational implementation while the adopted dates signify acceptance of a particular approach.

Figure 2 — Transformation theories

5.5.1 The International Terrestrial Reference Frame (ITRF)

In 1991, the International Union of Geodesy and Geophysics (IUGG) adopted a specification for the International Terrestrial Reference System (ITRS) having its origin at the center of mass of the Earth. The physical location and axial orientation of the ITRS is practically realized by the adopted coordinates of defining fiducial stations on the surface of the Earth, and the realization is known as the International

Terrestrial Reference Frame (ITRF). Because the relative station coordinates are affected by lateral tectonic motion on the order of centimeters per year, the ITRF is regularly re-estimated as a weighted, global combination of several analysis-center solutions. Sometimes, the ITRF solutions are identified by the calendar year of their publication, although these solutions have generally been constrained to minimize net rotation or frame shift with respect to previous realizations of the ITRF. For this reason, distinguishing between specific ITRF solutions is not usually required to describe locations in ITRF coordinates and changes in versions of the ITRF should be smaller than the observational errors for the purposes of orbit determination.[4]

5.5.2 The International Celestial Reference Frame (ICRF)

Starting on January 1, 1998, the IAU formally adopted the International Celestial Reference System (ICRS) to replace the IAU 1976 FK5 reference system (Arias et al., 1995). The ICRS is an ideally fixed, epoch-less, barycentric reference system defined by extragalactic radio sources so it does not rotate with time. The reference system includes a new precession-nutation model and uses the latest values of astronomical constants, the Barycentric and Geocentric Coordinate Times (TCB and TCG), and the latest solar-system ephemerides. The fiducial directions of the ICRS were selected to align with the dynamical equinox and mean celestial pole at J2000.0 of the former IAU-76/FK5 system, to within the formal uncertainty of that system.

The practical realization of the ICRS coordinate system is established through observations of extragalactic radio sources from Very Long Baseline Interferometry (VLBI) networks. This observed realization is technically known as the International Celestial Reference Frame (ICRF), and the alignment of radio and optical wavelengths is based on the adopted (optical) right ascension for radio source 3C 273 at epoch J2000.0 (Ma, 1998; Folkner et al., 1994). At optical wavelengths, the HIPPARCOS star catalog has been oriented on the ICRF and maintains continuity with the FK5 system (Kovalevsky et al., 1997). Other star catalogs, such as *Tycho 2, UCAC,* and *USNO B1.0,* provide densifications of the optical reference frame on the *Hipparcos Star Catalog*. The differences between the basis of the ICRF and the former reference system are about 20 milliarcseconds (mas), or about 10 cm at 1000 km. As the estimated relative positions of the defining radio sources are improved, and as more defining sources are added, the ICRF will be maintained such that there is no net rotation introduced with respect to the previous realizations. The Earth-centered counterpart to the barycentric ICRF is known as the Geocentric Celestial Reference Frame (GCRF). The ICRF is the coordinate frame of the *Jet Propulsion Laboratory* (JPL) *Development Ephemeris* 400 (DE400) series of planetary ephemerides.

IAU Resolution B1.8 (2000) introduced a fundamentally new system based on Earth kinematics only, rather than solar-system dynamics. The new intermediate system would have a moving reference origin that would replace the equinox of date. By definition, the intermediate nonrotating origin resides on the instantaneous celestial equator and is constrained to only move perpendicularly to—but not along—the celestial equator. Unlike the equinox, such an origin is not defined geometrically, but is maintained by the accumulated motion of the celestial equator and the conventionally adopted initial point of departure (i.e., the dynamical equinox of J2000.0). Two intermediate origins exist under such a system: a Celestial Intermediate Origin (CIO), and a Terrestrial Intermediate Origin (TIO). The TIO is the modern equivalent of the Greenwich meridian and is about 100m offset from the historical location (Kaplan 2005:54). The Earth-rotation angle between these two origins, and measured about the Celestial Intermediate Pole (CIP), supplants sidereal time under the new system. However, Resolution B1.8 also resolved that the IERS continue to provide users with data and algorithms for the conventional transformations, thus advocating two parallel methods to achieve (very nearly) the same outcome.

In August 2009, the XXVII IAU General Assembly adopted the second realization of the International Celestial Reference Frame (ICRF2) as the fundamental celestial reference frame as of 1 January 2010. The ICRF2 uses an extended and more stable set of astronomical radio sources compared to original

[4] The WGS-84 terrestrial frame is primarily used by the US Department of Defense and in GPS applications. The fundamental WGS-84 stations are actually constrained by their adopted ITRF coordinates during solution; thus, the axes of the modern WGS-84 and ITRF terrestrial frames spatially agree at the milliarcsecond level.

ICRF realization (ICRF1); a complete description of ICRF2 is available in IERS Technical Note 35. For almost all operational satellite applications the practical distinction between the ICRF1 and the ICRF2 is negligible.

The introduction of new systems and practices requires some new nomenclature, and unfortunately, minor differences in terminology and mathematical prescriptions now exist. While the IAU Working Group on Nomenclature for Fundamental Astronomy (NFA), the International Earth Rotation and Reference System Service (IERS), *The Astronomical Almanac* (2006), and the U.S. Naval Observatory (USNO) Circular 179 (Kaplan, 2005) introduced updated descriptors and definitions and further attempted to clarify many subtle technical issues, some legacy descriptors cannot precisely convey what is meant given the new reference systems. For example, reference to a "J2000 reference system" is ambiguous now because the 2000 IAU resolutions introduced an entirely new reference system relative to that epoch.

Several texts exist that describe the new coordinate frames in detail (Seidelmann, 1992; Kovalevsky & Seidelmann, 2004; Kaplan, 2005 are recommended).

5.5.3 Geocentric Celestial Reference System

The Geocentric Celestial Reference System (GCRS) will often be found described as the geocentric ICRS because the spatial orientation of the GCRS is determined by the Barycentric Celestial Reference System (BCRS). However, the relative orientation of these two systems is embodied in the 4-dimensional transformation, which is itself embodied in those algorithms used to compute observable quantities from BCRS (ICRS) reference data. Another perspective is that the GCRS is merely a rotation (or sequence of rotations) of the global geodetic system. The geodetic system rotates with the crust of the Earth, while the GCRS, to which it is referred, has no rotation relative to extragalactic objects.

A dynamically nonrotating, freely falling, locally inertial, geocentric reference system would slowly precess with respect to the BCRS, the largest component being called geodesic (or de Sitter–Fokker) precession. Geodesic precession and nutation is a relativistic effect solely caused by the fact that the orbit of the geocenter is not moving linearly, but follows a geodesic in the BCRS, thus producing an apparent relativistic perturbing force on satellite motion related to the dynamics of the barycenter of the Earth-moon system. Geodesic precession amounts to 19.2 mas per year and geodesic nutation is dominated by an annual term with amplitude 0.15 mas. By imposing the constraint of kinematical nonrotation to the GCRS, these Coriolis-type perturbations must be added (via the tidal potential in the metric) to the equations of motion of bodies referred to the GCRS. The motion of the celestial pole is defined within the GCRS, and geodesic precession therefore appears in the precession-nutation theory rather than in the transformation between the GCRS and BCRS, per IAU Resolution B1.6 (2000).

The GCRF is a reference frame for applications involving geocentric satellites. Hereafter in this document the letters (IJK) are used to identify its axes: the I-axis is approximately directed toward the mean vernal equinox at J2000, the K-axis is approximately directed toward the mean celestial pole at J2000 perpendicular to the equatorial plane, and the J-axis lies 90 degrees ahead (Eastward) in the equatorial plane, thus completing the right-handed coordinate system.

5.5.4 Implementation of the International Celestial Reference Frame

While the ICRF can be determined and maintained to an accuracy of about 0.2 mas, the extragalactic radio sources serving as its basis are optically faint. For this reason, alternative implementations are required at optical wavelengths.

The *Hipparcos Reference Catalog* results from the European Space Agency astrometric satellite mission from 1989-1993. About 120,000 stars down to 11^{th} magnitude were observed as the primary mission of Hipparcos. The catalog stars without problems are the basis for the implementation of the ICRS at optical

wavelengths. At its epoch of 1991.25, this catalog is accurate to about 1 mas, but since the proper motions have about 1 mas/year uncertainties, the accuracy of the catalog is continually degrading.[5]

The *Tycho 2 Catalog* is also based on Hipparcos satellite observations and is likewise limited to 11th magnitude, but it includes ~2,000,000 stars. It thereby adds density to the *Hipparcos Reference Catalog,* with accuracy reduced to about 20 mas at epoch. The proper motions for the *Tycho 2 Catalog* were based on about 120 Earth-based catalogs from the 20th century.

The USNO CCD Astrograph Catalog (UCAC3) is a pole-to-pole, overlapping CCD-exposure survey reaching about 16th magnitude at accuracies ranging from 20 to 70 mas, depending on magnitude. It contains the Hipparcos and Tycho Reference Catalogs and the Tycho 2 Catalog. The catalog was released in 2009 and contains over 95 million stars; for 45.4 million of these the proper motion is based on only 2 epochs, whereas for 49.5 million stars at least 3 epochs were available.

The *USNO B1.0 Catalog* is based on the Precise Measuring Machine measurements of faint sky surveys, including the Palomar Sky surveys, the various Schmidt southern surveys, and the northern and southern proper-motion surveys. The result is a catalog of ~1,000,000,000 stars down to 21st magnitude with accuracies around 200 mas. It also includes proper motions and photometric magnitudes in several colors.

5.5.5 CIP, CIO, and TIO

The IAU defined a new Celestial Intermediate Pole (CIP), replacing the Celestial Ephemeris Pole (CEP). It is determined by the precession-nutation model. The CIP is the pole of the intermediate equator of date. The IAU introduced the word “intermediate” for the reference frame between the celestial and terrestrial reference frames.

Since the ICRS is independent of the moving equinox, there is no need for the orientation of the x-axis, or departure point, of the moving reference frame of date to be tied to the equinox. After considering a number of possible choices for a departure point, the Celestial Intermediate Origin (CIO), was chosen as an alternative to the equinox. This has some significant advantages:

- It avoids the confusion between the catalog equinox and dynamical equinox, which itself has several possible definitions.
- The CIO is defined such that its motion on the fixed sphere has no motion along the equator. This means that the instantaneous movement of the CIO is always at right-angles to the instantaneous equator. The CIO has been called the nonrotating origin in previous papers. (Guinot, 1979).
- The angle, called the Earth rotation angle, measured along the equator between the CIO and the Terrestrial Intermediate Origin (TIO), in the International Terrestrial Reference Frame (ITRF), is such that it yields UT1 through a strictly linear relation. The time derivative of UT1 is proportional to the instantaneous angular velocity of the Earth.

The location of the CIO on the equator is defined by an integral that involves the path of the precessing-nutating pole since the reference epoch (Capitaine et al., 1986). This can be computed from the precession-nutation model and from observations. The position of the CIO has a zig-zag secular motion across the ICRF over long periods of time (tens of thousands of years). The small motion of the CIO is due to the choice of the constant of integration and the x-axis of the ICRF being near the equinox of J2000.0. The small motion of the CIO is based on the true motion of the CIP. The hour angle of the CIO is the Earth rotation angle, which is equivalent to sidereal time.

The Earth rotation angle is the replacement for the Greenwich Apparent Sidereal Time (GAST). The origin of the GAST is the equinox, which has components of motion along the equator; these are due to

[5] While the ICRF is epoch-less as a frame, optical stars have proper motions, so stellar epochs must be specified and stellar positions have to be corrected to specific dates by means of the proper motions.

the motion of the equator and ecliptic with respect to each other. Thus, the relationship between GAST and UT1 includes terms due to precession and nutation. The Earth Rotation Angle, and its relation to UT1, does not depend on combinations of precession and nutation.

The International Terrestrial Reference System (ITRS) is defined by the International Union of Geodesy and Geophysics (IUGG, 1992) and represented by the International Terrestrial Reference Frame (ITRF), which is a catalog of positions and velocities of point marks on the Earth. The longitude origin in the ITRF is the Terrestrial Intermediate Origin (TIO).

5.5.6 Celestial and Terrestrial Frame Transformations

The celestial frame is related to a time-dependent terrestrial frame through an Earth orientation model, represented by the standard matrix-multiplication sequence of transformational rotations:

$$\mathbf{r}_{\text{GCRF}} = \left[\mathbf{BPN}(t)\right]\left[\mathbf{R}(t)\right]\left[\mathbf{W}(t)\right]\mathbf{r}_{\text{ITRF}} \tag{5}$$

where $\mathbf{r}_{\text{GCRF}}$ is location with respect to the GCRF, $\mathbf{BPN}$ is the bias-precession-nutation matrix of date t, $\mathbf{R}$ is the sidereal-rotation matrix of date t, $\mathbf{W}$ is the polar-motion matrix of date t, and $\mathbf{r}_{\text{ITRF}}$ is the location with respect to the ITRF. The conventional Earth orientation models may be subdivided into partial rotational sequences, where intermediate frames are sometimes defined between these partial sequences. The BPN matrix may be subdivided into separate matrices or maintained as a single matrix operator, depending on the theory adopted.

Under the IAU 2000 resolutions, an improved IAU 2000A precession-nutation model was adopted. A new fiducial point was introduced—the Celestial Intermediate Origin (CIO)—which is based on the so-called "nonrotating origin" and serves as an alternative to the moving equinox. While the mean equinox has celestial motion along the equator due to precession, the CIO is defined to have no motion along the instantaneous equator. By definition, it only moves perpendicular to the instantaneous equator and results in a slow saw-tooth motion along a mean celestial equator during the precession cycle (~26,000 years).

Until 2002, the equinox method was the only one in effect, where the equinox and pole were officially modeled by the IAU 1976 Theory of Precession and the IAU 1980 Nutation model. Upon the adoption of the ICRF after 1997, the IERS began maintaining tabulated corrections to the IAU 1980 Nutation model to relate the ITRF to the ICRF, because a sufficiently accurate IAU model had yet to be developed. In 2000, the XXIVth IAU General Assembly passed additional resolutions that would significantly impact operational methods for modeling Earth orientation relative to the ICRF

The GCRF origin is offset from the theories by a tiny amount because the directional origin of the GCRS was defined by radio catalog positions before the theories were finalized. For the direction-cosine-based theory, the bias is implicit. For the IAU2000 equinox-based theory, the bias is explicit but static (Kaplan, 2005). For the IAU76/FK5 theory, the bias is explicit, time-varying, and is included in the $\delta\Delta\psi$ and $\delta\Delta\varepsilon$ of the corrected nutation theory.

In 2006 the new IAU 2006 Precession Theory was adopted (Hilton, 2006). This precession theory is based on Capitaine et al. (2003). This precession theory should be used with the nutation model of IAU 2000A.

In 2006 the IAU Working Group on Precession and the Ecliptic recommended that the terms "lunisolar precession" and "planetary precession" be replaced by "precession of the equator" and "precession of the ecliptic," respectively. They also recommended that the ecliptic pole be defined by the mean orbital angular momentum vector of the Earth-moon barycenter in the BCRS. This means that the rotating ecliptic, which follows the geometrical path of the Earth-moon barycenter and has been historically used since Newcomb, is being replaced by the inertial ecliptic, which follows the Earth-moon barycentric orbital angular-momentum vector in the BCRS.

There are different approaches currently available to perform the transformations: the CIO-based approach, an equinox-based approach, and even the application of tabular corrections to the former IAU-76/FK5-based technique. The challenge is to transform between these coordinate frames in a consistent and accurate manner. Because the newer techniques contain extensive series evaluations, computationally limited approaches may consider interpolating values from pre-computed tables. Vallado et al. (2006) show that using a simple cubic spline interpolation can reduce the level of computational effort for all methods.

The current IAU reference system transformations include several approaches (Figure 3) to implement the equinox-based transformations.

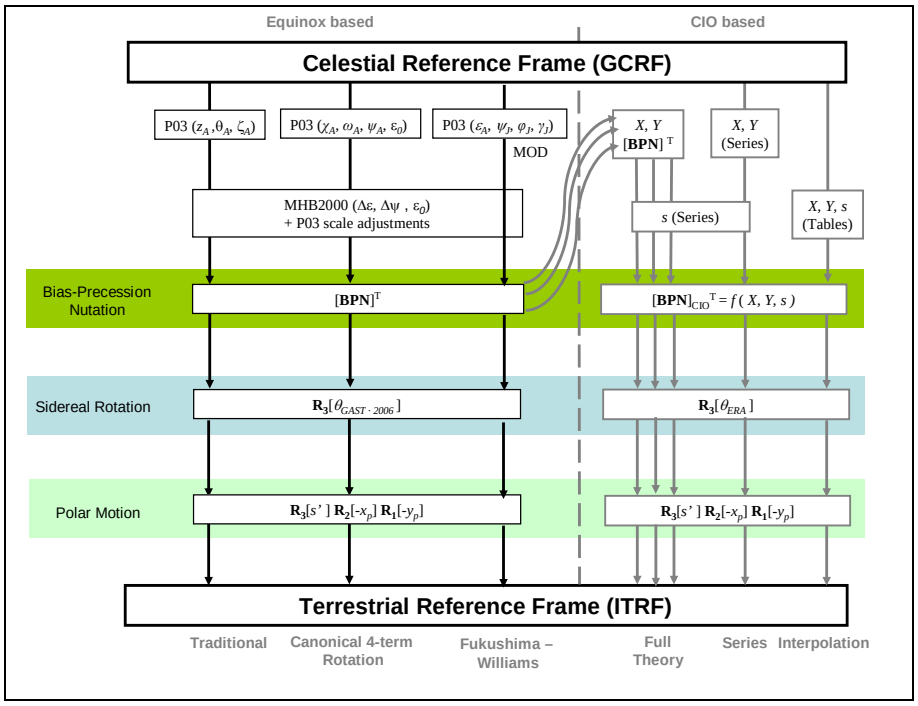

NOTE Several approaches transform between terrestrial (ITRS) and celestial coordinate systems (GCRS). Equinox-based approaches have been the basis of most existing transformation techniques over the years. Direction cosines *X* and *Y* for the CIO method are realized as the (3,1) and (3,2) elements of the equinox-based [BPN] matrix.

Figure 3 — Celestial to terrestrial coordinate transformations

The original MHB2000 model used an updated IAU-76 precession model that applied empirically observed adjustments to the precession constant and to rate of change of obliquity. However, this corrected precession model did not constitute a new, dynamically consistent precession theory, so IAU Resolution B1.6 (2000) encouraged the development of new expressions for precession consistent with the new IAU 2000A nutation model. Consequently, the XXVIth IAU General Assembly passed Resolution B1 (2006) adopting the (so-called) P03 precession model to replace the MHB2000 precession, effective 1 January 2009.

IAU Resolution B1 (2006) acknowledged that the choice of precession parameters should be left to the user, because one cannot expect any consensus on what precession parameters may be “best” for particular studies. Capitaine and Wallace (2006) suggest that the traditional Euler-angle form for precession is “no longer useful” due to the need to apply an additional small rotation to account for this bias, thus causing the traditional angles to undergo rapid changes around the J2000 epoch which are not as concisely approximated by a traditional time polynomial. An alternative representation was therefore proposed by Capitaine *et al.* (2003) involving the so-called ecliptic-precession angles, which attempts to cleanly separate (luni-solar) precession of the equator from (planetary) precession of the ecliptic. This

canonical 4-term rotation accounts for a slight bias between the fundamental axes of the ICRF and the directions of the CIP and CIO at epoch J2000. The Fukushima-Williams (F-W) form of precession has also been proposed for use with the P03 theory to avoid a singularity caused by bias offsets near the epoch of origin. The F-W form has an additional operational advantage since some of the terms serve as corrections to the angles in the nutation theory. The result is that precession and nutation can be realized *in combination* using only four rotations.

For further discussion of the precision of the new precession-nutation theories, see Coppola et al. (2009). The equations for these methods can be found in several documents (Kaplan, 2005 for instance).

5.5.6.1.1 Technical Definition

Fey, A., Gordon, D., & Jacobs, C. S. (Eds.). 2009. The Second Realization of the International Celestial Reference Frame by Very Long Baseline Interferometry, (IERS Technical Note 35). Frankfurt am Main, Germany: Verlag des Bundesamts für Kartographie und Geodäsie. http://www.iers.org/IERS/EN/Publications/TechnicalNotes/tn35.html

Kaplan, G. H. 2005. The IAU Resolutions on Astronomical Reference Systems, Time Scales, and Earth Rotation Models, Explanation and Implementation. *U.S. Naval Observatory Circular No. 179*. http://aa.usno.navy.mil/publications/docs/Circular_179.html.

Simon, J. L. et al. 1994. Numerical Expressions for Precession Formulae and Mean Elements for the Moon and the Planets. *Astronomy and Astrophysics, 282*: 663-683.

5.5.6.2 IAU-76/FK5

The International Astronomical Union (IAU) 1976 reference system and the Fifth Fundamental Catalog (FK5) were the bases of the IAU celestial reference system before 1998 (Kaplan 1981). The IAU 1976 Reference System is defined, in part, by the IAU 1976 Precession model, the IAU 1980 Theory of Nutation, the IAU 1982 Definition of Sidereal Time, the Jet Propulsion Laboratory (JPL) Development Ephemeris 200 (DE200), and the FK5 catalog, which was realized from observations of nearby stars observed at optical wavelengths.

5.5.6.2.1 Technical Definition

Kaplan, G. H. (Ed.). 1981. The IAU Resolutions on Astronomical Constants, Time Scales, and the Fundamental Reference Frame. USNO Circular No. 163. Washington DC: U.S. Naval Observatory.

A realization of the ITRS by a set of instantaneous coordinates (and velocities) of reference points distributed on the topographic surface of the Earth (mainly space geodetic stations and related markers). Currently the ITRF provides a model for estimating, to high accuracy, the instantaneous positions of these points, which is the sum of conventional corrections provided by the IERS convention center (solid Earth tides, pole tides, etc.) and of a regularized position. At present, the latter is modeled by a piecewise linear function, the linear part accounting for such effects as tectonic plate motion, postglacial rebound, and the piecewise aspect representing discontinuities such as seismic displacements. The initial orientation of ITRF is that of the BIH Terrestrial System at epoch 1984.0.

5.5.6.2.2 Technical Definition

Resolution No. 2 adopted at the 20th IUGG General Assembly of Vienna, 1991.

5.5.6.2.3 Sample Computer Code

http://maia.usno.navy.mil/conv2000/chapter5/NU2000A.f

http://www.iau-sofa.rl.ac.uk/

http://aa.usno.navy.mil/software/novas/novas_info.html

5.5.7 Origins of Celestial Coordinate Frames

The designations used to indicate the principal origins of celestial coordinate frames are as follows:

— Topocentric: viewed or measured from the surface of the Earth.

— Geocentric: viewed or measured from the center of the Earth.

— Selenocentric: viewed or measured from the center of the moon.

— Planetocentric: viewed or measured from the center of a planet (with corresponding designations for individual planets).

— Heliocentric: viewed or measured from the center of the Sun.

— Barycentric: viewed or measured from the center of the mass of the solar system (or of the Sun and a specified subset of planets).

The heliocenter and the barycenter are not coincident. The heliocenter has a small orbit about the solar system barycenter. The resulting positional error does not exceed 0.1 mas in the worst case.

The principal celestial reference planes through the appropriate origins are as follows:

— Horizon: the plane that is normal to the local vertical (or apparent direction of gravity) and passes through the observer.

— Local Meridian: the plane that contains the local vertical and the direction of the axis of rotation of the Earth.

— Celestial Equator: the plane that is normal to the axis of rotation of the Earth and passes through the Earth's center.

— Ecliptic: the mean plane (i.e., ignoring periodic perturbations) of the orbit of the Earth around the Sun.

— Planet's Meridian: a plane that contains the axis of rotation of the planet and passes through the observer.

— Planet's Equator: the plane that is normal to the axis of rotation of the planet and passes through the planet's center.

— Orbital Plane: the plane of the orbit of a body around another (e.g., of a planet around the Sun or barycenter).

— Invariable Plane or Laplacian Plane: the plane that is normal to the axis of angular momentum of a system and passes through its center.

— Galactic Equator: the mean plane of the Milky Way normal to the North Galactic Pole—which is in the constellation of Coma Berenices at $\alpha(2000) = 192.89548$, $\delta(2000) = 27.12825$—and passes through the Galactic Center which is in the constellation Sgr A at $\alpha(2000) = 266.40000$, $\delta(2000) = -28.93333$ (Kovalevsky and Seidelmann (2004, 168).

The lines of intersection of the plane of the meridian with the planes of the horizon and equator define the directions from which azimuth (A) and local hour angle (h) are measured. Azimuth is measured in the plane of the horizon from the north, increasing in positive value toward the east. Local hour angle is measured in units of time—1 hour for each 15° positive to the west with respect to the local meridian.

The latitudinal angles with respect to the horizon and equator are known as elevation (El) and declination (δ). Elevation is measured positively toward the zenith; in astronomy the zenith distance ($z = 90^\circ - \mathrm{El}$) is more generally used. Declination is measured from the equator, positive toward the north pole of rotation. The zenith distance of the North Pole, which is the same as the co-declination of the local vertical (or

zenith), is equal to the geographic co-latitude of the point of observation. This relationship is the basis of the astronomical methods for the determination of geographic latitude.

5.5.8 Satellite-Based Coordinate Frames

For satellite operations, it is convenient to use coordinate systems attached to the spacecraft, or aligned with the satellite orbital plane. There are many differences in the literature with respect to nomenclature, symbols, and use of these systems. Therefore, we identify a name for each system, representative letters, a figure, equations to form the basis vectors, and a discussion of the alternate uses in the literature. The Perfiocal system is shown in Figure 4. The coordinate frames described below should not be interpreted as an exhaustive list of acceptable frames, rather the user of this Standard should express work in the frame that is most convenient for the user and the purpose. It should be noted, however, that whatever frame is utilized should be rigorously defined as in the examples below. Finally, we use a generic IJK representation for GCRF inertial axes in these examples.

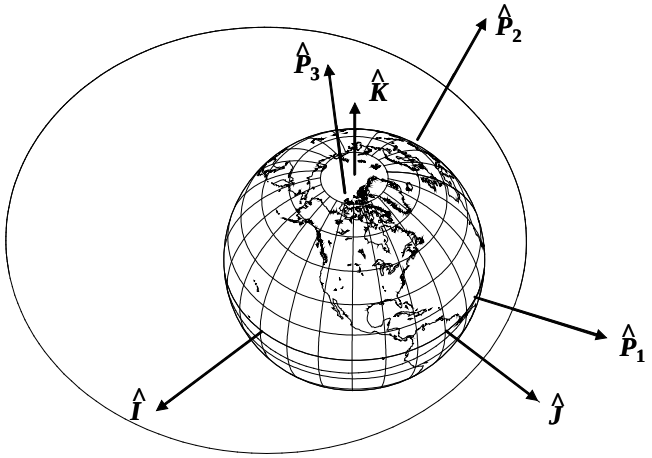

This system points towards perigee. Satellite motion is in the P1 – P2 plane. P3 is normal to the orbital plane. This particular orbit is inclined about 10 deg to the equatorial plane. Figure adapted from Vallado (2007: 164).

Figure 4 — Perfiocal coordinate system

- **Perifocal** ($(\hat{P}_1, \hat{P}_2, \hat{P}_3)$): The fundamental plane is defined by the satellite orbit and the origin is the orbit's focus. $\hat{P}_1$ points from the orbit focus (the center of the Earth) towards perigee (coincident with the eccentricity vector), $\hat{P}_3$ is coincident with the osculating orbital angular momentum vector, and $\hat{P}_2$ completes the right-handed triad ($\hat{P}_2 = \hat{P}_3 \times \hat{P}_1$). This system is often identified with the PQW letters.

The next two satellite based coordinate systems are very useful for describing relative positions, errors, and orientations. Figure 5 shows the general geometry.

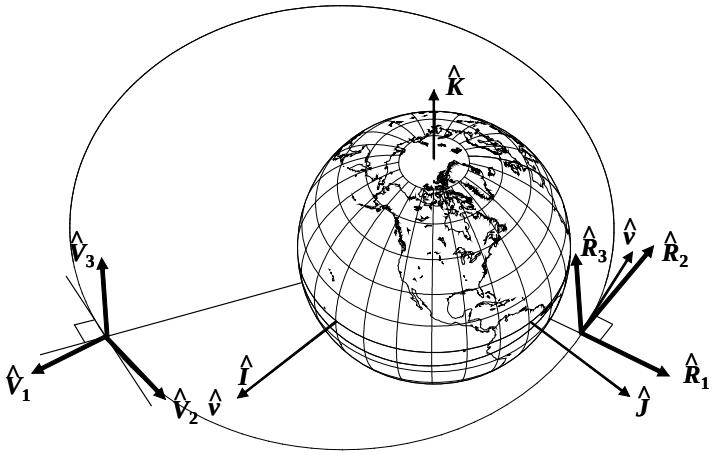

NOTE Both these coordinate systems move with the satellite. For the radial system, the $\hat{R}_1$ vector points out from the satellite along the radius vector from the geocenter, the $\hat{R}_3$ axis is normal to the orbital plane, and the $\hat{R}_2$ axis completes the right handed triad ($\hat{R}_2 = \hat{R}_3 \times \hat{R}_1$). In the Velocity system, the $\hat{V}_2$ axis is in the velocity vector direction, the $\hat{V}_3$ axis is normal to the orbital plane, and the $\hat{V}_1$ axis completes the right handed triad ($\hat{V}_1 = \hat{V}_2 \times \hat{V}_3$). Figure adapted from Vallado (2007: 165).

Figure 5 — Satellite-based coordinate systems

— Velocity ($(\hat{V}_1, \hat{V}_2, \hat{V}_3)$): This system is coincident with the spacecraft center of mass. $\hat{V}_2$ is the direction of satellite velocity, $\hat{V}_3$ is coincident with the osculating orbital angular momentum vector, and $\hat{V}_1$ completes the right-handed triad ($\hat{V}_1 = \hat{V}_2 \times \hat{V}_3$). This coordinate system is especially useful for highly eccentric orbits. It is sometimes used with normal, tangential or in-track, and cross-track (orbit plane normal) nomenclature.

— Radial ($(\hat{R}_1, \hat{R}_2, \hat{R}_3)$): This system is coincident with the spacecraft center of mass. $\hat{R}_1$ is directed outward along the satellite position vector from the orbit focus (the center of the Earth), $\hat{R}_3$ is coincident with the osculating orbital angular momentum vector, and $\hat{R}_2$ completes the right-handed triad ($\hat{R}_2 = \hat{R}_3 \times \hat{R}_1$) It is also sometimes used with radial, transverse or along-track, and cross-track (orbit plane normal) nomenclature.

Finally, we describe a local-vertical, local horizontal (LVLH) coordinate system that is very common with attitude operations. Figure 6 shows the geometry. Note the similarities, but pronounced differences to the Radial system.

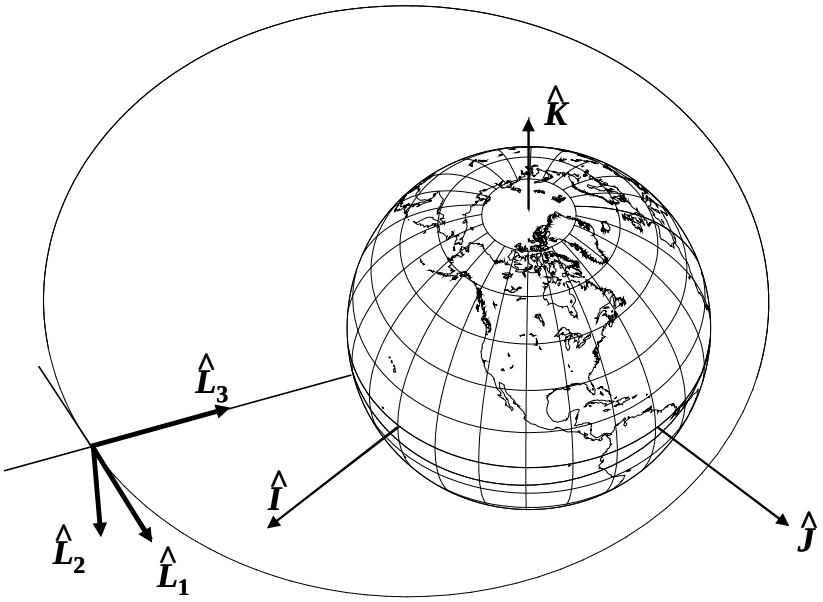

NOTE The LVLH system is similar to the Radial system, but oriented differently. The L3 axis points to the center of the Earth. The L2 axis is opposite the angular momentum vector, and the L1 axis completes the right handed coordinate system.

Figure 6 — Satellite-based LVLH coordinate system

— LVLH ($(\hat{L}_1, \hat{L}_2, \hat{L}_3)$): Spacecraft attitude engineers often use the Local Vertical Local Horizontal (LVLH) coordinate system in which $\hat{L}_3$ is defined along the position vector but towards the center of the Earth (i.e., the nadir direction). $\hat{L}_2$ is opposite the satellite angular momentum vector, and $\hat{L}_1$ completes the right-handed triad ($\hat{L}_2 \times \hat{L}_3 = \hat{L}_1$). Some organizations use an inverted LVLH frame (not pointing towards the Earth). The use depends on the particular organization. Consistency and documentation are the important requirements.

5.5.9 Recommended Practice

1) Use accepted and well-defined coordinate systems in all operations.

2) Use precise nomenclature when describing coordinate systems (ITRF, GCRF, etc.).

3) The ICRF is recommended as the celestial frame of reference. The geocentric counterpart, the GCRF, is recommended for geocentric applications, such as the exchange of satellite locations and ephemerides.

4) New software, and legacy software well positioned for changing coordinate-system methods, should make use of the CIO-based transformations. Although the corrected equinox-based method can give equivalent accuracy and may be easier to implement today, it may not be operationally supported indefinitely.

5) Computing platforms that are computationally limited should examine the interpolation of the $X/Y/s$ parameters, or $\Delta\psi_{2000}$ and $\Delta\varepsilon_{2000}$, for equinox-based approaches. Cubic splines or polynomial interpolation (5th order) are likely sufficient, but requirements should be verified through testing.

6) Existing programs can apply $\delta\Delta\psi_{1980}$ and $\delta\Delta\varepsilon_{1980}$ and precession corrections to the IAU-76/80/82 conventions to realize the GCRF.

7) Use complete reductions in every step of a numerical propagation.

8) The true-equator, mean-equinox (TEME) system is synonymous with the uniform equinox of date (Seidelmann, 1992:116), which is a computationally convenient, but unconventional, astronomical basis. Unfortunately, systems that claim to use this basis operationally often approximate its realization and do not mathematically relate it to more conventional systems. This results in loss of accuracy and cannot be generally recommended.

9) Use of an inverted LVLH frame depends on the particular organization. Consistency and documentation are the important requirements.

6 Force Models

6.1 Overview

The accuracy of orbit determination largely depends on the fidelity of the modeling of all physical forces affecting the motion of the Earth satellite or spacecraft in its orbital path through space. By far the largest perturbation(effect of the force causing the difference between the actual orbit and a reference orbit like the two-body orbit) is due to gravity, usually followed by atmospheric drag, third body perturbations, solar radiation pressure (SRP) effects, and a suite of smaller perturbative effects such as tides, albedo, and several others. Vallado (2005) shows the relative effect of various forces on several satellites. The satellite parameters were chosen to illustrate force model effects. Although specific satellites are listed, only their orbital characteristics were used. Each parameter was held constant ($C_D = 2.2$, $C_R = 1.2$, $A/m = 0.04$ m^2/kg). The simulation time, 2003 January 4, was chosen as the epoch to propagate as this was a moderate period of solar activity ($F_{10.7}$ ~ 140).

Figure 7 reproduces these quantitative effects of physical forces in terms of positional differences for one satellite. The baseline for comparison in all cases was a two-body orbit, except for the gravity cases which were compared to the next nearest case (2×0 compared to two-body orbit, 12×12 compared to 2×0, 24×24 compared to 12×12, and so forth). This was selected to best show the individual contributions. There is coupling between some forces, particularly gravity and atmospheric drag, but the effects are generally less than the other individual forces. Over time, their growth can become noticeable, but they are still usually much less than the predominant forces. Figure 7 shows representative results for a low-Earth satellite.

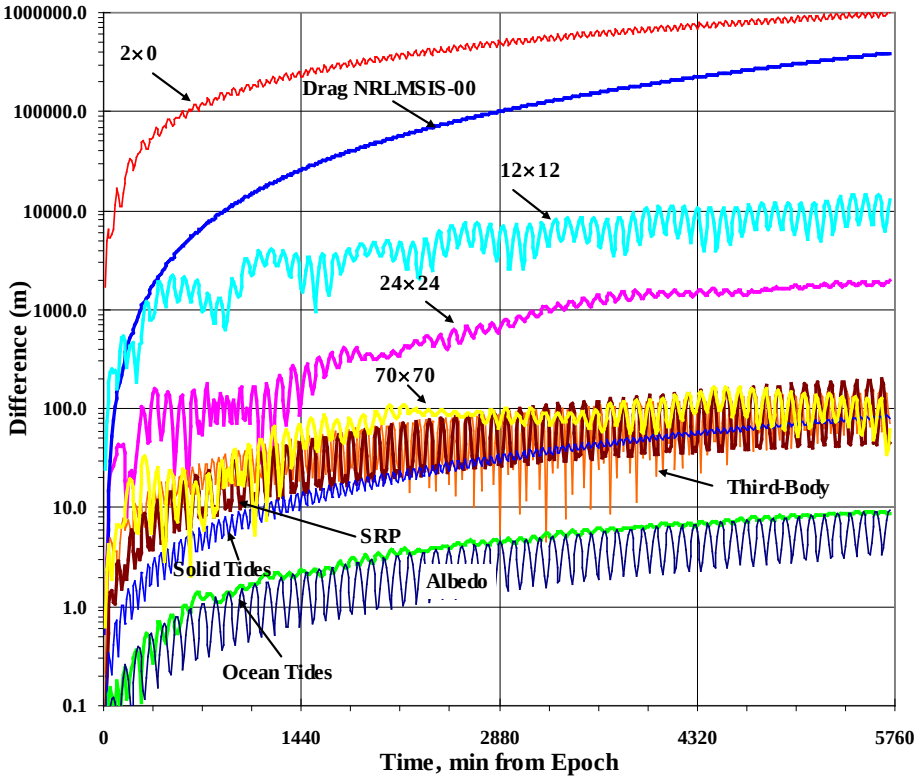

NOTE This figure shows the positional difference over time (four days) from using various force models on the same initial state. Each comparison is made with respect to a two-body orbit, except for the gravity runs which compare to the nearest gravity case. Thus, "12×12" is a comparison of a 12×12 WGS84/EGM96 gravity field to a WGS84/EGM96 2×0 gravity field ephemeris, and a "24×24" is a comparison of a 24×24 WGS84/EGM96 gravity field to a WGS84/EGM96 12×12 gravity field ephemeris, etc. The "third-body" is a comparison of a two-body orbit to an ephemeris including third-body perturbations. This is for JERS, SSC# 21867.

Figure 7 — Force model comparisons: LEO 500 × 500 km, 51.6°

The logarithmic scale was chosen to permit viewing all the forces on a single graph. Table 1 summarizes the individual results of several cases. Cases include a low-altitude (~500 km), sun-synchronous orbit, a highly eccentric orbit (~200 × 20,000 km), and others. Included are the final value and an average of the differences during the last period of the satellite's orbit. This average is intended to give an estimate of the variability in the results.

In general, gravity was the largest single perturbation source (shown in kilometers in Table 1) for the 0×0 case), so additional tests were conducted to determine the sensitivity of this perturbation force. Atmospheric drag was generally second for lower orbits, but third-body effects were much higher for higher altitude satellites. Because the study results indicated the conservative forces could be matched to cm-level, no additional studies were performed on third-body forces. Drag was considered separately. It is important to note that these are prediction differences resulting from the propagation of identical state vectors with differing acceleration models. A study of orbit determination accuracy using differing acceleration models could produce a very different set of results.

Table 1 — Summary force model comparisons

Secular (Average over the last period)													
Name	Apogee alt (km)	Perigee alt (km)	Incl (deg)	vs 2x0	vs 12x12	vs 24x24	vs 70x70	vs MSIS00	vs ThirdBody	vs SRP	vs SolidTides	vs OceanTides	vs Albedo
ISS	389	377	51.60	4179448.02	4475.43	558.03	418.60	2200700.77	455.60	95.74	46.49	10.60	3.62
JERS	490	475	97.60	559985.25	25983.24	325.83	16.85	222855.71	29925.24	725.71	33.42	12.11	34.99
Starlette	1100	800	49.80	1649331.98	14790.04	1505.60	5.62	1868.78	200.95	121.35	76.73	5.10	11.97
Vanguard 2	3023	550	32.86	2799810.40	54047.23	1956.43	305.60	6727.46	1008.79	2443.25	55.92	6.52	97.51
TOPEX	1347	1340	66.06	2140804.23	12809.29	768.07	22.66	309.47	414.42	142.41	83.31	4.31	3.54
NAVSTAR 50	20282	20282	55.24	43563.66	521.52	0.00	0.00	0.05	10137.84	1632.52	3.74	6.58	1.95
SL-12 R/B	21371	186	46.70	600259.59	17167.00	47.24	372.21	4981564.90	5996.97	407.38	10.10	1.50	6.20
Molnyia 3-35	38026	285	62.05	1649331.98	14790.04	1505.60	5.62	1868.78	200.95	121.35	76.73	5.10	11.97
Galaxy 11	35790	35785	0.03	69198.46	5779.77	0.00	0.00	0.00	27247.77	2849.94	0.93	0.08	1.21
Periodic (std dev over the last period)													
Name	Apogee alt (km)	Perigee alt (km)	Incl (deg)	vs 2x0	vs 12x12	vs 24x24	vs 70x70	vs MSIS00	vs ThirdBody	vs SRP	vs SolidTides	vs OceanTides	vs Albedo
ISS	389	377	51.60	160767.20	2061.85	113.52	7.85	22565.24	3.64	33.29	0.67	1.03	2.23
JERS	490	475	97.60	429353.68	18980.24	67.95	7.39	142934.82	26313.26	487.30	9.15	7.85	22.69
Starlette	1100	800	49.80	261369.54	1704.03	22.70	1.73	43.25	32.78	33.94	1.97	0.70	2.62
Vanguard 2	3023	550	32.86	92256.76	4209.46	218.57	14.44	806.20	222.20	311.03	11.72	0.71	12.05
TOPEX	1347	1340	66.06	93836.85	100.98	42.77	0.53	4.12	24.41	79.76	0.90	0.44	2.03
NAVSTAR 50	20282	20282	55.24	12064.61	213.37	0.00	0.00	0.00	832.04	972.10	0.17	0.42	0.80
SL-12 R/B	21371	186	46.70	184280.90	7621.10	16.55	152.63	2514036.34	2242.38	168.06	1.64	0.63	4.10
Molnyia 3-35	38026	285	62.05	261369.54	1704.03	22.70	1.73	43.25	32.78	33.94	1.97	0.70	2.62
Galaxy 11	35790	35785	0.03	7567.86	931.76	0.00	0.00	0.00	4819.47	1840.33	0.11	0.05	0.56

NOTE This table lists the overall results from the force model comparisons of several satellites (all values are in meters). Two sections are provided – secular and periodic. The secular is the average over the last revolution at the end of the time span, in this case 4 days. The periodic values are the standard deviations of the differences over the last revolution before the 4 day time. The baseline for comparison is a two-body orbit. Because the effect is so large, the gravity cases refer to the previous case, thus "vs 24×24" is the difference of a 24×24 gravity field, and a 12×12 gravity field propagation.

6.2 Central Body Gravitational Attraction

The general equation for the gravitational potential uses a spherical harmonic potential expansion in an Earth-centered, Earth-fixed reference frame. The fundamental expression for Earth's gravitational potential acting on a satellite is usually given in the familiar form of Earth's geopotential with the origin at Earth's center of mass:

$$V = \frac{\mu}{r}\left[1 + \sum_{n=2}^{\infty}\sum_{m=0}^{n}\left(\frac{R_{\oplus}}{r}\right)^{n} P_{nm}\left(\sin\phi_{gcsat}\right)\left(C_{nm}\cos m\lambda_{sat} + S_{nm}\sin m\lambda_{sat}\right)\right] \tag{6}$$

where μ is the gravitational parameter, r is the satellite radius magnitude, ϕ_{gcsat} and λ_{sat} are the geocentric coordinates of the satellite, $R_{\oplus}$ is the Earth radius, n and m are the degree and order, respectively, and C_{nm} and S_{nm} are the gravitational coefficients. Notice the presence of the Legendre polynomials

$$P_{nm}\left(\sin\phi_{gcsat}\right) = \left(\cos\phi_{gcsat}\right)^{m}\frac{d^{m}}{d\left(\sin\phi_{gcsat}\right)^{m}}P_{n}\left(\sin\phi_{gcsat}\right) \tag{7}$$

$$P_{n}\left(\sin\phi_{gcsat}\right) = \frac{1}{2^{n}n!}\frac{d^{n}}{d\left(\sin\phi_{gcsat}\right)^{n}}\left(\sin^{2}\phi_{gcsat} - 1\right)^{n} \tag{8}$$

A Legendre function (polynomial or associated function) is referred to as a zonal harmonic when $m = 0$, sectoral harmonic when $m = n$, and tesseral harmonic when $m \neq n$.

For computational purposes, this expression is often used in the *normalized* form. This results from replacing P_{nm}, C_{nm}, and S_{nm} with $\bar{P}_{nm}$, $\bar{C}_{nm}$, and $\bar{S}_{nm}$ where

$$\bar{P}_{nm} = \sqrt{\frac{(2n+1)k(n-m)!}{(n+m)!}} P_{nm}, \quad \textit{and} \quad \begin{Bmatrix} \bar{C}_{nm} \\ \bar{S}_{nm} \end{Bmatrix} = \sqrt{\frac{(n+m)!}{(2n+1)k(n-m)!}} \begin{Bmatrix} C_{nm} \\ S_{nm} \end{Bmatrix}, \tag{9}$$

with $k = 1$ for $m = 0$, and $k = 2$ for $m \neq 0$.

When normalized coefficients are used, they must be used with the corresponding normalized associated Legendre function:

$$\bar{P}_{nm} = \frac{P_{nm}}{\Pi_{nm}} \tag{10}$$

such that $\bar{C}_{nm}\bar{P}_{nm} = C_{nm}P_{nm}$ and $\bar{S}_{nm}\bar{P}_{nm} = S_{nm}P_{nm}$ and the standard model is preserved. Computer software programs should use double precision values when converting these coefficients.

6.2.1 Earth Gravitational Models

The first attempts to standardize models of the Earth's gravitational field and the shape of the Earth began in 1961. A series of gravitational constants in the form of low degree and order spherical harmonic coefficients were published based on Sputnik, Vanguard, Explorer, and Transit satellite tracking data by special investigators. The gravity models developed in the late 1950s and early 1960s for use within the astrodynamics community for the various satellite programs, including Projects Mercury, Gemini, and Apollo, consisted of a mix of gravity coefficient estimates from several sources, with widely varying uncertainties. This was largely due to the sparsity of observations available for analysis, the lack of satellites at varying inclinations, the inaccuracies in the prevailing measurement systems and the state of maturity built into the computer programs used for processing the observations.

Gravity models are in a long term state of development and enhancement based on new geodetic satellite missions. The EGM-08 model has been initially released and is on the order of 100 times more accurate than EGM-96. It includes data from GRACE with 20 cm rms global accuracy over 5 arc-min grid. Currently there are several prevailing gravitational models being used within the scientific community for a variety of purposes. These models were determined from a wide range of measurement types including surface gravity measurements and satellite altimetry data, satellite inclinations and altitudes. Figure 8 shows various models.

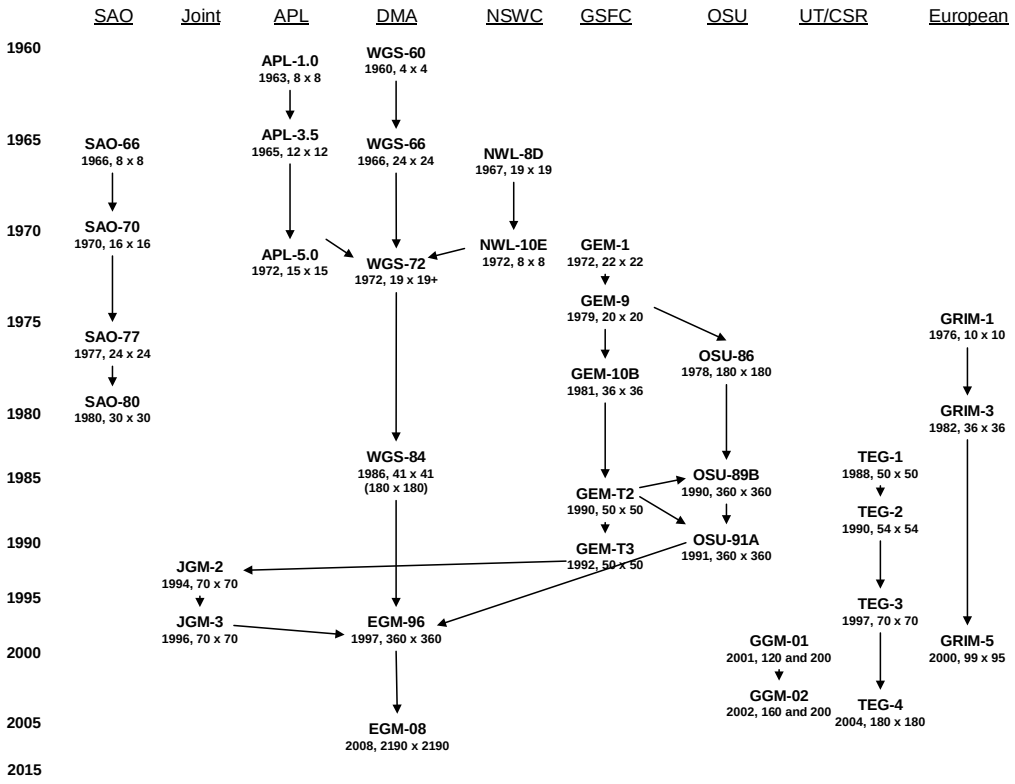

NOTE The *Joint Gravity Models* (JGM) were developed by a consortium of organizations including Goddard Space Flight Center (GSFC), Ohio State University (OSU), University of Texas at Austin (UT Austin), and the European communities. The *Earth Gravity Model* (EGM) combines the JGM work with Defense Mapping Agency efforts. The *Goddard Earth Model*s (GEM) were produced annually beginning with GEM-1 in 1972. Even numbered models contain satellite and surface gravity data. Odd numbered models contain only satellite data. WGS-72 had a few selected terms above 19 x 19, *Standard Earth* (SAO) and *Applied Physics Laboratory* (APL) models were among the first models. The GRACE gravity models (GGM) are square fields using either satellite data, or constrained with terrestrial information. The basic information is from Vetter (1994; 2001). (Source: Vallado 2007:598)

Figure 8 — Gravitational models

Four of the contemporary models, developed by individual agencies, are EGM-08/WGS-84, the University of Texas' TEG-4B, Ohio State University's OSU91A, and the European community's GRIM5-C1. The fifth, JGM-3, had been developed by a consortium of organizations including NASA/Goddard Space Flight Center (GSFC), University of Texas (UT Austin), the Centre National d'Etudes Spatiale (CNES), and Ohio State University (OSU). These are representative of the highest degree and order models currently in existence, any one of which is useful for Earth science applications requiring orbit computation accuracies in the submeter range. However, for geophysics and high precision geodetic applications where cm-level accuracies are needed, the EGM-08 gravity model is recommended. The EGM-08 gravity model has a global rms accuracy of < 15cm and a 5cm accuracy over CONUS. This model is complete to degree and order 2190 and is derived from satellite data including recent GRACE measurements (radiometric, laser ranging, and altimeter data) combined with surface gravity anomaly data base information of 5'x5' resolution.

Although a rigorous approach to astrodynamics requires the complete field, many applications use reduced gravity field orders to speed computational processing and because of program limitations. For example, AFSPC's operational systems often use a blanket 24×24 field for LEO orbits, rapidly truncating the gravity field as the orbits get higher in altitude. This may speed up the orbit processing, but may not be the

most accurate approach to determine the orbit. Barker et al. (1996) suggested a link between accuracy and the zonal truncation. Other studies have examined the average behavior of a square gravity field on the satellite orbit ephemeris. Vallado (2005) investigated the behavior of truncations for several satellites. One example is shown in Figure 9 for a satellite in a circular orbit at approximately 500 km altitude.

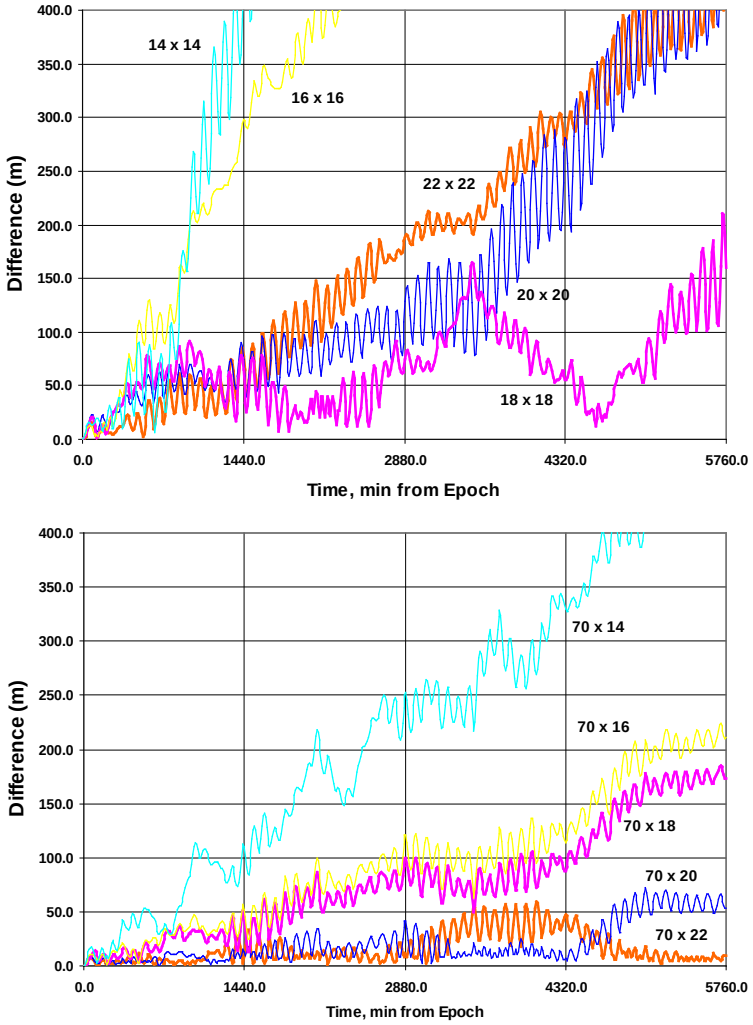

NOTE Truncated gravity fields are compared to ephemeris runs for a complete EGM-08 70×70 field for a satellite at about 500 km altitude. The top plot is for a square gravity field. The bottom plot includes all the zonals (70) in the truncations. The results do not always improve with a larger field (due to neglecting the OD contribution in forming the initial state), but the accuracy generally improves as the nonsquare truncation is reduced (the differences from 70×70 for 22×22 are greater than 18×18 on the top, but the 70×22 is smaller than the 70×18 on the bottom).

Figure 9 — Gravity field comparisons

An important assumption was used in that no orbit determination (OD) was performed with each different force model. Usually, there is a match between the OD and propagation processes. The OD adjusts the initial state based on the available force models during the OD run. Each time the gravity field is changed, the potential energy of the system changes, and an OD process produces a different state vector to reflect this change. Although the most precise way to evaluate each force model would be to perform an OD on each individual case, the process would be unnecessarily long because we are only trying to establish the relative trends for each perturbation, not specific values for an individual case. By keeping the same initial state vector, we added a certain amount of uncertainty that would have been minimized by individual OD runs.

There are two plots—a square gravity field on the top and the nonsquare is on the bottom. Each propagation is for 4 days. Differences are referenced to a complete 70×70 field. Thus, the 70×18 is a comparison between an ephemeris generated using the 70×70 field, to an ephemeris generated using a 70×18 field (70 zonal harmonics plus 18 sectoral terms). The scales are the same for each to allow easy scanning of the results. As computers have become faster, the best approach is to use a complete gravity field.

6.2.1.1 EGM-96, Earth Gravity Model

Collaborative effort with UT Austin/CSR, NGA, OSU, etc. Standard field is 360 x 360. The next update came out in 2008 and is known as EGM-08 (2160 x 2160). For details, refer to http://earth-info.nga.mil/GandG/wgs84/gravitymod/egm2008/index.html

6.2.1.1.1 Technical Definition

Lemoine, F. G. et al. 1998. *The Development of the Joint NASA GSFC and NIMA Geopotential Model EGM96* (NASA/TP-1998-206861). NASA Goddard Space Flight Center, Greenbelt, MD.

6.2.1.1.2 Data Coefficients

ftp://cddisa.gsfc.nasa.gov/pub/egm96/

Table 2 — Fundamental defining parameters (EGM-96)

Parameter	Symbol	Value
Earth Semimajor Axis	$a = r_{\oplus}$	6378136.3 meters
Flattening of the Earth	$1/f$	1/298.257
Angular Velocity of the Earth	$\omega_{\oplus}$	$7292115.8553\times10^{-11}$ rad/s
Earth's Gravitational Parameter (μ)	GM, μ	3.986004415×10^{5} km^3/s^2

Table 3 — Sample geopotential data (EGM-96)

n	m	$C_{n,m}$	$S_{n,m}$	$\Delta C_{n,m}$	$\Delta S_{n,m}$
2	0	-0.484165371736E-03	0.000000000000E+00	0.35610635E-10	0.00000000E+00
2	1	-0.186987635955E-09	0.119528012031E-08	0.10000000E-29	0.10000000E-29
2	2	0.243914352398E-05	-0.140016683654E-05	0.53739154E-10	0.54353269E-10
3	0	0.957254173792E-06	0.000000000000E+00	0.18094237E-10	0.00000000E+00
3	1	0.202998882184E-05	0.248513158716E-06	0.13965165E-09	0.13645882E-09
3	2	0.904627768605E-06	-0.619025944205E-06	0.10962329E-09	0.11182866E-09
3	3	0.721072657057E-06	0.141435626958E-05	0.95156281E-10	0.93285090E-10
4	0	0.539873863789E-06	0.000000000000E+00	0.10423678E-09	0.00000000E+00
4	1	-0.536321616971E-06	-0.473440265853E-06	0.85674404E-10	0.82408489E-10
4	2	0.350694105785E-06	0.662671572540E-06	0.16000186E-09	0.16390576E-09
4	3	0.990771803829E-06	-0.200928369177E-06	0.84657802E-10	0.82662506E-10
4	4	-0.188560802735E-06	0.308853169333E-06	0.87315359E-10	0.87852819E-10

NOTE The errors associated with each coefficient are also shown.

6.2.1.2 JGM 3

Several versions have been developed internally by CSR/UT Austin, labeled TEG models. They also participated in the Joint model development, labeled JGM-1 and JGM-2. The JGM-3 version was included in the EGM-96 effort.

6.2.1.2.1 Technical Definition

Tapley, B. D., et al. 1996. The Joint Gravity Model 3. *Journal of Geophysical Research*, Vol. 101, No B12, 28029-28049.

Nerem, R. S. et al. 1994. Gravity Model Developments for TOPEX/POSEIDON: Joint Gravity Models 1 and 2. *Journal of Geophysical Research.* 99 (C12):24, 421-24,447.

6.2.1.2.2 Data Coefficients

ftp://ftp.csr.utexas.edu/pub/grav/

Same as data in Table 2 and Table 3 for EGM-96.

6.2.1.3 WGS-84

World Geodetic Survey, 1984. Originally a U.S. military model, it contains both a datum and a gravitational model. Now it is used extensively with GPS observations and tied closely with the ITRF. The gravitational model also now references the EGM-96 model.

6.2.1.3.1 Technical Definition

National Imagery and Mapping Agency (NIMA). 2000. *Department of Defense World Geodetic System 1984.* NIMA-TR 8350.2, 3rd ed., Amendment 1. Washington, DC: NIMA.

6.2.1.3.2 Data Coefficients

http://earth-info.nga.mil/GandG/publications/tr8350.2/wgs84fin.pdf

Table 4 — Fundamental defining parameters (WGS-84)

Parameter	Symbol	Value
Earth Semimajor Axis	$a = r_{\oplus}$	6378137.0 meters
Flattening of the Earth	$1/f$	1/298.257223563
Angular Velocity of the Earth	$\omega_{\oplus}$	7292115.0×10^{-11} rad/s
Earth's Gravitational Parameter (μ)	GM, μ	3.986004418×10^{5} km^3/s^2

6.2.1.4 GGM-02, Grace Gravity Model

— The GGM-02 GRACE gravity model represents a new generation of Earth gravity models. GGM02S was determined solely from GRACE data which includes inter-satellite microwave (K-Band) range-rate measurements, GPS phase tracking using Blackjack dual-frequency on-board receivers and high precision on-board accelerometers. The K-Band measurements represent the changing gravity field of the Earth. The GPS and accelerometer measurements represent the nongravitational accelerations. The GGM02S model was estimated to degree and order 160 and is based on a joint program between NASA and DLR.

6.2.1.4.1 Technical Definition

Tapley, B. et al. 2005. GGM02—An Improved Earth Gravity Field Model from GRACE. *Journal of Geodesy*, Vol. 79, No. 8, pp. 467-478.

6.2.1.4.2 Data Coefficients

http://www.csr.utexas.edu/grace/gravity

6.2.1.5 Approved Variations

— Ensure that the gravitational parameters are consistent between organizations producing and using the data.

— Ensure all model constants (radius of the Earth, gravitational parameter, rotational velocity of the Earth, etc.) are consistent.

— Normalized coefficients may be useful for some applications.

6.3 Atmospheric Drag

The application of empirical atmospheric density models to astrodynamics in a real-world environment has been examined extensively since the launch of the first artificial satellites. Atmospheric density leads to significant drag effects for satellites below about 1000 km altitude, but its effects can be observed at altitudes well above this threshold. It's useful to review the basic acceleration equation (analysis adapted here from Vallado, 2005).

$$\vec{a}_{drag} = -\frac{1}{2}\rho\frac{C_D A}{m}v_{rel}^2\frac{\vec{v}_{rel}}{|\vec{v}_{rel}|} \tag{11}$$

ρ The density usually depends on the atmospheric model, EUV, $F_{10.7}$, K_p, a_p, prediction capability, atmospheric composition, etc. Each of these parameters contributes to differences. Popular parameters to examine today are the density and the exospheric temperatures. The density parameter represents perhaps the largest contribution to error in any orbit determination application.

C_D The coefficient of drag is related to the shape, as well as the satellite materials, but ultimately a difficult parameter to define. Gaposchkin (1994) discusses that the C_D is affected by a complex interaction of reflection, molecular content, attitude, etc. It will vary, but typically not very much as the satellite materials usually remain constant. Current research is being done to understand on-orbit changes to laboratory measurements.

A The cross sectional area changes constantly (unless the attitude maintains a constant orientation with respect to the satellite velocity, or the satellite is a sphere). This variable can change by a factor of 10 or more depending on the specific satellite configuration. Macro models are often used for modeling solar radiation pressure accelerations in orbit determination, but seldom if ever, for atmospheric drag. There could also be a benefit for applying this technique to atmospheric drag for propagation.

m The mass is generally constant, but thrusting, ablation, venting, etc., can change this quantity.

$\vec{v}_{rel}$ The velocity relative to the rotating atmosphere depends on the accuracy of the a-priori estimate, and the results of any differential correction processes. Because it's generally large, and squared, it becomes a very important factor in the calculation of the acceleration.

The ballistic coefficient ($BC = m/C_D A$; a variation is the inverse of this in some systems) is generally used to lump the mass, area, and coefficient of drag values together. It *will* vary, sometimes by a large factor. Several initiatives are examining the time-rate of change for this combined parameter without looking at the individual contributions. In high precision applications, it may not be best to model the combined parameter because all the components are potentially time-varying and are perhaps better modeled separately.

There are numerous atmospheric density models. Figure 10 (reproduced from Vallado, 2007:563) shows some of the more popular models.

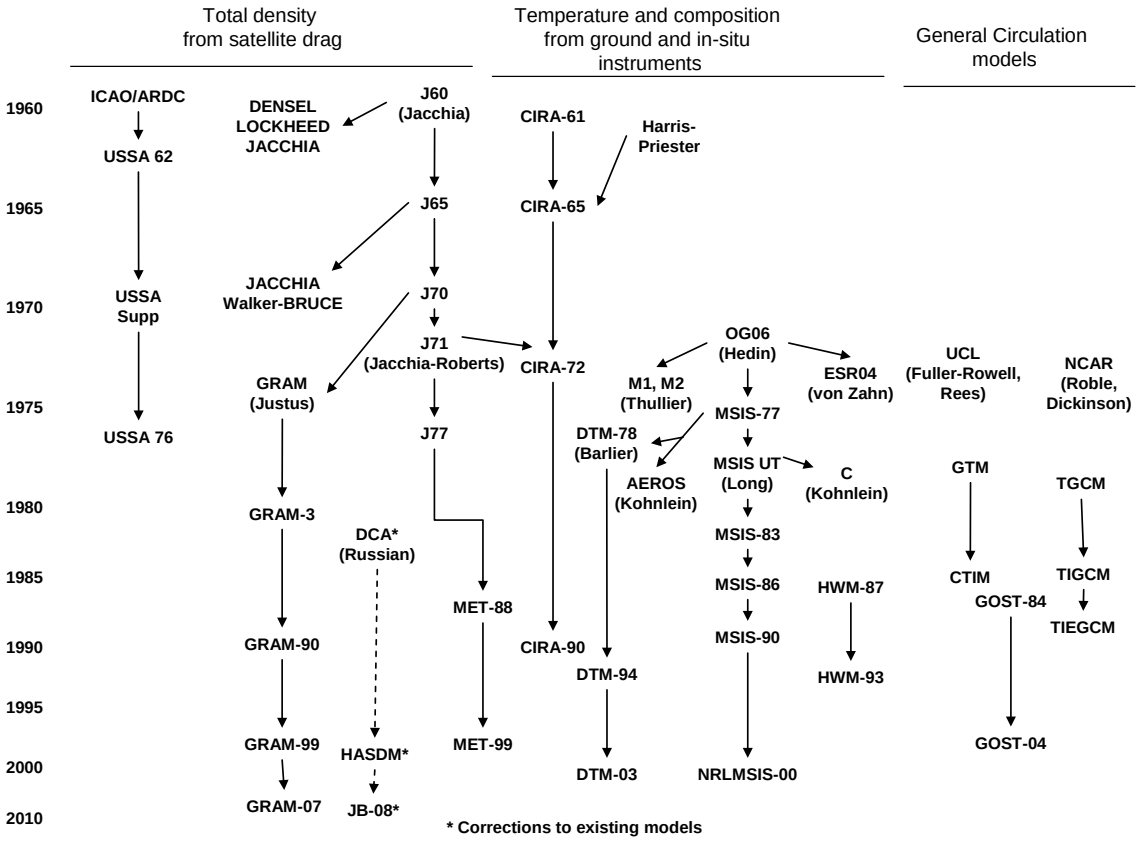

NOTE Flow of information among the three overall categories is limited (Marcos et al., 1993:20).The main models in use today are the Standard Atmosphere, USSA76; variations of the Jacchia-Roberts, J71, J77, and GRAM-07; COSPAR International Reference Atmosphere, CIRA90; Mass Spectrometer Incoherent Scatter, MSIS 00; Drag Temperature Model (DTM), Marshall Engineering Thermosphere (MET), the Russian GOST and general circulation models. The dynamic calibration of the atmosphere (DCA) series corrects other models and achieves some improvement in the density estimation.

Figure 10 — Atmosphere models

6.3.1 Corrections to Atmospheric Models

A new approach has been developing over the last few decades. Unlike the previous models, this approach isn't really a model, but rather a technique for improving or correcting atmospheric density. It gives fundamental scientific information about the variations in the density and the statistics of these variations. The work was pioneered by Nazarenko in the early 1980s (Gorochov & Nazarenko, 1982) and researched by Draper Laboratory (many documents including Cefola & Nazarenko, 1999; Granholm, 2000; Bergstrom, 2002; Yurasov et al., 2005; and Wilkins et al., 2006). Granholm (2000) and Wilkins et al. (2006) provide an excellent description of the technique, and Bergstrom (2002) showed results of implementing and testing the theory. The concept relies on changing the density directly.

The model determines the density corrections about every 3 hours from a set of "calibration" satellites. The three hour rate for density corrections is not unique. It came from a Russian consideration of determining the three hourly terms in the density from empirical inputs rather than observed geomagnetic data which they considered as unreliable in the early to mid 1980s. Note that in the recent work determining the density corrections from NORAD TLE information, the density corrections are determined once per day.

The “true” ballistic coefficient is used as an input, with processing about once every 20 days or so. This information becomes the basis of changing the atmospheric densities from an existing model—often Jacchia-Roberts-71 or an MSIS model.

The dynamic calibration work was later examined by the AFSPC (Storz, 1999). They investigated changing the temperature calculations and using spherical harmonics to extrapolate the results for global coverage. At the present time, there are a variety of AFSPC atmospheric model approaches implementing variations on the original DCA technique. Some are based on J70, while others use J71 with modifications. They use a variety of indices, some of which limit the time applicability of the model, and the performance is many times slower than the J70 model. The recent Jacchia-Bowman-08 model appears to be their chosen approach. See Marcos et al. (2006) and Bowman (2008) for additional information.

Wright and Woodburn (2004) have independently shown that using a Kalman filter, you can separate the atmospheric density errors from the modeling errors and bypass the additional computations with the density, spherical harmonics, fit spans, etc. This work was limited to the simultaneous estimation of the ballistic coefficient and atmospheric density correction for each satellite independently without extension to additional satellites. The separation of estimates for two linearly dependent states was enabled by the filter formulation which allows for both variables to be unknown functions of time, but restricting their variability with time to have greatly different time scales. Thus, all the variation on short time scales becomes attributable to density corrections while a long term bias is moved into the ballistic coefficient. The filter formulation could be extended to simultaneously estimate corrections to parameters within the global density model to provide an analog to the dynamic calibration work mentioned above.

The distinguishing feature of all the dynamic calibration approaches is that they permit the first breakthrough of the generally accepted 10% to 15% error in atmospheric models. All these approaches have significant applications to operational orbit determination. We do not yet cite these models as standards because they are all still in research stages, there has never been any release of data with which other organizations could independently verify results, and the complete models are not directly available for public release at this time.

6.3.2 Specific Details of Atmospheric Drag

The primary inputs to the drag calculation are the atmospheric density (handled via a specified model) and the BC. The mass and cross-sectional areas are usually assumed to be well known, and an estimate of the drag coefficient permits reasonable approximations. The atmospheric density models vary depending on several factors, including the satellite orbit, intensity of the solar activity, and the geomagnetic activity. Vallado and Kelso (2005) discuss how to compile a seamless file for operations. Their files are available at http://celestrak.com/SpaceData/.

Unlike any other force model discussed in this document, atmospheric drag receives extensive analysis and near-continual updates. The bottom line for drag (and to a lesser extent solar radiation pressure, as in Section 6.5) is to have as many options and choices as possible. While computer programming and certification tasks become more complicated, this nonconservative force is often the most difficult to match in ephemeris comparisons and having these options provides the user with a much greater ability to minimize differences with other programs.

There are three general observations that are important—the difference between atmospheric density models, treating the input data differently, and differing implementations of an approach. Vallado (2005) conducted a series of tests to determine the variability of different atmospheric density models for a given satellite using a single flight dynamics program and the differences resulting from the diverse treatment of the input solar weather data. The state vectors, epoch, BC, and solar radiation pressure coefficient $(m/C_R A_{sun})$ were held constant for all runs. The baseline used the Jacchia-Roberts atmospheric density model. The simulations were run during a time of “average” solar flux (2003 January 4, $F_{10.7}$ ~ 140). Minimum solar flux periods ($F_{10.7}$ ~ 70) will show little difference. Maximum periods ($F_{10.7}$ ~ 220) will show

much larger excursions. Figure 11 shows the results for a satellite (JERS) at about 500 km altitude. Additional runs were performed with different satellites and, as expected, the results were larger for lower and more eccentric orbits.

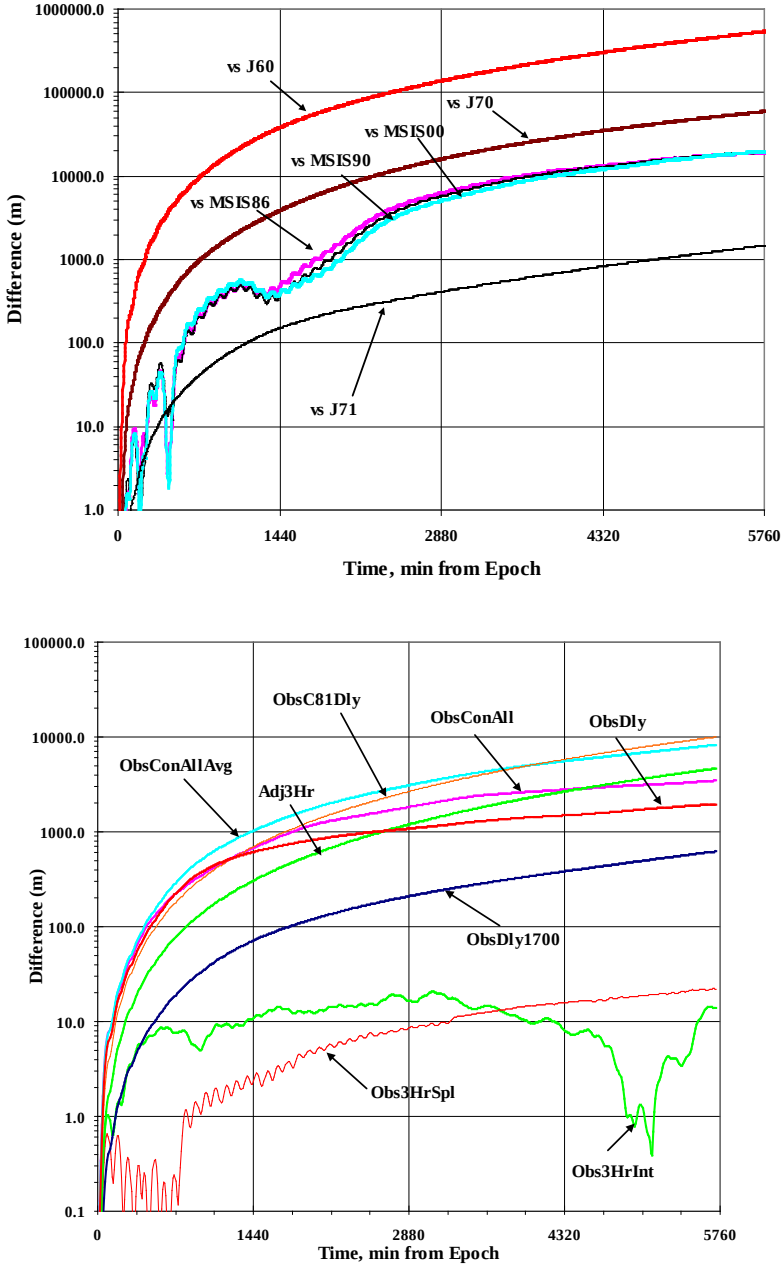

NOTE Positional differences are shown for a satellite at about 500 km altitude. Jacchia-Roberts density is the baseline for all runs with 3-hourly geomagnetic values. The top graph shows the variations by simply selecting different atmospheric density models. The bottom graph shows the effect of various options for treating solar weather data. Specific options are discussed in the text. Note that the scales are the same, and more importantly, the relative effect of different models and solar data options are about the same! Any transient effects quickly disappear as the effect of drag overwhelms the contributions.

Figure 11 — Sample atmospheric drag sensitivity

Most models, as implemented in computer code, do not follow the exact technical derivation defined in the literature. As a result, code often contains numerous short cuts, and many additional features that may be the result of internal studies and information. This makes comparison of atmospheric density models especially difficult.

The geomagnetic indices (K_p and a_p) also present an opportunity to standardize. The original work of Chapman and Bartels (1940) defined discrete values for corresponding indices. Unfortunately, the resulting scale is logarithmic, and not an exact transformation. Several forms of iteration and interpolation are available in the literature (Vallado and Kelso, 2005). The recommended approach uses cubic splines to interpolate intermediate values.

The formation of the geomagnetic data consists of averaging the K_p values from the worldwide sites (12 sites). These data are then reported to the nearest third, thus introducing a level of error to the observed data. Most models use K_p directly, while others (MSIS) use a_p.

Because atmospheric drag has perhaps the largest number of different models, defining an absolute standard is difficult to do, and could unnecessarily restrict research. There have been numerous studies to evaluate how well the atmospheric density models perform, yet no clear “winner” has ever emerged. After examining these and many other factors, Vallado (2005) concludes that no model is completely correct. Although each atmospheric density model is carefully designed, the treatment of solar weather data by each program adds so much variability, coupled with the lack of independent references and availability of observational data for comprehensive evaluation, makes it inappropriate for any one approach to be considered definitive for all cases.

Due to the large variability with atmospheric density models and input data, the following recommendations are set forth.

1) Density models should have an option to use either the last $F_{10.7}$ 81-day average, or the centered 81-day average. Atmospheric density model descriptions generally cite a centered average, but this is impractical for many operational systems, and a trailing 81-day average is often used.

2) K_p is a set of discrete categories defined by Chapman and Bartels (1940). Ideally, they should not be interpolated. In addition, atmospheric models should ideally use a_p as the input because it affords additional sensitivity not available in the K_p scale.

3) a_p values should be interpolated. The cubic spline routines discussed in Vallado and Kelso (2005) are recommended.

4) For models using the K_p index, the practical (and most common) method of operation is to interpolate the a_p values, and then select the discreet K_p value. However, this is not usually feasible, thus interpolation of K_p is an acceptable variation.

5) Programs should strive to use the newer Northern and Southern geomagnetic proxies (a_n and a_s respectively) as they represent a more rigorous approach. The older a_p values are still valid for historical continuity.

6) The codes should treat all $F_{10.7}$ measurements at the time the measurement is actually taken. The offset (2000 UTC after 1991 May 31, 1700 UTC before) should be used with all $F_{10.7}$ and average $F_{10.7}$ values. Any model specific “day before,” “6.7 hours before,” etc., should account for this offset. This can be a km-level effect.

7) The options for using a_p (or K_p) should be:

   a) Daily: Just the daily values are interpolated. All 3-hourly values are ignored.

b) 3-hourly: Just the 3-hourly values are used. The daily values are ignored and there is no interpolation. This will produce step function discontinuities.

c) 3-hourly interpolation: This should use the cubic splines. It should produce the smoothest transitions from one time to the next while preserving the discrete values. The measurements should reproduce exactly at the measurement times (e.g., 0000, 0300, 0600 UTC), and be smooth in between.

8) The lag time for a_p (K_p) values is often fixed to 6.7 hours, but other times have been proposed. Software should accommodate future changes to lag times without the need to re-compile.

9) The drag coefficient, area, and mass need to be included in state vector transmissions to permit increased accuracy in subsequent calculations.

In summary, atmospheric drag presents unique challenges for orbit determination and orbit propagation. The models are inherently limited by the degree to which they model reality. The generally accepted number is about 15% uncertainty in the density. The reasons for this are the lack of knowledge in the density of the upper atmosphere (which is not accurately modeled), the modeling of the forces needed to account for both the neutral gases and charged particles as they interact with the various satellite surfaces, and the effect of atmospheric particle flux on the varying attitude of nonspherical satellites. Equally large is how the input solar parameters are treated within a program. The newest models tend to do an excellent job of accounting for known physical phenomena. Unfortunately, there are still dynamic processes which scientists know little about, thus introducing error into any application involving atmospheric density. In addition, variations in many components (mass, area, C_D, material properties, etc.), are not generally included for orbit determination and propagation activities for satellites. This can introduce large errors in the accuracy of predictions and evaluations due to the rapidly changing behavior of these parameters. The necessity to use geomagnetic indices and their predictions in orbit determination and propagation is perhaps the single largest contributor to the effective use of atmospheric drag, along with the treatment of the input solar data. Finally, observations have the inherent error associated with any dynamic process. The combination of the aforementioned limitations and difficulties is the primary reason we have chosen not to recommend a particular model for use in all applications. The plethora of models indicates the dynamic nature of the problem, and it gives the practitioner several options to address specific or general application problems. Note that some of the older models (J64, Lockheed-Jacchia, etc.) tend to perform well for “extended” periods of time, whereas the newer models (MSIS, JR, DTM, GRAM, etc.) tend to perform better for short-term predictions. This phenomenon is likely due to the available data and the spans over which the data was analyzed. Thus, models and present references are listed that discuss the various merits of many of the models.

6.3.3 U.S. Standard 1976 (0–1,000 km) [Static]

“A hypothetical vertical distribution of atmospheric temperature, pressure and density which, by international agreement, is roughly representative of year-round, mid-latitude conditions. Typical usages are as a basis for pressure altimeter calibrations, aircraft performance calculations, aircraft and rocket design, ballistic tables, and meteorological diagrams. The air is assumed to obey the perfect gas law and the hydrostatic equation which, taken together, relate temperature, pressure and density with geopotential. Only one standard atmosphere should be specified at a particular time and this standard atmosphere must not be subjected to amendment except at intervals of many years” (U.S. Standard, 1976, xiv).

6.3.3.1 Technical Definition

U.S. Standard Atmosphere. 1976. Washington, DC: U.S. Government Printing Office.

6.3.4 DTM (200–1,200 km)

This model is similar to the MSIS models discussed later; however there are not as many constituent elements.

6.3.4.1 Technical Definition

Barlier, F., et al. 1978. A Thermospheric Model based on Satellite Drag Data. *Annales de Geophysics, 34*(1): 9–24.

Thuillier, G., Falin, J. L., & Barlier, F. 1977. Global Experimental Model of the Exospheric Temperature using Optical and Incoherent Scatter Measurements. *Journal of Atmospheric and Terrestrial Physics, 39*: 1195. Computer code in the paper.

6.3.5 Jacchia Models

Several versions exist with specific years as designators for each (1965, 1970, 1971, and the last, 1977). It is mostly designed for altitudes between 70-2500 km. The U.S. military uses the 1970 version extensively and has based the JB-08 corrections on this model.

6.3.5.1 Technical Definition

Jacchia, L. G. 1965. Static Diffusion Models of the Upper Atmosphere with Empirical Temperature Profiles. *Smithsonian Contributions to Astrop*hysics, *8*: 215-257.

Jacchia, L. G. 1970. *New Static Models for the Thermosphere and Exosphere with Empirical Temperature Profiles.* SAO Special Report No. 313. Cambridge, MA: Smithsonian Institution Astrophysical Observatory.

Jacchia, L. G. 1971. *Revised Static Models for the Thermosphere and Exosphere with Empirical Temperature Profiles.* SAO Special Report No. 332. Cambridge, MA: Smithsonian Institution Astrophysical Observatory.

Jacchia, L. G. 1977. *Thermospheric Temperature, Density, and Composition: New Models.* Smithsonian Institution Astrophysical Observatory Special Report 375. Cambridge, MA.

6.3.6 Jacchia-Roberts 1971

This modification to the J70 model contains analytical expressions for determining the exospheric temperature as a function of position, time, solar activity, and geomagnetic activity. Roberts (1971) recognized a tabular determination of atmospheric density and numerical integration to calculate partial derivatives for density is computationally intensive. So he analytically evaluated the J70 models and used partial fractions and other functions to integrate the J70 expressions.

6.3.6.1 Technical Definition

Roberts, C. E., Jr. 1971. An Analytic Model for Upper Atmosphere Densities Based upon Jacchia's 1970 Models. *Celestial Mechanics, 4*(314): 368–377.

6.3.7 MSIS Models

These models examine the molecular behavior of the atmosphere and its effect on the satellite. There are three primary versions associated with the year in which they were formulated (1986, 1990, and 2000).

6.3.7.1 Technical Definition

Hedin, A. E. 1987. MSIS-86 Thermospheric Model. *Journal of Geophysical Research, 92*: 4649-4662.

Hedin, A. E. 1991. Extension of the MSIS thermosphere model into the middle and lower atmosphere, *Journal of Geophysical Research, 96*: 1159-1172.

Picone, J. M., Hedin, A. E., & Drob, D. P. 2002. NRLMSISE-00 empirical model of the atmosphere: Statistical comparisons and scientific issues. *Journal of Geophysical Research, 107*(A12): 1468.

6.3.8 MET 88/MET 99

The Marshall Engineering Thermosphere Model (MET) is essentially a modified Jacchia 1970 model that includes some spatial and temporal variation patterns of the Jacchia 1971 model. In addition to thermospheric densities and temperatures the well-documented code provides also several often used parameters like gravitational acceleration and specific heat. MET was developed at NASA's Marshall Space Flight Center in Huntsville primarily for engineering applications. The MSIS model is generally considered superior to MET because of its larger data base and its more elaborate mathematical formalism.

6.3.8.1 Technical Definition

Hickey, M. P. 1988. *The NASA Engineering Thermosphere Model,* NASA CR-179359. Washington, DC. http://modelweb.gsfc.nasa.gov/atmos/met.html.

6.3.9 GRAM 07 (0–2,500 km)

The National Aeronautics and Space Administration's NASA/MSFC Earth Global Reference Atmospheric Model version 2007 (Earth GRAM-07) is a product of the Natural Environments Branch, NASA Marshal Space Flight Center. Like the previous versions of Earth GRAM, the model provides estimates of means and standard deviations for atmospheric parameters such as density, temperature, and winds, for any month, at any altitude and location within the Earth's atmosphere. Earth GRAM can also provide profiles of statistically-realistic variations (i.e., with Dryden energy spectral density) for any of these parameters along computed or specified trajectory. This perturbation feature makes Earth GRAM especially useful for Monte-Carlo dispersion analyses of guidance and control systems, thermal protection systems, and similar applications. Earth GRAM has found many uses, both inside and outside the NASA community. Most of these applications rely on Earth GRAM's perturbation modeling capability for Monte-Carlo dispersion analyses. Some of these applications have included operational support for Shuttle entry, flight simulation software for X-33 and other vehicles, entry trajectory and landing dispersion analyses for the Stardust and Genesis missions, planning for aerocapture and aerobraking for Earth-return from lunar and Mars missions, six-degree-of-freedom entry dispersion analysis for the Multiple Experiment Transporter to Earth Orbit and Return (METEOR) system, and more recently the Crew Exploration Vehicle (CEV). Earth GRAM-07 retains the capability of the previous version but also contains several new features.

6.3.9.1 Technical Definition

Justus, C. G., & Johnson, D. L. 1999. *The NASA/MSFC Global Reference Atmospheric Model – 1999 Version* (GRAM-99). NASA/TM 1999-209630. Washington, DC.

Justus, C. G., Duvall, A., & Keller, V. W. 2004. *Earth Global Reference Atmospheric Model (GRAM-99) and Trace Constituents.* C4.1-0002-04. Paper presented at 35th COSPAR Scientific Assembly, Paris, France.

6.3.10 GOST Russian (120–1,500 km)

GOST is an analytical method to obtain atmospheric density in an aspherical upper atmosphere from observations of Russian Cosmos satellites. It has been part of the Russian operational space surveillance system for more than 20 years, and it continues to incorporate updates from new satellite data. The elegant part of this algorithm is that it can turn factors affecting atmospheric density on or off by simply

omitting certain k factors. (For example, if diurnal variations are not needed, set k_2 to 1.) The variability in the Russian model gives a 1 sigma prediction error similar to the position error of actual data calculated with a Harris-Priester density model (Carter et al., 1987). The GOST model differed only 5–10% (Volkov, 1982) from the 1971 Jacchia density model. The Russian Earth's Upper Atmosphere Density Model for Ballistic Support of the Flight ff Artificial Earth Satellites, 2004, (Gost, 2004) is a product of the State Committee on Standardization and Metrology of the Russian Federation, Moscow. It was developed by the 4th Central Scientific Research Institute of the Ministry of Defense of the Russian Federation and adopted by the Russian Gosstandart on March 9, 2004.

6.3.10.1 Technical Definition

GOST. 2004. *Earth's Upper Atmosphere Density Model for Ballistics Support of Flights of Artificial Earth Satellites.* GOST R 25645.166-2004, Moscow, Publishing House of the Standards. (English translation accomplished by Vasiliy S. Yurasov in 2006 and edited by Paul J. Cefola in 2007.)

6.3.11 Approved Variations

— Some organizations use an inverted BC (where the units are kg/m^2). The use depends on the particular organization. Consistency and documentation are the important requirements

— The switch settings for the MSIS models are especially important and will cause great differences in the results. The SW(9) option is recommended as it calculates all the constituent parameters using the 3-hourly geomagnetic data.

We specifically do not recommend a single model for atmospheric density calculations because in reality, no single model stands out for all cases. However, because the results can vary significantly, communicating specific and detailed implementation information is crucial to any interoperability between organizations.

6.4 Third Body Perturbations

Although each planet contributes to the overall third-body force, the moon, sun, Venus, and Jupiter have the largest impact on satellite motion. In reality these are n-body perturbations that include the effect of geopotential accelerations of all planets acting on the satellite. The contributions are computed by assuming a point-mass formula. However, the sun and moon include an indirect effect as an interaction between a point-mass perturbing object and an oblate Earth. Thus, the third-body perturbation includes both direct and indirect terms of point mass third body perturbations.

The general form of the acceleration due to a single third body force is

$$\vec{a}_{3-body} = -\frac{G(m_{\oplus} + m_{sat})}{r_{Esat}^3}\vec{r}_{Esat} + Gm_3\left(\frac{\vec{r}_{sat3}}{\vec{r}_{sat3}^{\,3}} - \frac{\vec{r}_{E3}}{\vec{r}_{E3}^{\,3}}\right) \tag{12}$$

Analytical and numerically generated models are used for predicting the position of the perturbing third body. Many applications use the analytical approaches because they provide adequate accuracy. However, precise orbit propagation often requires the additional accuracy of the JPL numerical models.

6.4.1 Analytical

These routines are applicable for general purpose and approximate sun, moon and planetary positions. The accuracy is limited, but the speed of processing is quite good. The technique originally comes from the *Astronomical Almanac*.

6.4.1.1 Technical Definition

Vallado, David A. 2007. *Fundamentals of Astrodynamics and Applications* (3rd ed. pp. 279-283 (sun), pp. 287-291 (moon), pp. 297-300 (planets). El Segundo, CA: Microcosm.

6.4.2 Numerical (DE200, DE400 Series)

These accurate numerical models are valid over long periods of time (thousands of years) and are regarded as the standard for any precise orbit determination work. Note that the time argument is always TDB and as such, may need to be converted within an application. The ephemerides are intended for use with a specific coordinate system (e.g., DE200 series is designed for use with FK5 and DE400 series is designed for the IAU 2000).

6.4.2.1 Technical Definition

Standish, M. 1990. The Observational Basis for JPL's DELOD, the Planetary Ephemerides of the Astronomical Almanac. *Astronomy and Astrophysics.* 233: 252–271.

6.4.2.2 Data Files

http://www.willbell.com/software/jpl.htm

6.4.3 Approved Variations

— Because analytical routines are generally used for approximations only, there is wider latitude when selecting a particular technique. It is prudent to identify the source of the analytical technique when providing data or results using these approaches.

— Differences with JPL numerical models can arise from the use of a previous version (e.g., DE200 series instead of the current DE400 series) or using an incorrect coordinate system with the ephemerides. Consistency is recommended.

6.5 Solar Radiation Pressure

The nonconservative force due to solar radiation pressure (SRP) arises when photons from the sun impinge on a satellite surface and is absorbed (or reflected) thus transferring photon impulses to the satellite. In contrast to drag, the SRP force does not vary with altitude and its main effect is a slight change in the eccentricity and longitude of perigee. The effect of SRP depends on the satellite's mass and surface area and is most notable for satellites with large solar panels like communications satellites and GPS. In cases of geodetic precision orbits, complex models of the exposed satellite surfaces are created, usually using finite-element computer codes. This is the case with GPS where SRP represents an important force.

Vallado (2005) provides a background for SRP that is included herein. Although not studied as extensively in the literature, it poses many of the same challenges as atmospheric drag due to its nonconservative nature. This force has a significantly smaller effect than the other forces for LEO satellites but can be a noticeable contributor to the behavior of higher altitude satellites. Consider the basic equation.

$$\vec{a}_{srp} = -\rho_{SR} \frac{c_R A_{Sun}}{m} \frac{\vec{r}_{sat-Sun}}{\left|\vec{r}_{sat-Sun}\right|} \tag{13}$$

ρ_{SR} The incoming solar radiation pressure depends on the time of year and the intensity of the solar output. It's derived from the incoming solar flux (Vallado, 2007, pp. 574-578) and values of about 1358-1373 W/m^2 are common.

C_R The coefficient of reflectivity indicates the absorptive and reflective properties of the material and thus, the susceptibility of the satellite to the effects of incoming solar radiation.

A_{sun} The cross-sectional area (with respect to the sun) changes constantly (unless there is precise attitude control or it is spherical). This variable can change by a factor of 10 or more depending on the specific satellite configuration. Macro models are often used for geosynchronous satellites. This area is generally *not* the same as the cross-sectional area for drag.

m The mass is generally constant, but thrusting, ablation, and so forth can change this quantity.

$r_{sat-Sun}$ The orientation of the force depends on the satellite-sun vector—again a difference with atmospheric drag.

Despite the simple expression, accurate modeling of solar radiation pressure is challenging for several reasons. The major error sources are:

— Use of a shadow model.

— Use of macro models/attitude—this is perhaps the largest difference between programs.

— Use of differing shadow models (umbral/penumbral regions, cylindrical, none, etc.).

— Using a single value for the incoming solar luminosity, or equivalent flux at 1 AU.

— Use of an effective Earth radius for shadow calculations (23 km additional altitude is common)—this approximates the effect of attenuation from the atmosphere.

— Using different methods to account for seasonal variations in the solar radiation pressure.

— Not integrating to the exact points of arrival and departure at the shadow boundary.

— Use of the time for light to travel from the Sun to modify the satellite position. There are 3 primary approaches: treating the time from the Sun to the satellite as instantaneous, using the light time delay to the central body, and using the light time delay to satellite.

Figure 12 shows the impact of each of these items on the Starlette satellite.

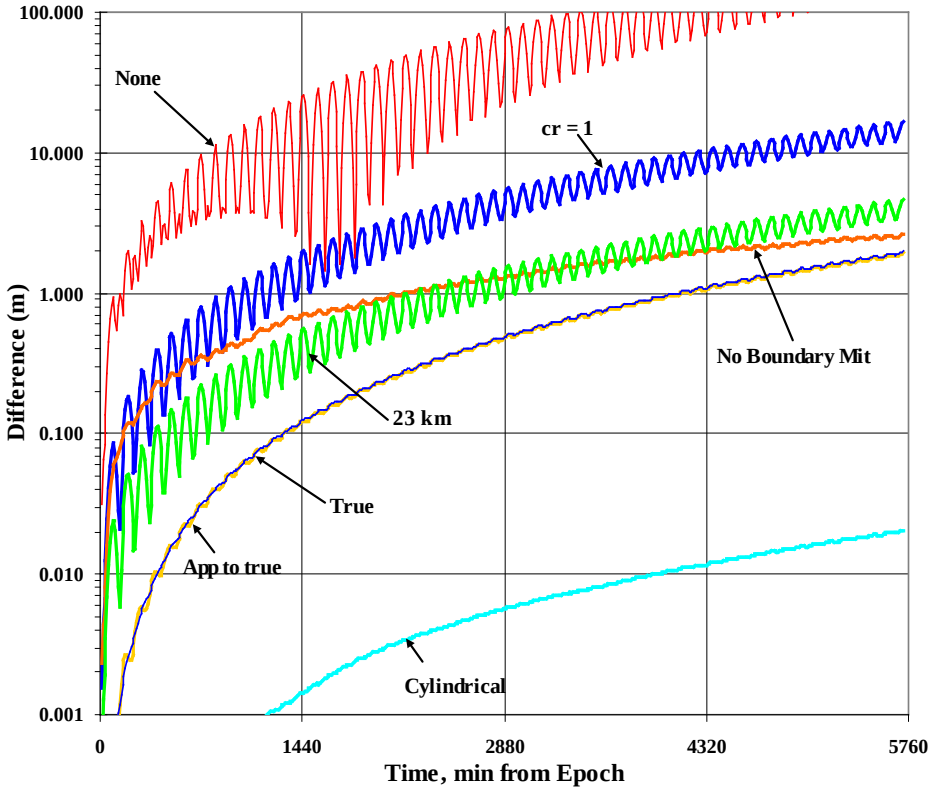

NOTE Positional differences are shown for the Starlette satellite (NORAD 07646) using options from STK/HPOP. The baseline is a dual-cone (umbra/penumbra) shadow model. Using no shadow model (none) produces the largest differences. Changing the solar radiation coefficient from 1.5 to 1.0 (C_R = 1) also produces large variations. A simple cylindrical model introduces modest differences. Shadow boundary mitigation ("No Boundary Mit") and the effective Earth size (23 km) contribute noticeable differences. The treatment of light travel time between the Sun and central body (app to true) and instantaneous travel (true), produce smaller, but still detectable results (Vallado, 2007).

Figure 12 — Sample solar radiation pressure sensitivity

6.5.1 Analytical Model of Solar Radiation Pressure Effects

There are several levels of analytical models which may be used for determining the effects of SRP. The simplest techniques use approximate methods to find the sun and moon positions. The best approach is to numerically evaluate the positions.

6.5.1.1 Technical Definition

Ries, J. C., Shum, C. K., & Tapley, B. D. 1993. Surface Force Modeling for Precise Orbit Determination. *Geophysical Monograph,* 73(13): 111-124.

6.5.2 Approved Variations

— If data providers are unwilling or unable to share specific satellite surface models, vectors used for interchange of information should estimate corrections using a simple model and distribute those results.

6.6 Temporal Variation of the Gravity Field

The temporal variation of the Earth's gravity field is composed of several effects: solid tides, ocean tides, pole tides, seasonal variations due to meteorological mass redistribution, and long-term response due to postglacial rebound. The solid Earth and ocean tidal perturbations on satellites arise from third bodies

such as the sun and moon pulling on the Earth, causing deformation and changes in its gravitational field. This in turn affects the satellite. Because the Earth is partially elastic and has a significant portion of its surface covered with liquid water, additional tidal variations are induced. The pole tide arises from the centrifugal deformation of the Earth due to a difference between the instantaneous and mean geographic pole locations. The dominant effect in seasonal variations is due to atmospheric mass transport. The postglacial rebound of the Earth's mantle, Antarctic ice sheet buildup, and glacial discharge all contribute to a very long period effect that over the lifetime of a satellite can be treated as a secular change in the gravity field.

Most of the data that have resulted in definitive models have come about within the last several years from Earth observation satellites such as TOPEX and GRACE. The basis of the models for pole, solid Earth and ocean tide models can be found in IERS Conventions (McCarthy, 2003). There are a variety of different approaches in handling these effects and properly implementing these approaches can become important if very precise comparisons are desired. Today, many models exist (especially for the ocean tides), but no single method has been recognized as the standard.

6.6.1 Solid Tides

With over 20 years of precision measurements on orbiting satellites, the historical model of the Earth as a rigid body has changed to account for an elastic body. The latest and best example of this is the IERS model. Solid Earth tidal contributions are computed as corrections to the spherical harmonic coefficients but for high precision applications become very complex as the ocean and solid Earth deformations influence each other and the anelasticity of the Earth's mantle causes frequency dependent phase lags in the Earth's response to the sun and moon. In its most simple form, derived by integrating the tidal potential over the Earth, solid tides can be represented as time-varying components of the normalized geopotential coefficients (*j* represents each disturbing body):

$$\begin{bmatrix} \Delta\bar{C}_{\ell m}(t) \\ \Delta\bar{S}_{\ell m}(t) \end{bmatrix} = \frac{k_{\ell m}}{2\ell+1}\sqrt{\frac{(\ell-m)!(2\ell+1)!(2-\delta_{0m})}{(\ell+m)!}}\sum_{j=1}^{2}\frac{\mu_j}{\mu_\oplus}\left(\frac{R_\oplus}{r_j}\right)^{\ell+1} P_{\ell m}(\cos\theta_j)\begin{bmatrix} \cos m\lambda_j \\ \sin m\lambda_j \end{bmatrix} \tag{14}$$

where

$k_{\ell m}$ The degree ℓ and order m Love number. The dominant Love numbers are the degree 2 terms. The order dependency for the Love numbers is less than 1% of the degree values. For example, the IERS gives the Earth degree 2 Love numbers as: k_{20} = 0.30190, k_{21} = 0.29830, and k_{22} = 0.30102. Therefore, for most applications, a single k_ℓ will suffice: $k_2 \approx 0.301$ and $k_3 \approx 0.093$.

r_j The distance from the center of the Earth to the disturbing body.

θ_j, λ_j The colatitude and longitude of the disturbing body.

The nonzero time-averaged contribution of the degree 2 solid Earth tide potential is called the *permanent tide*. When invoking the solid Earth tide perturbation, care should be taken to make sure that the gravity field being used is consistent with the solid Earth tide model. That is, if the permanent tide term is contained in the solid Earth tide computation, then the J_2 term of the gravity field should not also include this contribution. Conversely, the permanent tide can be directly incorporated into the gravity field and omitted from the solid tide. This can be confusing since at times gravity fields may list two entries for J_2, one with the permanent tide correction and one without. The user must ensure the proper value is being used. In terms of size, the permanent tide correction is about 4-5 orders of magnitude smaller than the nontidal J_2.

6.6.1.1 Technical Definition

McCarthy, D. D., & Petit, G. (Eds.). 2004. *IERS Conventions (2003).* IERS Technical Note No. 32, Frankfurt am Main, Germany: Verlag des Bundesamts fur Kartographie und Geodasie.

6.6.1.2 Approved Variations

— The solid tide models consist of varying Love number estimates whose values have not changed substantially over time. For example, some researchers still use either Cartwright and Tayler values or values from Wahr. The closeness of the k_2 values (all ~0.3 to within a few percent) implies that any of these values will suffice for most applications as long as consistency is maintained.

6.6.2 Ocean Tides

There exist a variety of ocean tide models that have been used since 1980 starting with the Swiderski hydrodynamic model. Cartwright and Ray updated ocean tide knowledge using 1980's altimetry from the GEOSAT mission. But these have been superseded by numerous models with the most current being CSR4.0 derived by The University of Texas, Center for Space Research (CSR). The early models had a 1 x 1 degree resolution with later models having higher resolutions.

As with the solid Earth tides, the ocean deformational response can also be analyzed in terms of temporal variations to the geopotential coefficients. The size of the corrections due to ocean tides is approximately an order of magnitude smaller than the solid Earth tide. It has been shown that the ocean tide generating potential can be represented as complex temporal variations of the geopotential coefficients. Note that the following expression is not the tide generating potential, rather the corrections to the coefficients.

$$\begin{bmatrix} \Delta C_{\ell m}(t) \\ \Delta S_{\ell m}(t) \end{bmatrix} = \frac{4\pi R_{\oplus}^2 \rho_w}{M} \left(\frac{(\ell+m)!}{(\ell-m)!\,(2\ell+1)\,(2-\delta_{0m})} \right)^{1/2} \left(\frac{1+k'_{\ell}}{2\ell+1} \right) \sum_{\mu} \begin{bmatrix} A \\ B \end{bmatrix}_{\mu\ell m} \tag{15}$$

$$\begin{bmatrix} A \\ B \end{bmatrix}_{\mu\ell m} = \begin{bmatrix} C^+ + C^- \\ S^+ - S^- \end{bmatrix}_{\mu\ell m} \cos\,(\overline{n}_{\mu} \cdot \overline{\beta}) + \begin{bmatrix} S^+ + S^- \\ C^+ - C^- \end{bmatrix}_{\mu\ell m} \sin\,(\overline{n}_{\mu} \cdot \overline{\beta}) \tag{16}$$

$$\begin{bmatrix} C^{\pm} \\ S^{\pm} \end{bmatrix}_{\mu\ell m} = \tilde{C}^{\pm}_{\mu\ell m} \begin{bmatrix} \sin\,(\overline{n}_{\mu} \cdot \overline{\beta}(t) \pm m\lambda) \\ \cos\,(\overline{n}_{\mu} \cdot \overline{\beta}(t) \pm m\lambda) \end{bmatrix} \tag{17}$$

$$\overline{n}_{\mu}\overline{\beta} = n_1\tau + n_2 s + n_3 h + n_4 p + n_5 N' + n_6 p_S \tag{18}$$

where

ρ_w The sea water mean density is approximately 1025 kg/m^3.

k'_{ℓ} The degree ℓ load deformation coefficient performs a similar function to the solid Earth Love number but refers to the ocean response as opposed to the solid Earth.

M The Earth's mass (5.9733328×10^{24} kg) (using EGM-96).

μ A summation is applied over all the separate tide constituents in the model. For CSR4.0 those are: S_{SA}, S_A, M_m, M_f, Q_1, O_1, P_1, K_1, N_2, M_2, K_2, S_2, T_2 and many other secondary constituents for a total of 223 separate tides.

$\overline{\beta}$ The Doodson variables are defined through the lunar and solar ephemeris and are closely related to the arguments used in the nutation series. There are six of them (τ, s, h, p, N', p_S) corresponding to periods of a lunar day (1.0035 days), nodical month

(27.3216 days), tropical year (365.2422 days), lunar perigee period (8.8473 years), lunar node period (18.6129 years) and solar perigee period (20940.2766 years).

$\overline{n}_{\mu} = (n_1, \ldots, n_6)$ are the integer multipliers for the Doodson variables. To get the final Doodson argument, the six-vector of the Doodson variables is dotted into the six-vector of the integer multipliers.

$\tilde{C}, \tilde{\varepsilon}$ These are, respectively, the amplitudes and phase angles of the ocean tide constituents.

6.6.2.1 Technical Definition

Eanes, R. J., & Bettadpur, S. V. 1995. *The CSR3.0 Global Ocean Tide Model.* Technical Memorandum CSR-TM-95-06. Austin, TX: Center for Space Research.

6.6.2.2 Approved Variations:

— While the solid Earth response is well known, the ocean response is very different. There are several models available, and Li et al. (1996) conducted a comparison of 11 available models (CSR3.0, RSC94, GSFC94, DW95.0, SR95.1, AG95.1, FES95.1, FES952.1, TPX0.2, Kantha, and ORI). The models were compared using approximately two years of TOPEX data and the analysis showed that they agreed to the 10 cm level (radial) in accurately reflecting the TOPEX orbit. Improvements are being made continually to the ocean tide models and many of these models (and others like CSR4.0, NAO.99, FES2004, and GOT99.2) have been updated or created using more complete TOPEX, JASON, and other satellite data. Additional satellites such as GRACE and GOCE are expected to contribute to a better model in the future. At the current time, the latter four models are the most up-to-date and any of them can be used with confidence. The following references are relevant.

NAO.99

Matsumoto, K., Takanezawa, T., & Ooe, M. 2000. Ocean Tide Models Developed by Assimilating TOPEX/POSEIDON Altimeter Data into Hydrodynamical Model: A Global Model and a Regional Model around Japan. *Journal of Oceanography,* 56: 567-581.

http://www.miz.nao.ac.jp/staffs/nao99/index_En.html

GOT99

Ray, R. D. 1999. A Global Ocean Tide Model From TOPEX/POSEIDON Altimetry: GOT99. NASA Tech. Mem. 209478. Greenbelt, MD: Goddard Space Flight Center.

http://www.miz.nao.ac.jp/staffs/nao99/index_En.html

CSR4.0

Eanes, R., & Bettadpur, S. 1995. The CSR 3.0 Global Ocean Tide Model, CSR-TM-95-06. Austin, TX: Center for Space Research.

http://www.miz.nao.ac.jp/staffs/nao99/index_En.html

FES2004

Letellier, T., Lyard, F., & Lefebre, F. 2004. *The New Global Tidal Solution: FES2004*. Paper presented at the Ocean Surface Topography Science Team Meeting, St. Petersburg, Florida.

http://www.legos.obs-mip.fr/en/soa/cgi/getarc/v0.0/index.pl.cgi?donnees=maree&produit=modele_fes

6.6.3 Pole Tides

Polar motion describes the behavior of the rotational axis relative to an Earth fixed reference frame that from space appears to show the physical Earth wobbling about its axis. Rigid Earth theory predicts a wobble period of 305 days. However, for a deformable, elastic Earth affected by movements in the oceans and the liquid core, the period is actually 435 days. In addition, seasonal variations in the atmosphere and in ocean currents cause an annual effect (365-day period) in the polar motion. The 435-day observed oscillation is the Chandler wobble—a free oscillation with some damping caused by earthquakes and mass redistributions.

Pole tides arise from the deformation of the Earth due to the centrifugal force exerted by polar motion and are described by modifications in the normalized C_{21} and S_{21} coefficients in the Earth's potential. The IERS gives the following expression for the deformation due to the polar tide:

$$\Delta\bar{C}_{21} = -4.332\times10^{-9}\ \left\{\mathrm{Re}\left[k_2\right]\left(x_p - \bar{x}_p\right) + \mathrm{Im}\left[k_2\right]\left(y_p - \bar{y}_p\right)\right\} \tag{19}$$

$$\Delta\bar{S}_{21} = -4.332\times10^{-9}\ \left\{\mathrm{Re}\left[k_2\right]\left(\bar{y}_p - y_p\right) + \mathrm{Im}\left[k_2\right]\left(x_p - \bar{x}_p\right)\right\} \tag{20}$$

where

x_p, y_p The instantaneous location of the geographic pole is published through the IERS Bulletins A and B as well as the United States Naval Observatory. The units are typically given in seconds of arc.

$\bar{x}_p, \bar{y}_p$ The mean location of the geographic pole is also given by the IERS and the United States Naval Observatory (Bulletins A and B). The units are typically given in seconds of arc.

k_2 The degree 2 Love number (~0.3077 + 0.0036*i*).

6.6.3.1 Technical Definition

McCarthy, D. D., & Petit, G. (Eds.). 2004. *IERS Conventions (2003).* IERS Technical Note No. 32. Frankfurt am Main, Germany: Verlag des Bundesamts fur Kartographie und Geodasie.

6.6.3.2 Approved Variations

— The EOP parameters are periodically updated and corrected. If the polar motion values are changed, the numerical values for the pole tide will change accordingly. There is also a dependency on the solid tide deformation Love number of degree 2. This quantity should be consistent with the solid Earth tide model that is being employed.

6.6.4 Seasonal and Secular Changes

The gravity field is not temporally constant, even after accounting for the tidal forces. It has short and long term, time-varying components. In the short term, seasonal variations exist as the mass of the Earth, particularly the atmosphere, undergoes changes in its distribution that alters the gravity field. The variations can be represented by seasonal changes in the values of the geopotential coefficients, C_{nm} and S_{nm}. These changes are extremely small and hence are necessary only for low degree and order coefficients ($n \leq 3$, $m \leq 2$ and $n \leq 5$, $m \leq 1$) and high precision applications. Orbit determination analysis of laser-ranged satellites has shown that atmospheric mass transport can affect orbits to the centimeter level.

Current models of the atmospheric mass transport are based upon global pressure distribution models such as the European Centre for Medium-Range Weather Forecasts (ECMWF) and National Meteorological Center (NMC) surface fields. These models include the entire atmosphere, not just the seasonal fluctuations. This means that the mean atmosphere needs to be removed from the gravitational model because the gravity field has already incorporated the mean atmosphere into the static gravity

field. The remaining effects can then be examined to determine an estimate of the bias, annual, and semiannual values. A sample set of values is shown in Table 5 based on the ECMWF pressure results. Again, the bias term is already in the estimated gravity field and so does not need to be incorporated into the perturbation.

Table 5 — Estimation of seasonal variations for low degree geopotential coefficients

Coefficient ($\times 10^{-11}$)	*Bias term*	*Annual cosine*	*Annual sine*	*Semi-annual cosine*	*Semi-annual sine*
C_{20}	-216.67	-0.62	8.19	0.31	-3.57
C_{21}	-1.87	5.93	2.93	1.79	-0.14
S_{21}	-80.33	10.32	-1.69	-0.81	-0.48
C_{22}	68.49	-6.34	-0.31	0.59	-1.00
S_{22}	-28.95	3.00	-3.02	-1.39	-0.69
C_{30}	180.82	-12.71	-5.31	-6.28	0.30
C_{31}	30.87	0.48	-0.44	-1.77	-1.08
S_{31}	-73.12	7.14	1.17	-1.51	-1.71
C_{32}	98.36	-4.20	-0.84	0.65	-0.01
S_{32}	-57.78	-1.56	0.08	-0.16	-1.11
C_{40}	-92.86	-3.33	3.95	3.13	-0.16
C_{41}	21.22	-2.57	0.08	0.99	-1.56
S_{41}	84.06	-3.31	-1.32	-0.40	0.78
C_{50}	116.49	3.34	3.39	-2.16	0.10
C_{51}	-8.30	-2.59	-1.58	-0.95	-2.88
S_{51}	2.22	1.67	-0.29	0.67	1.03

The effects of postglacial rebound and ice sheet buildup produce long period effects in the gravity field on the order of ice-age length. For the duration of spacecraft missions, this would appear as a secular change in the gravity field coefficients. Like the seasonal variations, this too is a very small effect and can be effectively limited to lumped secular changes in the low degree zonal terms, J_l. Various analysis exist in the literature, but typical values for $\dot{J}_2$ respectively range from -32×10^{-12} to -21×10^{-12} per year. Most gravity fields, such as EGM-96 and JGM3, contain a value for $\dot{J}_2$ that corresponds to the data reduction for that gravity field. Users should use the secular change in the zonal harmonics that is consistent with the chosen gravity model.

6.6.4.1 Technical Definition

Chao, B. F., & Eanes, R. J. 1995. Global Gravitational Changes due to Atmospheric Mass Redistribution as Observed by the Lageos Node Residual. *Geophysical Journal International,* 122(3): 755-764.

6.6.4.2 Approved Variations:

— Research continues on the temporal variation in the Earth's gravity field. The GRACE mission is producing the most up-to-date gravity fields on a monthly and an annual basis. The monthly values incorporate the seasonal changes. The GRACE gravity models also contain the correct associated $\dot{J}_2$ value (26×10^{-12}).

6.7 Earth Radiation Pressure

Radiation pressures on satellites consist of three types of effects: solar, Earth albedo (reflection of sunlight in the optical wavelengths), and Earth emissivity in the infrared. Solar radiation is the largest force on a satellite and it's generated from photons emitted from the sun hitting the surface of the satellite. As such, only the surface area directly exposed to the sun is impacted. The recommended solar radiation

pressure model is covered in Section 6.5. The Earth albedo may peak at up to 10-40% of the solar radiation pressure for low altitude satellites (it gets smaller as the altitude increases), while the Earth emissivity acceleration is about half the size of the Earth albedo effect.

The Earth acts as a reflecting body for the solar radiation in the visible (optical) wavelengths (Albedo). However, the mathematical expression is complicated by the fact that only a portion of the Earth is in sunlight at any given time. The force on the satellite is dependent upon how the satellite 'sees' that portion of the Earth that is reflecting the Sun's radiation. To get the net force on the satellite, the reflected radiation is integrated over that portion of the Earth that is both in sunlight, and visible to the satellite (Ξ). In practice, the integration is performed as a summation over as many as 20 different surface elements with each element of Ξ being located at a ground location (θ, λ) and being seen by a spacecraft with a nadir point of $(\theta_{SC}, \lambda_{SC})$. The form of the acceleration in the inertial reference frame is expressed as (note that in practice, a summation is usually used for individual surface elements, however, the most general form is an integration over the exposed surfaces):

$$\vec{a}_{op} = \frac{\rho_{sr}}{\pi\, c} \rho^2 \iint_{\Xi} \frac{c_{op} A_{eff}}{m} A_{op}(\theta, \lambda) \frac{\cos\psi_s (\cos\eta - \rho)}{\left(1 - 2\rho\cos\eta + \rho^2\right)^2} \begin{bmatrix} \sin\theta_{sc}\cos\lambda_{sc} - \rho\sin\theta\cos\lambda \\ \sin\theta_{sc}\sin\lambda_{sc} - \rho\sin\theta\sin\lambda \\ \cos\theta_{sc} - \rho\cos\theta \end{bmatrix} \sin\theta\, d\theta\, d\lambda \qquad (21)$$

where

c_{op} The satellite's reflectivity in the optical regime (either an aggregate value, or a specific portion of the satellite). This is typically close to the solar radiation pressure coefficient of reflectivity, c_R. It should be noted that in long-term analysis, the reflectivity coefficients can change with time as the surface of the satellite degrades.

A_{eff} The effective cross-sectional area presented towards the reflecting surface element on the Earth (not likely to be the same as the cross-sectional area used for drag and solar radiation pressure).

m The satellite mass at the time the integration is performed (may change with time).

ρ_{sr} The solar radiation pressure flux and can vary depending upon the time of year and solar activity but is typically between 1358 and 1373 W/m^2.

ρ The effective Earth radius is the distance of the satellite from the center of the Earth, measured from the center of the planet to the top of the reflective atmosphere. Values in the literature range from 6381 to 6401 km.

η The angle between the satellite position vector and the vector from the center of the Earth to the particular surface element at (θ, λ) reflecting the radiation.

ψ_s The angle between the Earth-sun vector and the vector from the center of the Earth to the surface element at (θ, λ).

A_{op} The Earth albedo model is typically a dimensionless zonal model with an additional annual signal in the odd degree components. One proposed model for the Earth albedo is as follows (where f_s is the true anomaly of the fictitious sun). Note that this is a simple zonal model, so there isn't any dependence on the latitude longitude as discussed previously.

$$A_{op} = 0.30 + 0.05\cos f_s \; P_{1,0}(\cos\theta) + 0.10 \; P_{2,0}(\cos\theta) + \left[0.03\cos f_s - 0.01\right] P_{3,0}(\cos\theta) + 0.04 \; P_{4,0}(\cos\theta) \tag{22}$$

The Earth, as well as the sun, emits an ambient radiation, but whereas the sun's radiation effect on a satellite is primarily in the visible range, the Earth's emitted radiation is composed of energy originally absorbed from the Sun and then re-emitted predominantly in the infrared portion of the electromagnetic spectrum. The expression for the Earth emissivity acceleration follows the same general form as the Earth albedo acceleration with the exception that the integration (or summation) is performed not over that portion of the Earth both in sunlight and visible to the spacecraft but instead simply over that portion of the Earth that the spacecraft sees:

$$\vec{a}_{ir} = \frac{1}{\pi\, c}\rho^2 \iint_{\Xi'} \frac{c_{ir} A_{eff}}{m} A_{ir}(\theta,\lambda) \frac{(\cos\eta - \rho)}{\left(1 - 2\rho\cos\eta + \rho^2\right)^2} \begin{bmatrix} \sin\theta_l \cos\lambda_l - \rho\sin\theta\cos\lambda \\ \sin\theta_l \sin\lambda_l - \rho\sin\theta\sin\lambda \\ \cos\theta_l - \rho\cos\theta \end{bmatrix} \sin\theta \, d\theta \, d\lambda \tag{23}$$

The definitions are the same as for the Earth albedo term although ρ is now the ratio of the true Earth radius (because the infrared radiation is coming from the surface of the Earth) to the distance of the satellite from the center of the Earth. Also, where

A_{ir} There are various albedo models available and the information is continuously being updated. One simple model containing the main central body term and the second order harmonic is given below (in W/m^2).

$$A_{ir} \approx 240 + 24 \; P_{2,0}(\cos\phi) \tag{24}$$

6.7.1 Technical Definition

Sehnal, L. 1981. Effects of the Terrestrial Infrared Radiation Pressure on the Motion of an Artificial Satellite. *Celestial Mechanics,* 25: 169-179.

6.7.2 Approved Variations

Research is ongoing for the Earth's reflectivity coefficients in the optical and infrared regimes. NASA's Earth Radiation Budget Experiment (ERBE) has provided most of the comprehensive global investigation into the topic. The ERBE database contains high-resolution models for both the Earth albedo and the Earth emissivity.

6.8 Relativity

General relativistic effects affect the motion of satellites in their orbits, the propagation of radio signals between satellites and near atomic clocks in the satellite itself such as used by GPS. The relativistic correction for clocks is accounted for by a change (reduction) in frequency due to the relativistic blue shift. The effect of General Relativity is very small and only becomes important when centimeter level orbit precision is needed. These effects must be modeled carefully and are based on complex relativistic mathematics carried out [generally] in a solar system barycentric frame of reference as opposed to an Earth centered inertial reference frame. It should be noted that in relativistic theory, mass does not attract an orbiting object directly. Instead the presence of energy and momentum cause the four-dimensional fabric of space-time to curve so that an orbiting object that appears in three-dimensional space to be following a conic section in its motion instead is simply following a straight line in the curved four-dimensional space-time.

The relativistic accelerations on a satellite can be quite complex and the full parameterization of the problem is more than a typical user would ever require. But by assuming that the Earth is the only relativistically significant body, the accelerations can be reduced largely into just a few components: the spherical central body term due to the gravitational energy of the Earth, the oblateness correction to this

expression, the geodesic precession, the relativistic rotational energy, and the Lense-Thirring acceleration due to angular momentum. Satellites such as the recently launched Gravity Probe B will try to measure and quantify the geodesic and Lense-Thirring precessions and verify and validate Einstein's theory of general relativity.

Geodesic precession is included in the equation below even though it normally would only be needed in a coordinate transformation between the solar system barycentric and geocentric coordinate systems. But since the orientation of the geocentric coordinate system is determined through VLBI measurements of distant quasars and hence already includes this additional precession, a transformation would normally be needed to account for the basis vector precession when examining satellites solely in the geocentric frame. By placing it in the dynamical equations, geodesic precession can be handled in a much simpler manner. The relativistic accelerations are (terms are listed with identifiers for convenience):

$$
\begin{aligned}
\bar{a}_{rel} = {} & \frac{\mu_\oplus}{c^2 r^3}\left\{\left[2(\gamma+\beta)\frac{\mu_\oplus}{r} - \gamma\left(\dot{\bar{r}}\cdot\dot{\bar{r}}\right)\right]\bar{r} + 2\,(1+\gamma)\,(\bar{r}\cdot\dot{\bar{r}})\,\dot{\bar{r}}\right\} && \text{Spherical central body} \\
& - \frac{\mu_s}{c^2 R_{es}^3}(1+2\gamma)\left[\bar{R}_{es}\times\dot{\bar{R}}_{es}\right]\times\dot{\bar{r}} && \text{Geodesic precession} \\
& + \ (1+\gamma)\,\frac{\mu_\oplus}{c^2 r^3}\,J_e\left\{\frac{3}{r^2}\left(\bar{r}\cdot\hat{\Omega}_\oplus\right)\left(\bar{r}\times\dot{\bar{r}}\right) + \left(\dot{\bar{r}}\times\hat{\Omega}_\oplus\right)\right\} && \text{Lense-Thirring} \\
& + \frac{\mu_\oplus}{c^2 r^3}\,2\,(\beta+\gamma)\,J_2\left(\frac{R_\oplus}{r}\right)^2\frac{\mu_\oplus}{r}\begin{pmatrix} x\,(2-9z^2/r^2) \\ y\,(2-9z^2/r^2) \\ z\,(5-9z^2/r^2)\end{pmatrix} && \text{Oblateness 1} \\
& + \frac{\mu_\oplus}{c^2 r^3}3(1+\gamma)J_2\left(\frac{R_\oplus}{r}\right)^2\left\{\left(1-5\frac{z^2}{r^2}\right)\left(\bar{r}\cdot\dot{\bar{r}}\right) + 2zv_z\right\}\dot{\bar{r}} && \text{Oblateness 2} \\
& - \frac{\mu_e}{c^2 r^3}\frac{3}{2}\gamma\,J_2\left(\frac{R_\oplus}{r}\right)^2\left(\bar{r}\cdot\dot{\bar{r}}\right)\begin{pmatrix} x\,(1-5z^2/r^2) \\ y\,(1-5z^2/r^2) \\ z\,(3-5z^2/r^2)\end{pmatrix} && \text{Oblateness 3} \\
& - \frac{3}{14}\,T_e\,(1+\gamma)\,\frac{\mu_\oplus}{c^2 r^3}\left(\frac{R_\oplus}{r}\right)^2\left\{\left[1-5\frac{z^2}{r^2}\right]\bar{r} + 2\left(\bar{r}\cdot\hat{\Omega}_\oplus\right)\hat{\Omega}_\oplus\right\} && \text{Rotational energy}
\end{aligned}
\tag{25}
$$

where

γ This parameter measures the curvature of space-time induced by the presence of a unit of mass (or equivalently energy). In General Relativity, this parameter is unity.

β This parameter measures the violation of the superposition principle. The superposition principle for gravity states that the solutions of a field composed of two subfields is equal to the sum of the solutions of the two subfields. If β = 0, the fields add linearly and the superposition principle holds, but in most theories β is not zero implying that two interacting gravitational fields produce curvature in excess of that produced by the two fields independently. In General Relativity, this parameter is unity.

L The Lense-Thirring parameter. In General Relativity, this parameter is also unity. Normally, a nonrotating gravitating body causes the fabric of space-time to curve; when it also has a rotation (angular momentum), the fabric of space is dragged in the direction of rotation. For this reason, the Lense-Thirring precession is also called frame-dragging.

$\bar{R}_{es}, \dot{\bar{R}}_{es}$ Vectors from the Earth to the sun.

J_e The Earth angular momentum per unit mass (980 km^2/sec based on a partially elastic Earth) and impacts the amount of frame-dragging that occurs.

T_e The rotational energy of the Earth per unit mass (0.0355 km^2/sec^2, also based on a partially elastic Earth). This term has the same form as the nonrelativistic Earth oblateness acceleration. Therefore, there is no way to separate the two effects; the J_2 that is recovered from gravity field estimation is actually a combination of the actual Earth J_2 and the relativistic rotational energy.

Ω_e The unitized spin vector of the Earth.

(x, y, z), (v_x, v_y, v_z) The components of the satellite state vector $(\bar{r}, \dot{\bar{r}})$.

Figure 13 shows the approximate levels of magnitude of the various relativistic accelerations as a function of semimajor axis.

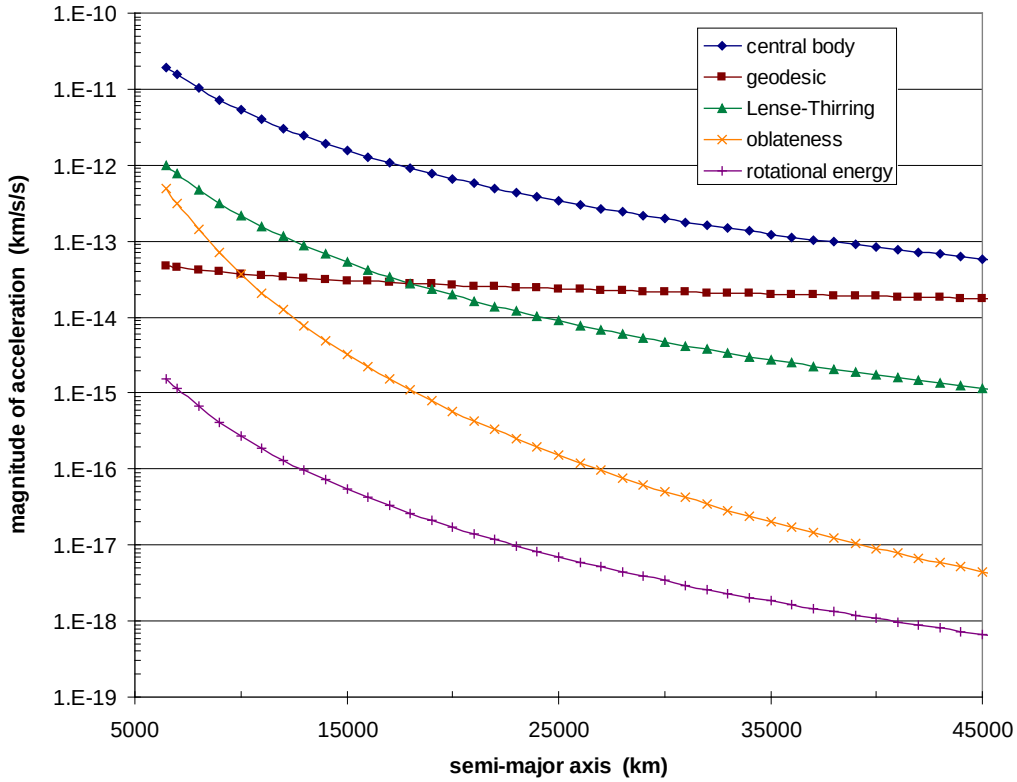

NOTE Most satellite applications do not require even the largest relativistic term. In comparison, the central body relativity term is about 2 orders of magnitude smaller than the largest solid Earth tide acceleration for LEO satellites and about 1 order of magnitude smaller than the largest solid Earth tide acceleration for GEO.

Figure 13 — Magnitudes of relativistic accelerations as a function of semimajor axis

6.8.1 Technical Definition

Soffel, M. 1989. *Relativity in Astrometry, Celestial Mechanics, and Geodesy*. Berlin, Germany: Springer-Verlag.

6.8.2 Approved Variations

— Other relativistic theories exist although the experimental results at the current time indicate that General Relativity is the closest representation of reality (to within 1%). These other variations are contained in an overall mathematical methodology called the Post-Parameterized Newtonian (PPN) framework that was developed in order to compare the various theories. However, the effects from the differences between these theories and General Relativity are at the submillimeter level and below, and therefore are not relevant to satellite applications at the current time.

6.9 Thermal Yarkovsky Forces

There are two Yarkovsky thermal radiation effects, one based on solar heating and the other deriving from the Earth. These satellite re-radiation accelerations arise from a differential heating of the satellite due to the relative position of the spin axis with respect to the radiating body. As radiation heats the satellite, a temperature gradient develops within the satellite between its hot and cold sides. As the cold side then heats and the hot side cools down, a thrust is developed that is directed along the spin axis.

The resulting Yarkovsky acceleration for the Earth can be expressed as:

$$\bar{a}_{ey} = -2\alpha_e \sin\delta \cos(u-\delta)\hat{s} \tag{26}$$

where

u This is the argument of latitude of the satellite.

δ The thermal lag angle is determined as part of the estimation process or a typical value is assumed. For laser-ranged geodetic satellites such as LAGEOS, the thermal lag angle is assumed to be approximately 55 deg.

α_e This coefficient combines the relevant physical properties of the satellite in question and is typically determined empirically through satellite estimation. Current estimates of the most highly observed satellites place the magnitude of α_e at around 10 picometers/sec^2.

$\hat{s}$ The satellite spin vector must be either known or estimated. The spin vector is difficult to model in that it will tend to migrate over time if not actively controlled and can behave in a chaotic fashion for some satellites.

The solar Yarkovsky is more complex than the Earth Yarkovsky because the satellite encounters periods of eclipse where the Sun no longer heats the satellite. In general, the solar Yarkovsky acceleration will have a form similar to the Earth's, but must include the continual heating and cooling resulting from the eclipses. The following form assumes an exponential cooling/heating trend:

$$\bar{a}_{sy} = -\alpha_s \cos\varepsilon \left[e^{-(t-t_1)/\tau} \right] \hat{s} \qquad \text{(eclipsed)} \tag{27}$$

$$\bar{a}_{sy} = -\alpha_s \cos\varepsilon \left[C + (1-C)\left(1 - e^{-(t-t_2)/\tau}\right) \right] \hat{s} \qquad \text{(unshadowed)} \tag{28}$$

where

α_s Similar to α_e, this is a combined parameter denoting the magnitude of the solar thermal acceleration, is usually determined empirically in the estimation process, and is about an order of magnitude larger than α_e at tens of picometers/sec^2.

ε This is the angle between the satellite spin axis and the Sun's direction.

t_1, t_2 These times indicate when the eclipse is entered and exited.

τ This is the thermal decay time (~30 minutes is typical).

C This constant is chosen to match the two terms at the shadow boundary.

6.9.1 Technical Definition

Rubincam, D. P. 1988. Yarkovsky Thermal Drag on Lageos. *Journal of Geophysical Research.* 93: 13805-13810.

6.9.2 Approved Variations

— The Yarkovsky accelerations are not known a priori as they depend upon the material properties of the spacecraft, how heat is conducted through the structure, and the spin axis. Therefore, they are typically used as empirical or modeled accelerations to account for systematic behavior in the orbit elements that cannot be accounted for in any other way. As such, αe and αs are unique for each satellite.

6.10 Thrust and Other Forces

In stationkeeping, it is often the case that a required burn magnitude is computed in the form of a small change in the spacecraft velocity. In this case, the change can be added as an impulse directly into the spacecraft velocity at the integration step boundary if small, and if large, it can be changed in to a constant acceleration that acts over the length of multiple integration time steps (finite burn). For continuous low thrust applications, the thrusting is best resolved into an equivalent acceleration that is applied over the entire duration of the thrust. Care must be taken when deciding upon a method as the type of integrator chosen can influence whether, and at what magnitude, changes in the velocity or the accelerations would require a re-start of the integrator.

6.11 Recommended Practice for Force Models

1) The gravity field being used should be explicitly identified as either including or not including the permanent tide deformation to avoid potential confusion with the solid tide model.

2) Use consistent constants from a single gravitational model. For instance, if using EGM-08, use the constants that are defined with the field.

3) Use the same geopotential for orbit determination and propagation. Using different models can actually change the energy of the orbit because the gravitational parameter could be different.

4) Use the proper radius of the Earth, gravitational parameter, and Earth angular velocity.

5) Use proper force models to capture the dominant error sources based on the requirements for each problem. Clearly specify the force models used.

6) Provide all satellite parameters whenever possible. This includes the drag coefficient C_D being estimated if at all possible. Therefore, A and M should be included in any solutions, where possible. The driving factor here is the availability of data.

7) Interpolate the $F_{10.7}$ and a_p values for use in the models.

8) Provide capability for 81-day average (trailing data values) calculations for operational applications, and centered 81-day averages for postprocessing (where the full data exists).

9) Computer programs should use original definitions of models or well documented, published, and available revisions that have vetted improvements and or corrections. Other approximations can only lead to confusion when later trying to perform comparisons. Basically, J70 becomes a modified J70.

7 Propagation Methods for Earth Satellites

7.1 Introduction

One of the primary requirements for orbital analysis is the ability to predict future, or past, locations of a satellite. This activity is formally known as propagation, and there are three primary types: analytical, numerical, and semianalytical. The importance of accurate propagation techniques is obvious, and as we use increasingly complex operations with faster computers, our ability to pick and choose among these techniques is expanding every day. Likewise, the applications that require propagation are becoming increasingly dependent upon the accuracy of techniques to complete a particular operation. We'll discuss each of the main methods of propagation in this section.

The major perturbations that affect the motion of a satellite include Earth gravitation, atmospheric drag, lunar and solar gravitation, and solar radiation pressure (discussed in Section 6). Depending on the orbital altitude and physical size of the satellite, the effect of each of these perturbations may be more or less important. The perturbations included in the model will result in short-period and long-period periodic terms as well as secular perturbations in the solution.

We begin with the analytical theories. An expanded introduction to these techniques is found in Chapters 8 and 9 of Vallado (2007).

7.2 Analytical Solutions of Earth Satellite Equations of Motion

Analytic theories describing the motion of planets, comets, asteroids, moons and other planetary bodies have been in existence since the time of Gauss and Laplace in the 18^{th} century. With the advent of Earth satellites, analytic theories were developed which include limited force terms and model the effects of the primary gravity perturbations and atmospheric drag. The early works of Brouwer and Kozai are notable examples and are in use even today for modeling general perturbation effects in such programs as Simplified General Perturbations-4 (SGP4) and Position Partials and Time (PPT3) for orbit propagation. These analytical theories generally have an accuracy of about 1 km at epoch. Different analytical solutions use such methods as the variation of parameters, averaging techniques and a variety of canonical transformations to simplify the equations of motion. Today there are numerous analytical solutions for solving unperturbed motion but the results obtained ultimately depend on the forces that are being modeled. This process usually relies on series expansions to express the motion—a source of practical difficulty. Transformations into a set of orbital elements provide insight into the behavior of the perturbation effects over time caused by the secular, short-periodic, and long-periodic motions. Although these distinctions help decide which effects to model, the practical difficulty of an infinite series still remains.

When selecting an analytical model, the question of accuracy often arises. The accuracy of a model is difficult to quantify because of the very nature of analytical solutions and real world uncertainties. There are two interpretations of the notion of orbital model accuracy. In an absolute sense, we can assess the degree to which the orbital model matches the real world behavior of a satellite. That is the hardest accuracy to assess because it depends not only on the extent of the model but also on the orbit determination and observational data used to initialize the model. In addition, there are physical aspects of the real world behavior such as atmospheric density that are still not totally understood or well predicted. Therefore, the in-track error can dominate and grow to the size of the orbit itself. However, the orbit solution (in terms of the slowly varying elements) may match very closely. The other interpretation of accuracy is based on assessing how well the analytical solution matches the exact solution of the differential equations for the forces selected for inclusion in the model. Usually, we accept a numerical integration of the same differential equations as the "exact" standard for comparison.

In either case, it is important to realize that analytical solutions are not perfect closed-form solutions of the differential equations. Inclusion of even the simplest perturbations in the model results in a complex system of six first-order differential equations. The usual solution methods employ a transformation of

variables to successively remove the short-period and long-period periodic terms. These transformations are not exact, but rather are developed to some order of accuracy. The resulting transformed differential equations still contain secular terms and are usually highly coupled. And because the transformations were only carried out to a certain order accuracy, the transformed differential equations will have similarly limited accuracy. For example, the Brouwer (1959) analytical solution was carefully developed to first-order periodic and second order secular in the small parameter J_2. Thus, one can conclude that the Brouwer solution will have errors on the order of $O(J_2^3)$ that grow linearly with increasing prediction time. The secular differential equations of Brouwer are unique in that they were no longer coupled and could be solved. Such is the exception rather than the rule. Including any other perturbations beyond the zonal gravitation results in highly coupled secular differential equations. There is little established methodology for solving such systems of differential equations. Thus, depending on the cleverness of the developer, the analytical solution of a system of secular differential equations that includes terms through second order may very well contain errors larger than the expected third order error growth with time. This is the place where accuracy assessment of analytical solutions becomes most fuzzy.

The analytical models discussed below represent two different development approaches. One approach is to develop a model that provides moderate accuracy for all orbital altitudes and satellite physical sizes. The U.S. Air Force model, SGP4, and the U.S. Navy model, PPT3, are examples of this approach. The other approach is to determine an accuracy requirement, partition outer space into several orbital classes, and develop a suite of models each of which provides the required level of accuracy within its orbital class. This is the approach taken by the Russians in their orbital modeling, and the AP model in section 7.2.6 is an example.

7.2.1 Two-Body Model

The simplest analytical model of satellite motion is the two-body model, which assumes that both the Earth and the satellite are point masses. This is the only orbit model for which we have a closed-form solution. The two-body model is useful for visualization and back of the envelope analysis, but does not have sufficient accuracy for operational use.

7.2.1.1 Technical Definition

Vallado, D. A. 2007. *Fundamentals of Astrodynamics and Applications* (3rd ed.). Hawthorne, CA: Microcosm/Springer. (pp 89, algorithm 7)

7.2.2 Simple Analytical Model

When simplicity is desired but the model is to be used for behavior analysis over longer periods of time (weeks or more), then it is advisable to include simple perturbation models in the analysis. The most significant perturbation is due to the oblateness of the Earth, which is modeled by the first zonal harmonic, J_2, of the geopotential. This perturbation causes three secular effects.

— Linear precession of the line of nodes.

— Linear precession of the argument of perigee.

— Offset in the mean motion from the two-body value.

The next most important perturbation is due to atmospheric drag. This perturbation causes these secular effects.

— Decrease in the semimajor axis which generates an accompanying acceleration in the velocity direction.

— Decrease in the eccentricity to a small limiting, but nonzero, value.

A complete model of these effects will contain periodic and secular terms as well as a complicated dependence on atmospheric density. However, if we are only interested in understanding the long-term

behavior, we can ignore the periodic effects and just consider the secular effects. This can be accomplished by selecting one of the models discussed below (e.g., the SGP model) and using only the secular terms. This model is useful for constellation design and back of the envelope analysis, but does not have sufficient accuracy for operational use.

7.2.2.1 Technical Definition

Vallado, D. A. 2007. Fundamentals of Astrodynamics and Applications (3rd ed.). Hawthorne, CA: Microcosm/Springer. (pp. 686-688, including secular effects from drag on semimajor axis and eccentricity).

7.2.3 Simplified General Perturbations (SGP)

One of three widely used analytical models is the Simplified General Perturbations (SGP) model developed in 1963. It is based on the solution of Kozai, which includes the effects of the first three zonal harmonics (J_2, J_3, J_4) for the gravity model. In order to gain efficiency, the SGP model was obtained by dropping geopotential periodic terms of order $O(J_2 e)$ or smaller. Atmospheric drag is modeled as a semiempirical time rate of change of mean motion and a constant perigee height assumption. The SGP model does not include any third body gravitational or resonance effects. One important point to note is that the mean motion in the SGP model is the total time rate of change of the mean anomaly and thus is not related to the semimajor axis in the usual Kepler relationship.

7.2.3.1 Technical Definition

Hoots, F. R., & Roehrich, R. L. 1980. *Models for Propagation of the NORAD Element Sets.* Project SPACETRACK Rep. No. 3. Alexandria, VA: USAF Aerospace Defense Command.

7.2.4 Simplified General Perturbations #4 Model (SGP4)

Another of the widely used analytical models is the Simplified General Perturbations-4 (SGP4) model. The basis for SGP4 is an extensive analytical model known as AFGP4, developed by Lane and Cranford in 1969 for the U.S. Air Force. It includes the effects of the first four zonal harmonics (J_2, J_3, J_4, J_5) for the gravity model as given in the solution of Brouwer. Atmospheric drag is included using a power-law density function developed by Lane, Fitzpatrick, and Murphy (see Fitzpatrick, 1970, p. 327). The SGP4 model was obtained from the AFGP4 model by dropping any geopotential periodic term of order $O(J_2 e)$ or smaller as well as dropping most drag periodic terms. SGP4 was developed by Cranford in the early 1970s but was not published at that time. Later in the 1970s Bowman and Hujsak developed modifications to SGP4 to include the effects of point-mass gravitation from the moon and sun. They also included terms to model the most important resonance effects of satellites in synchronous and highly eccentric 12-hour orbits.

7.2.4.1 Technical Definition

Hoots, F. R., Schumacher, P. W. & Glover, R. A. 2004. History of Analytical Orbit Modeling in the U. S. Space Surveillance System. *Journal of Guidance, Control, and Dynamics, 27*(2): 174-185.

7.2.5 Position and Partials as a Function of Time (PPT3)

The third of the three widely used analytical models is Position and Partials as a function of Time (PPT) developed for the U.S. Navy in 1964. The current version (PPT3) includes the effects of the first four zonal harmonics (J_2, J_3, J_4, J_5) for the gravity model as given in the solution of Brouwer. In contrast to SGP and SGP4, the PPT3 model retains all terms from the Brouwer work. Atmospheric drag is modeled as a semi-empirical time rate of change of mean motion and eccentricity. It was adapted from the work of King-Hele by Richard Smith. In 1997 the Lunar, Solar, and resonance terms from the SGP4 model were added to the Naval Space Command PPT model to provide improved prediction of higher altitude satellites. This modified model became known as PPT3 and is documented in the work of Paul

Schumacher and Bob Glover. One important point to note is that the mean motion in the PPT3 model is the total time rate of change of the mean anomaly and thus is not related to the semimajor axis in the usual Kepler relationship.

7.2.5.1 Technical Definition

Schumacher, P. W., Jr., & Glover, R. A. 1995. *Analytical Orbit Model for U.S. Naval Space Surveillance—an Overview*. Paper AAS-95-427 presented at the AAS/AIAA Astrodynamics Specialist Conference, Halifax, Nova Scotia, Canada.

7.2.6 Russian Analytical Prediction Algorithm With Enhanced Accuracy (AP)

The Russians independently developed orbital models, each tailored to a particular orbital altitude class. These models were developed in the 1970s but have only been openly published recently. Thus, they have not yet experienced widespread use outside the Russian Space Surveillance System. One of the Russian models is the Analytical Prediction Algorithm with Enhanced Accuracy (AP) and is designed for near Earth satellites with eccentricity, $e < 0.05$. It includes an 8 × 8 geopotential field as well as a model of atmospheric density that includes dependence on a specifiable value of $F_{10.7}$ solar activity. The model uses a nonsingular set of orbital elements to avoid singularities for small eccentricity or inclination. The prediction error of this model compared to exact integration of the force model chosen is given in the following table.

Table 6 — AP prediction error in days

Prediction Interval	1	2	3	5	7	10
400 km < H < 1500 km	1.0 km	1.7 km	2.7 km	4.7 km	7.0 km	15.0 km
H > 1500 km	0.9 km	1.3 km	1.6 km	1.9 km	2.7 km	3.4 km

7.2.6.1 Technical Definition

Boikov, V. F., Makhonin, G. N., Testov, A. V., Khutorovsky, Z. N., & Shogin, A. N. 2009. Prediction Procedures Used in Satellite Catalog Maintenance. *AIAA Journal of Guidance, Control and Dynamics*, *32*(4): 1179-1199

7.2.7 Russian Analytical Prediction Algorithm (A)

The Russians also discuss an analytical model called the Analytical Prediction Algorithm (A). This model is used for approximate calculations such as observation correlation and detection of new orbits where efficiency is more important than high accuracy. It includes a 6 x 2 geopotential field as well as a model of atmospheric density that includes dependence on a specifiable value of $F_{10.7}$ solar activity. It is restricted to satellites having $e < 0.05$. The model uses a nonsingular set of orbital elements to avoid singularities for small eccentricity or inclination.

7.2.7.1 Technical Definition

Boikov, V. F., Makhonin, G. N., Testov, A. V., Khutorovsky, Z. N., & Shogin, A. N. 2009. Prediction Procedures Used in Satellite Catalog Maintenance. *AIAA Journal of Guidance, Control and Dynamics, 32*(4): 1179-1199.

7.2.8 Approved Variations

— In general, analytical theories are useful for quick analyses with low to modest accuracy requirements. Because the mathematical theory is different, computer code is sometimes required for programs with insufficient documentation, validation, test cases, and so forth. Use of such techniques is discouraged until adequate documentation and testing can be independently verified and reproduced at numerous locations.

— For SGP4, according to official AFSPC policy, there are no acceptable variations. Unfortunately, this is impractical for many users. Thus, use of a consolidated code is recommended. The paper given by Vallado et al. (2006) presents an openly available source code and is recommended for applications using TLE data.

7.3 Numerical Solutions of Earth Satellite Equations of Motion

The method of special perturbations (also referred to as numerical methods and Cowell's formulation) are the simplest and most straightforward of all the perturbation methods. An overwhelming advantage is the fact that the solution contains all secular and periodic variations introduced by the perturbing forces. Although the modern computer has eliminated many of the computational constraints, obtaining the result usually takes longer than analytical methods but can produce more accurate results. The solution rests with solving the perturbed equation of motion

$$\bar{a} = -\frac{\mu r}{r^3}\vec{r} + \bar{a}_{non-spherical} + \bar{a}_{drag} + \bar{a}_{3-body} + \bar{a}_{srp} + \bar{a}_{tides} + \bar{a}_{other} \tag{29}$$

To get the total result, all of the accelerations are summed together and numerically integrated. Although this equation looks innocuous, its solution continues to be a challenge. To account for all the major perturbations (central body, drag, third-body, solar radiation, thrust, tides, albedo, other), realistic expressions for the accelerations must be employed—and these are sometimes quite complex.

The variation of parameter equations can also be numerically integrated. This process is really a special perturbation solution although it focuses on orbital elements, rather than position and velocity vectors. Depending on the application, the immediate availability of orbital elements throughout a program simulation is usually very beneficial.

There are not specific implementations of numerical solutions because the mathematical technique is the same. However, many programs offer numerical solution techniques, yet they are not all the same fidelity. The number of force models available for use, the types of integrators, the treatment of data, all contribute to the accuracy that can be achieved with each program. Numerical propagation includes several areas in which we can define standards: coordinate systems, time, force models, and integration techniques. Figure 14 depicts the interrelations of each of these areas.

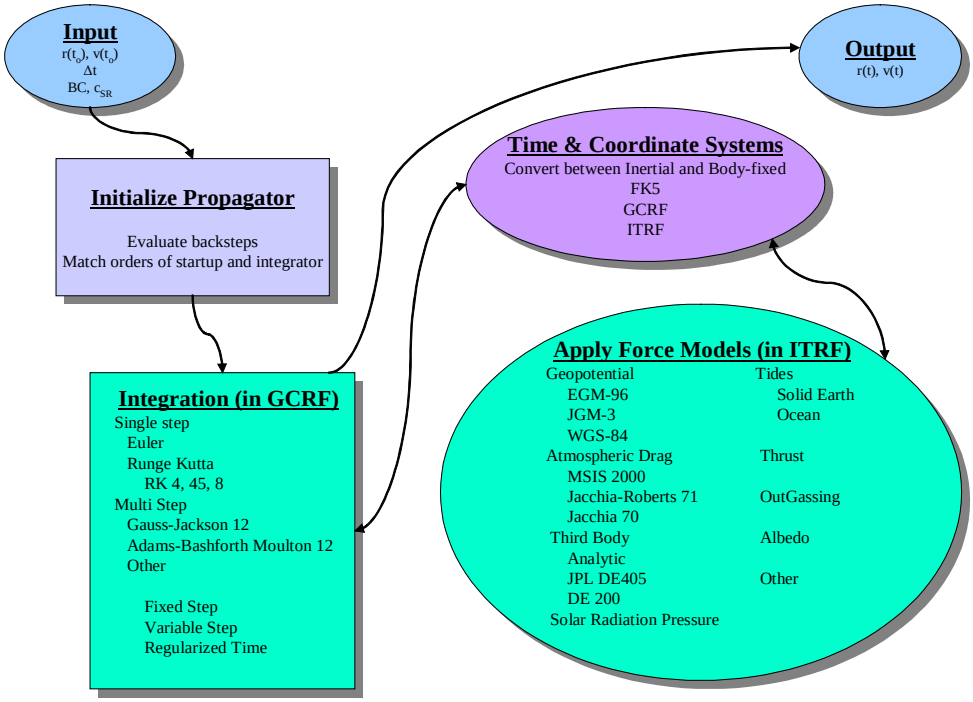

NOTE The interaction of several functions required for numerical propagation of an orbit is shown. Note the requirement to change from inertial and fixed reference frames at each integration step. The summation of forces can be accomplished in either the ITRF or the GCRF frames.

Figure 14 — Propagation flowchart

7.3.1 Integrators

In general, numerical techniques use fixed, variable, or regularized (e.g., *s*-integration) methods to move the satellite forward through time. The selection of one over another is generally based on the orbit type, but often on what is available. Because of the popularity of fixed-step methods, we describe those and simply introduce the others here.

Variable step size methods are often used for highly elliptical or "difficult" orbits. The technique uses smaller steps when the satellite is in higher perturbing effects regions, and larger steps in regions where the perturbations are less dynamic. The determination of the proper step size introduces additional computational complexity, but permits accurate evaluation of these special orbits. Variable step sizes are available for most popular integrators from Runge-Kutta to the Adams-Bashforth methods (See Krogh 1974 for instance). Unfortunately, one integrator isn't the best for *all* orbit types. The complexity of the integrating routine may be an additional hindrance because multistep methods usually require equally spaced values to form the polynomials. Adjusting the step size can require us to determine additional past values if the new step size doesn't match existing steps.

A generalized Sundman transformation can also be used to set up a regularization where time is replaced as the independent variable by another variable (*s*).

$$dt = cr^n\, ds$$

Several cases apply. If $n = 1$ and $c = \sqrt{\frac{s}{a}}$, s is the eccentric anomaly. If $n = 2$ and $c = \sqrt{\mu a(1-e^2)}$, s is the true anomaly. There is a computational price for this transformation because an additional equation

must be solved and the time steps for any back-substitution will no longer be equally spaced, but the increased performance for certain orbits may justify its use.

7.3.1.1 Runga–Kutta

Perhaps the most well-known numerical integrators are the Runge–Kutta methods originally developed by Carl Runge in 1895 and Wilhelm Kutta in 1901, which derive from a Taylor series. They differ from traditional Taylor series integrators because, instead of having to derive application-specific formulas for the higher derivative terms, the approximation is formed by simply using the slope at different points within the integration interval.

7.3.1.1.1 Technical Definition

Fehlberg, E. 1968. *Classical Fifth-, Sixth-, Seventh-, and Eighth-Order Runge-Kutta Formulas with Stepsize Control.* NASA Technical Report, TR-R-287. Huntsville, AL: NASA Marshall Space Flight Center.

7.3.1.2 Gauss-Jackson

Gauss-Jackson can be described as a Class II (or double-integration) multistep integrator. It uses backpoints as well as a summation term from epoch to compute the new position—and it integrates acceleration directly to position. It can be implemented as a predictor-corrector, or as a predictor only. The predictor-corrector scheme can also vary (i.e., PEC or PECE). Its main limitation is lack of step-size control, it is derived to be a fixed-step method. Using regularized time can help though for regulating the step about elliptical orbits.

7.3.1.2.1 Technical Definition

Berry, M. M., & Healy, L. M. 2004. Implementation of Gauss-Jackson Integration for Orbit Propagation, *Journal of the Astronautical Sciences,* 52(3): 331-357.

Maury, J. L. Jr., & Segal, G. P. 1969. *Cowell Type Numerical Integration as Applied to Satellite Orbit Computation.* NASA Technical Report TM-X-63542, X-553-69-46. Greenbelt, MD: Goddard Space Flight Center.

7.3.1.3 Adams-Bashforth

Vallado (2007: 529) provides a broad overview of the technique. Adams-Bashforth-Moulton is well established in existing programs. It's a multistep, fixed step-size method that estimates the state over time using previously determined back values of the solution. Although multistep methods perform only one evaluation for each step forward (compared to four for the fourth-order Runge-Kutta), they usually have a predictor and a corrector formula, so they often require two evaluations per step. Because these methods require back values, many aren't self-starting. Berry and Healy (2001) show that you can start multistep methods with iterative procedures that use the same method with the formulae shifted to correct the backpoints. You can also use a Runge-Kutta technique to supply the initial starting conditions, but you should match the order of both routines (e.g., eighth-order Runge-Kutta and an eighth-order Adams-Bashforth-Moulton).

7.3.1.3.1 Technical Definition

Bashforth, F., & Adams, J. C. 1883. *Theories of Capillary Action.* London: Cambridge University Press.

7.3.2 Approved Variations

Numerical integrators can affect the accuracy of an ephemeris. The lower order (e.g., 4^{th} order) Runge-Kutta techniques are useful for approximate studies. The higher order Runge-Kutta techniques, as well as the multistep methods, perform reasonably close as long as care is taken with respect to setting error

tolerances, step size, etc. These issues are beyond the current scope, but many references exist which discuss these trade-offs.

Numerical techniques have quickly become the standard for many operations. Vallado (2005) examined some basic steps required to ensure compatibility of results among different numerical integration programs. The conclusion was that mm-level comparisons are possible with proper understanding of the operation of each program. Nonconservative forces will require additional testing, and the variances can be larger, mostly due to the treatment of input data (geomagnetic and solar flux for instance).

7.4 Semianalytical Solutions of Artificial Earth Satellite Equations of Motion

Speed of computation has historically been the main reason for use of most analytical propagation theories. These theories, which were relatively easy to use and gave reasonable results, dominated numerical methods for many years. In fact, until modern times, numerical methods were not realistic for most problems. The analytical techniques were accurate enough for scientific uses of the day, but space flight to the planets would not have been possible without the use of numerical integration techniques. Semianalytical techniques were developed with modest computational capabilities, and they served to combine speed and accuracy for extended propagation intervals. Today's computers have made numerical integration possible and very popular for operational systems. These systems depend on numerical-integration programs with sophisticated mathematical models of perturbing accelerations, which yield very precise results, especially in the near future. However, semianalytical theories are a significant resource for large and accurate long-term studies, as well as understanding the nature of the perturbative effects on the orbital elements.

Speed and accuracy can be traded off by combining the best features of numerical and analytical techniques. A semianalytical approach gets the best speed and accuracy by taking advantage of the characteristics of the effects present on a satellite's orbit. The underlying approach separates the short-periodic contributions from the long-periodic and secular effects so that mean element rates can be numerically integrated. This is accomplished with three equations: equations of motion for the mean elements, equations for the short-periodic coefficients (which are functions of the mean elements), and a Fourier series that allows the construction of the short-periodic motion in the elements, given the short periodic coefficients. Because both the mean elements and the short-periodic coefficients are slowly varying, they are both open to interpolation processes, and therefore larger step sizes (typically on the order of a day). Hermite interpolation is appropriate for the mean elements because the mean element rates are available and Lagrange interpolation is appropriate for the short-periodic coefficients. The mean element and short-periodic coefficient interpolation grids do not have to be aligned. Many semianalytical techniques exist today—some of the better known techniques are listed in the technical definition section.

7.4.1 Technical Definitions

There are several semianalytical techniques in use today. Each has benefits and specific applications for use. Others are general purpose.

7.4.1.1 Draper Semianalytical Satellite Theory (DSST)

Paul Cefola and his colleagues at the Charles Stark Draper Laboratory developed this theory in the mid-1970s and early 1980s. Many conference proceedings and technical reports detail the approach. Cefola (1972), McClain (1992, 1978) and Danielson et al. (1995) present excellent summaries of the mathematical technique used in this theory. Early (1986) presents a broad overview of the rationale behind the theory. Neelon et al (1997) provided an updated snapshot of the status at that time. Several Masters Theses have been conducted using DSST, each of which has extended the capabilities (i.e., Lyon, 2004; Smith, 1999).

DSST has many distinctions over other semianalytical techniques, including an extensive treatment of perturbing forces (central body including tesseral harmonics, drag, third-body, solar-radiation, and others); great flexibility, so you can tailor the algorithm to the application; recent improvements to

documentation; and wide use. Although some applications don't require the ability to incorporate many force models, others do. It's useful to have a theory which accounts for all significant perturbations. History has shown that, once a theory gains widespread use, the inherent assumptions of the theory are soon forgotten, and it's often used inappropriately. A theory that handles many different scenarios lessens the possibility for failure due to unintended application.

Neither of the DSST interpolators (mean element or short-periodic coefficients) need to be constructed unless there is an 'off-grid' output point. DSST is cast in terms of the nonsingular equinoctial elements. Finally, the DSST equinoctial mean elements are very good as solve-for variables in a Kalman filter.

McClain, W. D. 1978. *A Recursively Formulated First-Order Semianalytic Artificial Satellite Theory Based on the Generalized Method of Averaging* (Vol. 2). CSC/TR-78/6001. Falls Church, VA: Computer Sciences Corporation.

McClain, W. D. 1992. *Semianalytic Artificial Satellite Theory. Vol. 1.* Cambridge, MA: Charles Stark Draper Laboratory.

Danielson, D. A., Neta, B., & Early, L. W. 1994. *Semianalytical Satellite Theory (SST): Mathematical Algorithms.* Technical Report NPS-MA-94-001. Monterey, CA: Naval Postgraduate School.

Danielson, D. A. et al. 1995. *Semianalytical Satellite Theory (SST): Mathematical Algorithms.* Technical Report NPS-MA-95-002. Monterey, CA: Naval Postgraduate School.

7.4.1.2 HANDE

The HANDE model was intended to replace the analytical SGP4 model. It incorporated the effects of the Jacchia dynamic atmosphere models for the average solar flux during the propagation interval, while retaining the speed and character of an analytic general perturbations model. It also included the full Brouwer gravity solution, much of which had been dropped for the SGP4 simplification. The code was implemented in the operational system, but its use is unknown.

HANDE uses numerical quadrature to get quantities related to atmospheric drag and this is a key concept in HANDE. But this calculation is done once, at epoch. After that, HANDE looks like an analytical theory.

Hoots, F. R. 1982. *An Analytical Satellite Theory Using Gravity and a Dynamic Atmosphere.* AIAA-82-1409. Paper presented at the AIAA/AAS Astrodynamics Conference, San Diego, CA.

Hoots, F. R., & France, R. G. 1987. An Analytic Satellite Theory Using Gravity and a Dynamic Atmosphere. *Celestial Mechanics*, *40*(1): 1–18.

7.4.1.3 SALT

The physical models for semi-analytical Liu theory (SALT) are the full Brouwer geopotential: zonals through J5, a Jacchia 1970 atmosphere density, and J2 short periodics.

Liu, J. 1973. *A Second-order Theory of an Artificial Satellite under the Influence of the Oblateness of the Earth.* M-240-1203. CA: Northrop Services.

Liu, J. 1974. Satellite Motion About an Oblate Earth. *AIAA Journal,* 12: 1511–1516.

7.4.1.4 USM

The Russians have several techniques for orbital propagation. Some, like the NA and NAP theories are space surveillance-specific satellite theories. They include much more physics than semianalytical techniques like SALT. The high eccentricity theory due to Testov is of particular interest. The USM method is a semianalytical technique comparable to the DSST method, but it uses analytical averaging on a simplified GOST-84 atmospheric drag model.

Yurasov, V. 1996. *Universal Semianalytic Satellite Motion Propagation Method.* U.S.–Russian Second Space Surveillance Workshop, Adam Mickiewicz University, Poznan, Poland.

Cefola, P. J., Yurasov, V. S., Folcik, Z. J., Phelps, E. B., Proulx, R. J., & Nazarenko, A. I. 2003. *Comparison of the DSST and the USM Semi-Analytical Orbit Propagators*. AAS 03-236. Paper presented at the AAS/AIAA Space Flight Mechanics Meeting, Ponce, Puerto Rico, February.

7.4.1.5 European Semianalytical Techniques

The Europeans have done some work on semianalytical theories, primarily with the work of Bruinsma, Metris, and Exertier (1997). The theory uses Delaunay canonical variables that allow the separation of short-periodic from the long-periodic and secular motion. At the time of publication, nonconservative forces were not included. The long and short periodic terms are separated using the Lie transformation of Deprit (1969). There is some discussion of eccentricity restrictions—probably from the restriction of the Poisson series.

Bruinsma, S., Exertier, P. , & Metris, G. 1997. *Semi-analytical Theory of Mean Orbital Motion: A New Tool for Computing Ephemerides.* Paper presented at 12th International Space Flight Dynamics Symposium, Darmstadt, Germany.

7.4.2 Approved Variations

As with analytical techniques, the semianalytical techniques will sometimes require actual computer code to provide consistent results. However, in this case, the need is generally driven by the complexity of the method as opposed to insufficient testing and documentation. Some techniques, like DSST and USM, are general purpose routines that are accurate over many satellite classes. Others, like SALT, are designed for a particular satellite orbital class, and are therefore limited. A key factor in choosing to use one technique over another rests on intended use (all satellite classes), required accuracy, availability to generate or use mean elements particular to that method, and documentation of the method.

7.5 Summary Recommended Practice for Propagation Methods

1) Regularized time formulations should be used for highly eccentric orbits if results indicate adequate performance is not achievable with existing standard formulations.

2) Although the choice of a particular numerical propagator rests on the desired accuracy and the tools/money available, the following guidelines are presented:

    a) Analytical techniques are best for low-accuracy, fast calculations.

    b) Numerical techniques are best for high-accuracy calculations in which computing time is not a major factor.

    c) Semianalytical techniques are best for calculations that have variable accuracy and speed requirements.

3) Fully define the reference system, the scale (e.g., gravitational parameter), mathematical technique, and the origin with all state vectors to remove ambiguity in the delivered product.

4) Include all estimated parameters in any numerically generated product.

5) Computer code is not a standard per se. There are a few exceptions where the code is publicly available and consistent with the technical documentation. The best approach is to fully document the mathematical equations and let that be the standard.

8 Bibliography

For useful references related to the topic of propagation, refer to Annex A.

Barlier, F., et al. 1978. A Thermospheric Model Based on Satellite Drag Data. *Annales de Geophysics*, 34(1): 9-24.

Bashforth, F., & Adams, J. C. 1883. *Theories of Capillary Action.* London: Cambridge University Press.

Berry, M. M., & Healy, L. M. 2004. Implementation of Gauss-Jackson Integration for Orbit Propagation, *Journal of the Astronautical Sciences*, *52*(3): 331-357.

Boikov, V. F., Makhonin, G. N., Testov, A. V., Khutorovsky, Z. N. and.Shogin, A. N., Prediction Procedures Used In Satellite Catalog Maintenance, *AIAA Journal of Guidance, Control and Dynamics, 32*(4): 1179-1199.

Bruinsma, S., Exertier, P. & Metris, G. 1997. *Semi-analytical Theory of Mean Orbital Motion: A New Tool for Computing Ephemerides.* Paper presented at 12th International Space Flight Dynamics Symposium, Dramstadt, Germany.

Chao, B. F., & R. J. Eanes. 1995. Global Gravitational Changes due to Atmospheric Mass Redistribution as Observed by the Lageos Node Residual. *Geophysical Journal International, 122,*3: 755-764.

Danielson, D. A., Neta, B., & Early, L. W. 1994. *Semianalytical Satellite Theory (SST): Mathematical Algorithms*. Technical Report NPS-MA-94-001. Monterey, CA: Naval Postgraduate School.

Danielson, D. A. et al. 1995. *Semianalytical Satellite Theory (SST): Mathematical Algorithms*. Technical Report NPS-MA-95-002. Monterey, CA: Naval Postgraduate School.

Eanes, R. J., & Bettadpur, S. V. 1995. The CSR3.0 Global Ocean Tide Model. *Technical Memorandum CSR-TM-95-06,* Center for Space Research, The University of Texas at Austin.

Fehlberg, E. 1968. *Classical Fifth-, Sixth-, Seventh-, and Eighth-Order Runge-Kutta Formulas with Stepsize Control.* NASA Technical Report, TR-R-287. Huntsville, AL: NASA.

Fey, A., Gordon, D., & Jacobs, C. S. (Eds.). 2009. The Second Realization of the International Celestial Reference Frame by Very Long Baseline Interferometry. IERS Technical Note 35. Frankfurt am Main, Germany: Verlag des Bundesamts für Kartographie und Geodäsie. http://www.iers.org/IERS/EN/Publications/TechnicalNotes/tn35.html

GOST. 2004. Earth's Upper Atmosphere Density Model for Ballistics Support of Flights of Artificial Earth Satellites. GOST R 25645.166-2004, Moscow: Publishing House of the Standards. (English translation by Vasiliy S. Yurasov in 2006 and edited by Paul J. Cefola in 2007).

Hedin, A. E. 1987. MSIS-86 Thermospheric Model. *Journal of Geophysical Research, 92:* 4649-4662.

Hedin, A. E. 1991. Extension of the MSIS Thermosphere Model Into the Middle and Lower Atmosphere. *Journal of Geophysical Research, 96:* 1159-1172.

Hickey, M. P. 1998. *The NASA Engineering Thermosphere Model,* NASA CR-179359, Washington, D.C. http://modelweb.gsfc.nasa.gov/atmos/met.html.

Hoots, F.. R. 1982. *An Analytical Satellite Theory Using Gravity and a Dynamic Atmosphere.* Paper AIAA-82-1409 presented at the AIAA/AAS Astrodynamics Conference, San Diego, CA.

Hoots, F. R., & France, R. G. 1987. An Analytic Satellite Theory Using Gravity and a Dynamic Atmosphere. *Celestial Mechanics, 40*(1): 1–18.

Hoots, F. R., & Roehrich, R. L. 1980. *Models for Propagation of NORAD Element Sets.* Spacetrack Report #3. Washington, DC: Aerospace Defense Command, U.S. Air Force.

Hoots, F. R., Schumacher, P. W., & Glover, R. A. 2004. History of Analytical Orbit Modeling in the U. S. Space Surveillance System. *Journal of Guidance, Control, and Dynamics, 27*(2): 174-185.

Jacchia, L. G. 1965. Static Diffusion Models of the Upper Atmosphere with Empirical Temperature Profiles. *Smithsonian Contributions to Astrophysics*, *8:* 215-257.

Jacchia, L. G. 1970. *New Static Models for the Thermosphere and Exosphere with Empirical Temperature Profiles*. SAO Special Report No. 313. Cambridge, MA: Smithsonian Institution Astrophysical Observatory.

Jacchia, L. G. 1971. *Revised Static Models for the Thermosphere and Exosphere with Empirical Temperature Profiles*. SAO Special Report No. 332. Cambridge, MA: Smithsonian Institution Astrophysical Observatory.

Jacchia, L. G. 1977 Thermospheric Temperature, Density, and Composition: New Models. SAO Special Report 375. Cambridge, MA: Smithsonian Institution Astrophysical Observatory.

Justus, C. G., & Johnson, D. L. 1999. *The NASA/MSFC Global Reference Atmospheric Model – 1999 Version (GRAM-99).* NASA/TM 1999-209630. Huntsville, AL: NASA.

Justus, C. G., Duvall, A., & Keller, V. W. 2004. Earth Global Reference Atmospheric Model (GRAM-99) and Trace Constituents. Paper C4.1-0002-04, Presented at 35th COSPAR Scientific Assembly Paris, France.

Kaplan, G. H. (Ed.). 1981. The IAU Resolutions on Astronomical Constants, Time Scales, and the Fundamental Reference Frame. USNO Circular No. 163. Washington, DC: U.S. Naval Observatory.

Kaplan, G. H. 2005. The IAU Resolutions on Astronomical Reference Systems, Time Scales, and Earth Rotation Models, Explanation and Implementation. U.S. Naval Observatory Circular No. 179. http://aa.usno.navy.mil/kaplan/Circular.html

Letellier, T., Lyard, F., & Lefebre, F. 2004. The New Global Tidal Solution: FES2004. Paper presented at the Ocean Surface Topography Science Team Meeting, St. Petersburg, Florida.

Lemoine, F. G. et al. 1998. The Development of the Joint NASA GSFC and NIMA Geopotential Model EGM96. NASA/TP-1998-206861. Greenbelt, MD: NASA Goddard Space Flight Center.

Liu, J. 1973. A Second-order Theory of an Artificial Satellite Under the Influence of the Oblateness of the Earth. M-240-1203. Northrop Services.

Liu, J. 1974. Satellite Motion About an Oblate Earth. *AIAA Journal, 12*: 1511–1516.

Matsumoto, K., Takanezawa, T. & Ooe, M. 2000. Ocean Tide Models Developed by Assimilating TOPEX/POSEIDON Altimeter Data into Hydrodynamical Model: A Global Model and a Regional Model around Japan. *Journal of Oceanography, 56,* 567-581:, 2000.

Maury, J. L. Jr., & Segal, G. P. 1969. Cowell Type Numerical Integration as Applied to Satellite Orbit Computation. NASA Technical Report TM-X-63542, X-553-69-46. Greenbelt, MD: NASA Goddard Space Flight Center.

McCarthy, D. D., & Petit, G. (Eds.). 2004. *IERS Conventions (2003)*, IERS Technical Note No. 32. Frankfurt am Main, Germany: Verlag des Bundesamts fur Kartographie und Geodasie.

McClain, W. D. 1978. *A Recursively Formulated First-Order Semianalytic Artificial Satellite Theory Based on the Generalized Method of Averaging.* Vol. 2. CSC/TR-78/6001: Greenbelt, MD: Computer Sciences Corp.

McClain, W. D. 1992. *Semianalytic Artificial Satellite Theory.* Vol. 1. Cambrigde, MA: Charles Stark Draper Laboratory.

Nerem, R. S. et al. 1994. Gravity Model Developments for TOPEX/POSEIDON: Joint Gravity Models 1 and 2. *Journal of Geophysical Research*, *99* (C12): 24, 421-24, 447.

NIMA. 2000. *Department of Defense World Geodetic System 1984.* NIMA-TR 8350.2, 3rd ed, Amendment 1. Washington, DC: Headquarters, National Imagery and Mapping Agency.

Picone, J. M., Hedin, A. E., & Drob, D. P. 2002. NRLMSISE-00 Empirical Model of the Atmosphere: Statistical Comparisons and Scientific Issues. *Journal of Geophysical Research,* 107, A12: 1468.

Ray, R. D. 1999. A Global Ocean Tide Model from TOPEX/POSEIDON Altimetry: GOT99. NASA TM 209478. Greenbelt, MD: Goddard Space Flight Center.

Ries, J. C., Shum, C. K., & Tapley, B. D. 1993. Surface Force Modeling for Precise Orbit Determination. *Geophysical Monograph, 73,* 13: 111-124.

Roberts, C. E., Jr. 1971. An Analytic Model for Upper Atmosphere Densities Based upon Jacchia's 1970 Models. *Celestial Mechanics*. 4, 314: 368–377.

Rubincam, D. P. 1988. Yarkovsky Thermal Drag on Lageos. *Journal of Geophysical Research. 93,* 13805.

Schumacher, P. W., Jr., & Glover, R. A. 1995. Analytical Orbit Model for U.S. Naval Space Surveillance—an Overview. Paper AAS-95-427 presented at the AAS/AIAA Astrodynamics Specialist Conference. Halifax, Nova Scotia, Canada.

Sehnal, L. 1981. Effects of the Terrestrial Infrared Radiation Pressure on the Motion of an Artificial Satellite. *Celestial Mechanics, 25,* 169.

Soffel, M. 1989. *Relativity in Astrometry, Celestial Mechanics, and Geodesy.* Berlin, Germany: Springer-Verlag.

Standish, M. 1990. The Observational Basis for JPL's DELOD, the Planetary Ephemerides of the Astronomical Almanac. *Astronomy and Astrophysics, 233*: 252-271.

Tapley, B. et al. 2005. GGM02 - An improved Earth gravity field model from GRACE. *Journal of Geodesy*, *79*: 467-478.

Tapley, B. D. et al. 1996. The Joint Gravity Model 3. *The Journal of Geophysical Research*, *101*, B12: 28029-28049.

Thuillier, G., J., Falin, L., & Barlier, F. 1977. Global Experimental Model of the Exospheric Temperature Using Optical and Incoherent Scatter Measurements. *Journal of Atmospheric and Terrestrial Physics, 39*: 1195. Computer code in the paper.

U.S. Standard Atmosphere. 1976. Washington, DC: U.S. Government Printing Office.

Annex A References (Informative)

Arsenault, J. L., Chaffee, Lois, and Kuhlman, J. R. 1964. General Ephemeris Routine Formulation Document. ESD-TDR-64-522, Aeronutronic Publication U-2731.

Astronomical Almanac. 2010. Washington, DC: U. S. Government Printing Office. http://asa.usno.navy.mil/index.html

Baker, R. M. 1967. *Astrodynamics, Applications and Advanced Topics.* New York: Academic Press.

Barkstrom, B. R. 1984. The Earth Radiation Budget Experiment (ERBE). *Bulletin of American Meteorological Society*, *65:* 1170-1185.

Bergstrom, S. 2002. *An Algorithm for Reducing Atmospheric Density Model Error Using Satellite Observation Data in Real-time*. (M.S. Thesis.) Department of Aeronautics and Astronautics, Massachusetts Institute of Technology, Cambridge.

Bevington, P., & Robinson, D. K. 2002. *Data Reduction and Error Analysis for the Physical Sciences*. New York: McGraw Hill.

Bowman, B. 1971. *A First Order Semi-Analytic Perturbation Theory for Highly Eccentric 12 Hour Resonating Satellite Orbits.* Peterson AFB, CO: NORAD.

Bowman, B. 2008. *A New Empirical Thermospheric Density Model JB2006 Using New Solar Indices.* AIAA-2008-6438. Paper presented at the AIAA/AAS Astrodynamics Specialist Conference. Honolulu, HI.

Brouwer, D. 1959. Solutions of the Problem of Artificial Satellite Theory Without Drag. *Astronomical Journal,* 64, 1274: 378–397.

Brouwer, D., & Hori, G. 1961. Theoretical Evaluation of Atmospheric Drag Effects in the Motion of an Artificial Satellite. *The Astronomical Journal*, *66,* 5:193-225.

Brouwer, D., & Clemence, G. M. 1961. *Methods of Celestial Mechanics.* New York: Academic Press.

Capitaine, N., & Wallace, P. T. 2006. High precision methods for location the celestial intermediate pole and origin. *Astronomy & Astrophysics*, 450: 855-872.

Capitaine, N., Wallace, P. T., & Chapront, . 2003. Expressions for IAU 2000 Precession Quantities. *Astronomy and Astrophysics,* 412: 567-586.

Carter, D., McClain, W. D., & Cefola, P. J. 1987. *LANDSAT Orbit Determination Study Technical Report.* #CSDL-R-1952. Cambridge, MA: Charles Stark Draper Laboratory.

Cartwright D. E., & Ray, R. D. 1990. Oceanic Tides from Geosat Altimetry. *Journal of Geophysical Research, 95:* 3069.

Cartwright, D. E., & Tayler, R. J. 1971. New computations of the tide-generating potential. *Geophysical Journal Royal Astronomical Society, 23*: 45-74.

Cefola, P. J. 1972. *Equinoctial Orbit Elements—Application to Artificial Satellite Orbits.* AIAA 72-937. Paper presented at the AIAA/AAS Astrodynamics Conference, Palo Alto, CA.

Cefola, P. J., & Fonte, D. J. 1996. *Extension of the Naval Space Command Satellite Theory to Include a General Tesseral m-daily Model.* AIAA-96-3606. Paper presented at the AIAA/ AAS Astrodynamics Conference, San Diego, CA.

Cefola, P. J., Nazarenko, A. I., et al. 1999. *Neutral Atmosphere Density Monitoring Based on Space Surveillance System Orbital Data.* AAS-99-383. Paper presented at the AAS/AIAA Astrodynamics Specialist Conference, Girdwood, AK.

Champion, K. S. W., Cole, A.E. & Kantor, A. J. 1985. Standard and Reference Atmospheres. In A. S. Jursa (Ed.), *Handbook of Geophysics and the Space Environment* (pp. 14-1-14-43). Hanscomb AFB, MA: Air Force Geophysics Laboratory.

Chao, B. F., & Au, A. Y. 1991. Temporal Variation of Earth's Zonal Gravitational Field Caused by Atmospheric Mass Redistribution, 1980-1988. *Journal of Geophysical Research, 96:* 6569-6575.

Chapman, S., & Bartels, J. 1940. *Geomagnetism.* (2 vols.). Oxford, England: Chapman Press.

Cheng, M. K., Eanes, R. J., Shum, C. K. , Schutz, B. E., & Tapley, B. D. 1989. Temporal Variations in Low Degree Zonal Harmonics from Starlette Orbit Analysis. *Geophysical Research Letters, 16:* 393.

Coppola. V., Seago, J. H., & Vallado, D. A. 2009. The IAU 2000A and IAU 2006 Precession-Nutation Theories and Their Implementation. Paper AAS 09-159. In Segerman, A. M. et al. (Eds.), Spaceflight Mechanics 2009: Advances in the Astronautical Sciences (vol. 134, pp. 919-938). San Diego, CA: American Astronautical Society.

de Sitter, W. 1916. On Einstein's Theory of Gravitation and its Astronomical Consequences. *Monthly Notice of the Royal Astronomical Society, 77,* 155.

Defense Mapping Agency. 1987. Supplement to Department of Defense World Geodetic System 1984 DMA Technical Report: Part I - Methods, Techniques, and Data Used in WGS 84 Development. DMA TR 8350.2-A. Washington, DC: U.S. Naval Observatory.

Defense Mapping Agency. 1987. Supplement to Department of Defense World Geodetic System 1984 Technical Report: Part II - Parameters, Formulas, and Graphics for the Practical Application of WGS 84. DMA TR 8350.2-B. Washington, DC: U.S. Naval Observatory.

Doodson, A. T. 1921. The Harmonic Development of the Tide-Generating Potential. *Proceedings of the Royal Society of London, Series A, 100,* 704: 305-329.

Eanes, R. J., & Bettadpur. S. V. 1996. Temporal Variability of Earth's Gravitational Field From Satellite Laser Ranging. In R. H. Rapp, A. A. Cazenave, & R. S. Nerem (Eds.), *Global Gravity Field and its Variations, IAG Symposia, 116.* Berlin, Germany: Springer-Verlag.

Eanes, R. J., Tapley, B. D., & Schutz, B. E. 1983. Earth and Ocean Tide Effects on Lageos and Starlette. *Proceedings of the Ninth International Symposium on Earth Tide* (pp. 239-250). Stuttgart, Germany: Schweizerbart.

Early, L. W. 1986. A Portable Orbit Generator Using Semianalytical Satellite Theory. AIAA 86-2164-CP Paper presented at the AIAA/AAS Astrodynamics Conference, Williamsburg, VA.

Fairhead, L., & Bretagnon, P. 1990. An Analytical Formula for the Time Transformation TB-TT. *Astronomy and Astrophysics,* 229: 240-247.

Fitzpatrick, P. M. 1970. *Principles of Celestial Mechanics.* New York: Academic Press.

Fitzpatrick, P. M., & Findley, G. B. 1960. *The Tracking Operation at the National Space Surveillance Control Center.* Directorate of Aerospace, Air Proving Ground Center, Eglin AFB, Florida.

Folkner, W. M. et al. 1994. Determination of the extragalactic-planetary frame tie from joint analysis of radio interferometric and lunar laser ranging measurements. *Astronomy and Astrophysics,* 287: 279-289.

Gaposchkin, E. M. 1987. Evaluation of Recent Atmospheric Density Models. Paper AAS-87-557. *Proceedings of 1987 AAS/AIAA Astrodynamics Conference,* San Diego, CA.

Gaposchkin, E. M. 1994. *Calculation of Satellite Drag Coefficients.* Technical Report 998. Lexington, MA: MIT Lincoln Laboratory.

Gaposchkin, E. M., & Coster, A. J. 1987. Evaluation of New Parameters for Use in Atmospheric Models. Paper AAS-87-555. *Proceedings of 1987 AAS/AIAA Astrodynamics Conference,* San Diego, CA.

Gorochov, Y. P., & Nazarenko, A. I. 1982. *Methodical Points in Building Models of the Fluctuation of the Atmosphere Parameters.* Astronomicheskii Sovet Akademii Nauk SSSR, Vol. 80. A copy was obtained by the MIT Lincoln Laboratory Library in January 2004 from the CISTI Document Delivery Service and translated by MIT Aeronautics and Astronautics Department graduate student Kalina Galabova in February 2004.

Granholm, G., Cefola, P., Nazarenko, A., & Yurasov, V. 2000. *Near-Real Time Atmospheric Density Correction Using NAVSPASUR Fence Observations.* Paper AAS-00-179 presented at the AAS/AIAA Spaceflight Mechanics Conference, Clearwater, FL.

Guinot, B. 1979. Basic Problems in the Kinematics of the Rotation of the Earth. In D. D. McCarthy & J. D. H. Pilkington (Eds.), *Time and the Earth's Rotation: Proceedings of the Eighty-Second IAU Symposium* (A79-53001 24-89), pp. 7-18. Dordrecht, The Netherlands: D. Reidel Publishing.

Guinot, B., & Seidelmann, P. K. 1988. Time scales: Their History, Definition and Interpretation. *Astronomy and Astrophysics*, *194*: 304-308.

Harada, W., & Fukushima, T. 2003. Harmonic Decomposition of Time Ephemeris TE405. *The Astronomical Journal*, *126*: 2557–2561.

Heiskanen, W. H., & Moritz, H. 1967. *Physical Geodesy.* San Francisco, Freeman.

Hilton, C. G. 1963. *The SPADATS Mathematical Model.* ESD-TDR-63-427, Aeronutronic Publication U-2202.

Hilton, C. G., & Kuhlman, J. R. 1966. *Mathematical Models for the Space Defense Center.* Philco-Ford Corporation Publication U-3871, pp. 17-28.

Hoots, F. R. 1998. *A History of Analytical Orbit Modeling in the United States Space Surveillance System*. Third U.S./Russian Space Surveillance Workshop, Washington, DC.

Huang, C., Ries, J. C., Tapley, B. D. & Watkins, M. M. 1990. Relativistic Effects for Near-Earth Satellite Orbit Determination. *Celestial Mechanics, 48,* 2:167-185.

Hujsak, R. S. 1979. *SPACETRACK Report #1: A Restricted Four Body Solution for Resonating Satellites Without Drag.* Colorado Springs, CO: USAF Aerospace Defense Command.

Jacchia, L. G. 1981. Empirical Models of the Thermosphere and Requirements for Improvements. *Advances in Space Research, 1,* 12: 81-86.

Jacchia, L. G., & Slowey, J. W. 1981. Analysis of Data for the Development of Density and Composition Models of the Upper Atmosphere. Air Force Geophysics Laboratory Report AFGL-TR-81-0230 (AD-A-100420). Hanscom AFB, MA.

James, T. S., & Ivins, E. R. 1995. Present-day Antarctic Ice Mass Changes and Crustal Motion. *Geophysical Research Letters 22:* 973-976.

Jursa, A. S. (Ed.). 1985. *Handbook of Geophysics and the Space Environment*. Air Force Geophysics Laboratory, Air Force Systems Command, Cambridge, MA.

Kaula, W. M. 1966. *Theory of Satellite Geodesy*. Waltham, MA: Blaisdell.

King-Hele, D. 1964. *Theory of Satellite Orbits in an Atmosphere.* London: Butterworths.

Kinoshita, H., McCarthy, D. D., & Seidelmann, P. K. 1982. The New Definition of Universal Time. *Astronomy and Astrophysics*, *105*: 359-361.

Kovalevsky, J. et al. 1997. The HIPPARCOS Catalogue as a Realisation of the Extragalactic Reference System. *Astronomy and Astrophysics, 323*: 620-633.

Kovalevsky, J. & Seidelmann, P. K. 2004, Fundamentals of Astrometry. London: Cambridge University Press.

Kozai, Y. 1959. The Motion of a Close Earth Satellite. *Astronomical Journal,* 64, 1274: 367–377.

Krogh, F. T. 1974. *Changing Stepsize in the Integration of Differential Equations Using Modified Divided Differences.* JPL Internal Technical Memorandum No. 312 (March 20, 1973).

Lambeck, K. 1988. *Geophysical Geodesy: The Slow Deformations of the Earth.* London: Oxford University Press.

Lane, M. H. 1965. *The Development of an Artificial Satellite Theory Using Power-Law Atmospheric Density Representation.* AIAA 65-35. Paper presented at the 2nd Aerospace Sciences Meeting, New York.

Lane, M. H., & Cranford, K. H. 1969. *An Improved Analytical Drag Theory for the Artificial Satellite Problem.* AIAA 69-925. Paper presented at the AIAA/AAS Astrodynamics Conference, Princeton, NJ.

Lane, M. H., Fitzpatrick, P. M., & Murphy, J. J. 1962. *On the Representation of Air Density in Satellite Deceleration Equations by Power Functions with Integral Exponents*. Deputy for Aerospace, Air Proving Ground Center, Eglin AFB, Florida.

Lane, M. H., & Hoots, F. R. 1979. *SPACETRACK Report #2. General Perturbations Theories Derived From the 1965 Lane Drag Theory.* Colorado Springs, CO: USAF Aerospace Defense Command.

Lense, J., & Thirring, H. 1984. Uber die Einfluss der Eigenrotation der Zentralkrper auf die Bewegung der Planeten und Monde nach der Einsteinschen Gravitationstheorie. *Phys. Zeitschrt., 19,* 156, 1918; English translation by B. Mashoon, et. al., *Gen. Relativ. Gravit., 16,* 711.

Li, X., Shum, C. K., & Tapley, B. D. 1996. *Accuracy Evaluations of Global Ocean Tide Models.* Technical Memorandum CSR-96-3. Texas: Center for Space Research, The University of Texas at Austin.

Lombardi, M. A. 2002. NIST Time and Frequency Services. *NIST Special Publication 432 (Revised)*, p. 21. http://www.boulder.nist.gov/timefreq/general/pdf/1383.pdf

Lyddane, R. H. 1963. Small Eccentricities or Inclinations in the Brouwer Theory of the Artificial Satellite. *The Astronomical Journal*, *68*, 8: 555-558.

Lyon, R. H. 2004. *Geosynchronous Orbit Determination Using Space Surveillance Network Observations and Improved Radiative Force Modeling*. (Master's Thesis). Cambridge, MA: Massachusetts Institute of Technology.

Ma, C. et al. 1998. The International Celestial Reference Frame as Realized by Very Long Baseline Interferometry. *Astronomical Journal, 116*: 516-546.

Marcos, F. A. et al. 1993. *Satellite Drag Models: Current Status and Prospects.* AAS-93-621. Paper presented at the AAS/AIAA Astrodynamics Specialist Conference, Victoria, BC, Canada.

Marcos, F. A. et al. 2006. *Accuracy of the Earth's Thermospheric Neutral Density Models.* AIAA-2006-6167. Paper presented at the AIAA/AAS Astrodynamics Specialist Conference, Keystone, CO.

McCarthy, D. 1996. *IERS Conventions (1996).* IERS Technical Note #21. Paris: IERS.

Moritz, H. 1988. Geodetic Reference System 1980. *Bulletin Geodesique, 54*, 3: 395-405.

Müller, E. A. (Ed.) 1977. *Transactions of the International Astronomical Union, Vol. XVIB: Proceedings of the Sixteenth General Assembly*. Dordrecht, The Netherlands: Kluwer Academic Publishers.

Nazarenko, A. 1999. T*he Description of a Theoretical Fundamentals of Universal Semianalytical Method. Development Formulas for Perturbation Account.* Report CSDL-C-6502 prepared by the Scientific Industrial Firm NUCOL for the Charles Stark Draper Laboratory, Cambridge, MA.

Neelon, J. G., Cefola, P. J., & Proulx, R. J. 1997. *Current Development of the Draper Semianalytical Satellite Theory Standalone Orbit Propagator Package.* AAS-97-731. Paper presented at the AAS/AIAA Astrodynamics Specialist Conference, Sun Valley, ID.

Nordvedt, K., & Will, C. M. 1972. Conservation Laws and Preferred Frames in Relativistic Gravity II: Experimental Evidence to Rule out Preferred-Frame Theories of Gravity. *Astrophysical Journal, 177:* 775.

Oza, D. H., & Friertag, R. J. 1995. *Assessment of Semi-empirical Atmospheric Density Models for Orbit Determination.* AAS 95-101. Paper presented at the AAS/AIAA Spaceflight Mechanics Conference, Austin, TX.

Pardini, C., & Anselmo, L. 1999. *Calibration of Semi-empirical Atmosphere Models Through the Orbital Decay of Spherical Satellites.* AAS 99-384. Paper presented at the AAS/AIAA Astrodynamics Specialist Conference, Girdwood, AK

Ries, J. C., Eanes, R. J., Tapley, B. D., & Peterson, G. E. 2002. Prospects for an Improved Lense-Thirring Test With SLR and the GRACE Gravity Mission. *Proceedings of the 13th International Workshop on Laser Ranging.* Washington, DC.

Rubincam, D. P., & Weiss, N. R. 1986. Earth Albedo and the Orbit of Lageos. *Celestial Mechanics, 38,* 233-296.

Scharoo, R., Walker, K. F., Ambrosious, B. A. C. , & Noomen, R. 1991. On the Along-track Acceleration of the Lageos Satellite. *Journal of Geophysical Research, 96,* 729-740.

Schwiderski, E. W. 1980. Ocean Tides, Part I: Global Ocean Tidal Equations. *Marine Geodesy, 3,* 161-217.

Schwiderski, E. W. 1980. Ocean Tides, Part II: A Hydrodynamical Interpolation Model. *Marine Geodesy, 3,* 219-255.

Seidelmann, P. K. 1982. IAU (1980) Theory of Nutation. *Celestial Mechanics, 27:* 79-106.

Seidelmann, P. K. 1992. *Explanatory Supplement to the Astronomical Almanac*. Mill Valley, CA: University Science Books.

Seidelmann, P. K., & Kovalevsky, J. 2002. Application of the New Concepts and Definitions (ICRS, CIP and CEO) in Fundamental Astronomy. *Astronomy and Astrophysics, 392*: 341-351.

Seidelmann, P. K., & Seago, J. H. 2005. *Relativistically Correct Celestial Reference Systems.* AAS 05-352. Paper presented at the AIAA/AAS Astrodynamics Specialist Conference and Exhibit, Lake Tahoe, CA.

Simon, J. L. et al. 1994. Numerical Expressions for Precession Formulae and Mean Elements for the Moon and the Planets. *Astronomy and Astrophysics, 282*: 663-683.

Smith, J. E. 1999. *Application of Optimization Techniques to the Design and Maintenance of Satellite Constellations* (M.S. Thesis, CSDL-T-1336). Cambridge, MA: Department of Aeronautics and Astronautics, Massachusetts Institute of Technology.

Standish, E. M. 1982. The JPL Planetary Ephemerides. *Celestial Mechanics, 26:* 181-186.

Standish, E. M. 1998. Time Scales in the JPL and CfA Ephemerides. *Astronomy & Astrophysics*, *336:* 381-4.

Stephens, G. L., Campbell, G. G., & Vonder Haar, T. H. 1981. Earth Radiation Budgets. *Journal of Geophysical Research, 86,* 9739-9760.

Stewart, R. H., Fu, L. L., & Lefebre, M. 1986. *Science Opportunities From the TOPEX/POSEIDON Mission.* Rep. No. 86-18. Pasadena, CA: Jet Propulsion Laboratory.

Storz, M. 1999. *Satellite Drag Accuracy Improvements Estimated From Orbital Energy Dissipation Rates.* AAS 99-385. Paper presented at the AAS/AIAA Astrodynamics Specialist Conference, Girdwood, AK.

Tanygin, S., & Wright, J. R. 2004. *Removal of Arbitrary Discontinuities in Atmospheric Density Modeling*. AAS 04-176. Paper presented at the AAS/AIAA Space Flight Mechanics Conference, Maui, HI.

Tapley, B. D., Schutz, B. E., Eanes, R. J., Ries, J. C., & Wartkins, M. M. 1993. LAGEOS Laser Ranging Contributions to Geodynamics, Geodesy, and Orbital Dynamics. *Contributions of Space Geodesy to Geodynamics: Earth Dynamics, 24:* 147-174.

Taylor, B. N. (Ed.). 2001. The International System of Units (SI). NIST Special Publication 330. Washington, DC: U.S. Government Printing Office.

Taylor, B. N. (Ed.). 1995. Guide for the Use of the Internal System of Units (SI), NIST Special Publication 811. Washington, DC: U.S. Government Printing Office. http://physics.nist.gov/Document/sp811.pdf

Taylor, B. N., & Kuyatt, C. E. 1994. Guidelines for Evaluating and Expressing the Uncertainty of NIST Measurement Results. NIST Technical Note 1297. Washington, DC: U.S. Government Printing Office.

U.S. Standard Atmosphere. 1976. Environmental Science Services Administration, National Aeronautics and Space Administration, and U.S. Air Force. Washington, DC: U.S. Government Printing Office.

Vallado, D. A. 2007. *Fundamentals of Astrodynamics and Applications* (3rd ed.). Hawthorne, CA: Microcosm/Springer.

Vallado, D. A. 2005. *An Analysis of State Vector Propagation Using Differing Flight Dynamics Programs.* AAS 05-199. Paper presented at the AAS/AIAA Space Flight Mechanics Conference, Copper Mountain, CO.

Vallado, D. A., & Kelso, T. S. 2005. *Using EOP and Space Weather Data for Real-time Operations.* AAS 05-406. Paper presented at the AAS/AIAA Astrodynamics Specialist Mechanics Conference, Lake Tahoe, CA.

Vallado, D. A. et al. 2006. *Revisiting Spacetrack Report #3.* AIAA 2006-6753. Paper presented at the AIAA/AAS Astrodynamics Specialist Conference, Keystone, CO.

Vetter, J. R., Nerem, R. S., Cefola, P., & Hagar, H. 1993. *A Historical Survey of Earth Gravitational Models Used in Astrodynamics From Sputnik and Transit to GPS and TOPEX.* AAS 93-620. Paper presented at the AAS/AIAA Astrodynamics Specialist Conference, Victoria, BC, Canada.

Volkov, I. I., Knyazeva, Y. I., & Kugayenko, B. V. 1982. Refining a Model of Atmospheric Density for Ballistic Calculations. *Nablyudeniya Iskusstvennykh Nebesnykit Tel* (Moskva), *80:* 126-135.

Wahr, J. M. 1981. The Forced Nutations of an Elliptical, Rotating, Elastic, and Oceanless Earth. *Geophysical Journal of the Royal Astronomical Society, 64,* 3: 705-727.

Wielicki, B. A., Wong, T., Loeb, N., Minnis, P., Priestley, K., & Kandel, R. 2005. Changes in Earth's Albedo Measured by Satellites. S*cience, 308,* 5723: 825.

Wilkins, M. P. et al. 2006. *Practical Challenges in Implementing Atmospheric Density Corrections to the NRL-MSISE-00 Model.* AAS-06-170. Paper presented at the AAS/ AIAA Spaceflight Mechanics Conference, Tampa, FL.

Wright, J. R., & Woodburn, J. 2004. *Simultaneous Real-time Estimation of Atmospheric Density and Ballistic Coefficient.* AAS-04-175. Paper presented at the AAS/AIAA Space Flight Mechanics Conference. Maui, HI.

Yurasov, V. 1996. *Universal Semianalytical Satellite Motion Propagation Method.* Paper presented at U.S.-Russian Space Surveillance Workshop, Poznan, Poland.

Yurasov, V., et al. 2006. *Density Corrections for the NRLMSISE-00 Model.* AAS-05-168. Paper presented at the AAS/AIAA Spaceflight Mechanics Conference, Copper Mountain, CO.

American Institute of
Aeronautics and Astronautics

1801 Alexander Bell Drive, Suite 500
Reston, VA 20191-4344

www.aiaa.org

ISBN 1-60086-842-8